

Design of Carbonaceous Mercury Adsorbents from Waste Materials

by

Teresa Marie Bisson

A thesis submitted in partial fulfillment of the requirements for the degree of

Doctor of Philosophy

in

Chemical Engineering

Department of Chemical and Materials Engineering
University of Alberta

© Teresa Marie Bisson, 2014

Abstract

Mercury is an air pollutant emitted from coal fired power plants. Once released into the environment, mercury undergoes conversion to organomercury compounds, which cause health concerns for both humans and animals. Many studies have been completed with the goal of reducing mercury emissions from flue gases of coal fired power plants using various types of sorbent and catalytic technologies. Mercury removal has most commonly been accomplished in full scale applications through injecting powdered activated carbon-based sorbents into flue gas streams, including several commercial operations in North America. In particular, brominated activated carbon has been proven to be effective at improving the mercury removal efficiency. In order to reduce the cost associated with activated carbon injection, the research of this thesis studied an alternative carbon source, biomass ash waste, which is a by-product from combustion of waste wood for power generation. A chemical-mechanical bromination procedure was used to impregnate the wood ash with bromine (Br-Ash). The mercury capture performance of Br-Ash was found to be comparable to that of a commercial brominated activated carbon (Br-AC). Both Br-Ash and Br-AC captured mercury up to 390°C. Bromine was found to be stable on the Br-Ash up to high temperatures, but leached considerably when exposed to water at all pH values and liquid to solid mass ratios. The mercury concentration in the leachate was very low at neutral pH and high liquid to solid mass ratios. However, at low or high pH values, the mercury concentration in the leachate was above the amount set by the Environmental Protection Agency (EPA) for classifying hazardous waste. Decreasing the liquid to solid mass ratio in the leach tests (from 20:1 to 2:1) further increased the concentration of mercury in the leachate. The high mercury concentration in this case was due to increased bromine concentration in the leachate.

Based on these results, it was recommended to consider landfill conditions before disposal of the spent sorbent. In order to reduce environmental impact, the sorbent was re-designed to minimize the amount of Br required for mercury capture. The design of the new sorbent was based on studying the mercury removal mechanisms for Br-Ash compared to Br-AC using x-ray absorption spectroscopy (XAS). The mechanism of mercury capture by Br-Ash was proposed to involve oxidation of the mercury by the surface of the sorbent followed by binding to carbon near Br on the surface. In the case of Br-AC, the mercury was bound to sulfide groups that were not present on the Br-Ash. Understanding the mechanism of mercury capture led to the design of an optimal sorbent containing both Br and sulfide groups. Elemental sulfur was used to impregnate the wood ash, followed by bromination with a lower amount of Br (2 drops). Compared with sorbents containing only 2 drops Br (2D-Br-Ash) or sulfur (S-Ash), the combination of Br and sulfur (2D Br-S-Ash) significantly improved mercury capture. Optimum sulfur loading was achieved at a sulfur:carbon mass ratio of 1:20. The mercury capture mechanism of the 2D Br-S-Ash sorbent was also studied by XAS and was proposed to involve surface enhanced oxidation of mercury, followed by binding of the oxidized mercury to S, Br, or C on the surface of the sorbent. In addition, leach tests on the 2D Br-S-Ash sorbent showed a significant reduction of Hg and Br in the leachate at low liquid to solid ratios. Overall, a new type of carbon based sorbent containing both Br and S was designed with high mercury capture efficiency based on a study of mercury removal mechanisms.

Preface

The format of this thesis is a compilation of several papers; some of which are published and others are to be submitted for publication. Some of the papers and chapters are co-authored and the following list indicates the contributions for each paper.

- Chapter 1: Introduction: Original work by T.M. Bisson
- Chapter 2: Literature Review: Original work by T.M. Bisson
- Chapter 3: A version of this chapter has been published as “Chemical–mechanical bromination of biomass ash for mercury removal from flue gases,” co-authored by Teresa M. Bisson, Zhenghe Xu, Rajender Gupta, Yadollah Maham, Yan Liu, Hongqun Yang, Ian Clark, and Manoj Patel. in: *Fuel*. **2013**. *108*. p.54-59. Bisson was responsible for mercury pulse injection tests, thermogravimetric analysis, surface area measurements and manuscript preparation. Bisson prepared Figures 3-8. Liu and Yang were responsible for preparation of the Br-Ash and analysis of the sorbents tested at the power station, as well as preparing Figures 1, 2 and 9. Clark and Patel were responsible for arranging and conducting the tests in real flue gases of the power station, reviewing results and providing insight based on industrial perspective. Maham supervised the thermogravimetric analysis portion of the paper and provided insight into data interpretation as well as proofreading. Gupta and Xu supervised the project, assisted with data interpretation and proofread the manuscript prior to submission.
- Chapter 4: This chapter is to be submitted as “Potential Hazards of Brominated Carbon Sorbents for Mercury Emission Control,” co-authored by Teresa M. Bisson and Zhenghe Xu. Bisson was responsible for experimental design, data collection and interpretation as well as manuscript preparation. Xu supervised the work and made suggestions to include x-ray photoelectron spectroscopy analysis. Xu also proofread the manuscript before submission.
- Chapter 5: A version of this chapter has been published as “Characterization of Mercury Binding onto a Novel Brominated Biomass Ash Sorbent by X-ray Absorption Spectroscopy,” co-authored by Teresa M. Bisson, Lachlan C. W. MacLean, Yongfeng Hu, and Zhenghe Xu. in: *Environ. Sci. Technol.* **2012**, *46*, 12186–12193. Bisson was

responsible for conducting the mercury loading tests, analysis of the sorbents, and writing the sections pertaining to mercury loading and analysis, as well as the section regarding implications for Hg capture. MacLean was responsible for the x-ray absorption spectroscopy and x-ray fluorescence data collection and analysis, and was responsible for writing the corresponding sections. Hu supervised the x-ray absorption data collection and analysis, and was also responsible for proofreading the manuscript. Xu was responsible for supervising the mercury loading tests and analysis and proofread the manuscript before submission.

- Chapter 6: This chapter is to be submitted as “Sulfur Loading on Brominated Carbon Sorbent for Improved Mercury Capture,” co-authored by Teresa M. Bisson, Zong Qian Ong, Aimee MacLennan, Yongfeng Hu and Zhenghe Xu. Bisson was responsible for mercury loading on sorbents, data interpretation, manuscript preparation, and for synthesis and testing of the high and low sulfur ashes. Ong was a summer student working under Bisson’s supervision and was responsible for assisting in loading sulfur onto ash, mercury pulse injection tests and drawing the sulfur loading schematic. MacLennan and Hu were responsible for x-ray absorption data collection and analysis, writing the experimental section for x-ray absorption, and proofreading the paper. Xu supervised the work and proofread the manuscript.
- Chapter 7: Conclusion: Original work by T.M. Bisson

Dedicated to my husband Blair

Acknowledgements

Financial support of this work was provided by the Natural Sciences and Engineering Research Council of Canada (NSERC). The Brominated Ash project was supported by Alberta Energy Research Institute (Alberta Innovates) and EPCOR (Capital Power), Edmonton, Alberta. Financial support for Canadian Light Source (CLS) is provided by NSERC, National Research Council, Canadian Institutes of Health Research, and the University of Saskatchewan.

I am extremely thankful for my supervisor, Dr. Zhenghe Xu, who has been a mentor to me since I worked in his lab as a WISEST student in my teenage years. I am grateful for his keen scientific insight, which has substantially improved the quality of my research. I am also thankful for him for encouraging my scientific curiosity, and providing me with many opportunities to share my work with the scientific community.

I would also like to thank my supervisory committee members; Dr. Rajender Gupta and Dr. Arno de Klerk, for their insightful comments and scientific discussions that have helped me complete this work more effectively. In particular, I would like to thank Dr. Gupta for allowing me to use the Clean Coal Lab facilities for many of my experiments. It has been a privilege to be a part of the Clean Coal research group.

I also would have not achieved my career goals so far without some strong mentors who have helped me along the way. I would like to thank Dr. Yadollah Maham for his kindness and support throughout both my undergraduate and graduate degrees. His encouragement has given me confidence and I am grateful for his support. I would also like to thank my mentors Dr. Mary Bourke and Mr. Frank Vagi, who have helped me grow from a “young engineer” to a more mature engineer. I appreciate their example of professionalism, career path discussions, and I am grateful for our continued friendship.

The work in this Thesis would not have been complete without participation from various laboratory facilities. I would like to thank the Alberta Center for Surface Engineering and Science (ACSES) for providing surface analysis of my samples, and in particular would like to thank Dr. Dimitre Karpuzov, Dr. Shihong Xu and Dr. Anqiang He for the valuable discussions and help with CasaXPS software. I would also like to acknowledge the Integrated Nanosystems Research Facility (INRF) at the National Institute of Nanotechnology (NINT) for the use of their facilities. I would also like to thank CLS for the use of the synchrotron facilities along with my

colleagues Dr. Yongfeng Hu, Dr. Lachlan MacLean and Aimee MacLennan. I would also like to thank the staff at CLS for technical support, in particular Dr. Ning Chen and Dr. Weifeng Chen. Thank you to Mike Xia, Tong Qiu and Lan Wu for help with surface area measurements.

Over the course of my thesis work, I have had the privilege to work with several summer students; Shunbin Xia, Zhe Bai, and Zong Qian Ong, who have helped me collect the data in this thesis and brought energy and excitement into the laboratory. Thank you for your hard work and scientific curiosity. I would also like to thank all of the C⁵MPT and Oilsands group members for interesting scientific discussions and support during this thesis work. Thank you to our technicians, Mr. Jim Skwarok and Ms. Jie Ru, for your technical assistance and expertise. I would also like to thank Ms. Lisa Carreiro, Ms. Gayle Hatchard, Mr. Kevin Heidebrecht, Ms. Lily Laser, Mr. Walter Boddez, Mr. Shiraz Merali, Mr. Richard Cooper, Mr. Wayne Moffat, Ms. Jela Burkus, Dr. Mingsheng Ma, Mr. Les Dean, Ms. Andrée Koenig, Mr. Jack Gibeau, Mr. Clark Bicknell, Mr. Herb Green, Mr. James Mckinnon, Mr. Dave Parlin, Mr. Robert Smith, Mr. Jason Dibbs, and any others who provided administrative and technical assistance to me for the duration of this degree. Dr. David Kelly and the staff at Capital Power who assisted with the flue gas tests are also acknowledged. Thank you also to my colleagues and friends, Dr. Erin Bobicki, Ms. Natalie Kuznicki, Dr. Meijiao Deng and Ms. Shiau Yin Wu for your friendship and support throughout this degree. I am grateful to Blair Bisson, Rachel Dueck, Sylvia Bisson, Cheryl Fortin and Natalie Kuznicki for proofreading portions of this thesis and other papers I have published.

On a personal note, I would like to thank my heavenly Father who has guided my path. I am forever grateful and forever changed by Your love. I would also like to thank my parents, Richard and Delene Van Ember for the sacrifices they have made to ensure I had a good education, for raising me to be a good person and for encouraging me to follow my dreams. I would not be who I am today without such incredible parents as my first teachers. I am also grateful for my sister, Christina Van Ember, who is always available to lend a listening ear when I need to talk. Thank you to my mother in law Sylvia Bisson for your encouraging words during my studies. To my husband Blair, I am so thankful for your love, encouragement and companionship, especially during these last few years of completing this doctorate degree. I would not have been able to complete this without your support. To my daughter Jacqueline, I am so grateful for the love and joy you bring into my life.

Table of Contents

Chapter 1: Introduction	1
1.1. Background on Mercury Pollution Control	1
1.1.1 Mercury in Coal and Flue Gases.....	2
1.2. Objectives and Thesis Outline	5
1.3. References.....	8
Chapter 2: Literature Review.....	10
2.1. Introduction.....	10
2.2. Activated Carbon Sorbents	10
2.3. Sulfur Functionalized Sorbents.....	12
2.3.1 H ₂ S Oxidation	13
2.3.2 Elemental Sulfur (S ⁰) Impregnation.....	14
2.3.3 Other Sulfur Addition Methods	17
2.4. Halogenated Activated Carbon Sorbents	19
2.4.1 Brominated Activated Carbon	20
2.5. Flue Gas Effects:.....	21
2.6. Mechanisms of Hg ⁰ Removal by Activated Carbon Sorbents.....	22
2.7. Conclusion	26
2.8. References.....	27
Chapter 3: Chemical–Mechanical Bromination of Biomass Ash for Mercury Removal from Flue Gases	33
3.1. Introduction.....	33
3.2. Experimental	34
3.2.1 Novel Bromination Procedure	35

3.2.2 Mercury Injection Tests	35
3.2.3 Flue Gas Exposure Tests.....	36
3.2.4 Sorbent Characterization.....	37
3.3. Results and Discussion	37
3.3.1 Surface Composition.....	37
3.3.2 Surface Morphology	38
3.3.3 TG Analysis	40
3.3.4 Mercury Capture Results	43
3.3.5 Flue Gas Exposure Results	44
3.4. Conclusion	46
3.5. References.....	47
Chapter 4: Characterization of Mercury Binding onto a Novel Brominated Biomass Ash Sorbent by X-ray Absorption Spectroscopy	49
4.1. Introduction.....	49
4.2. Experimental Section.....	51
4.2.1 Sample Preparation	51
4.2.2 Mercury Pulse Injection Test.....	52
4.2.3 Mercury Loading Test.....	52
4.2.4 X-ray Fluorescence (XRF) Spectroscopy	53
4.2.5 X-ray Absorption Spectroscopy (XAS).....	53
4.2.6 XAS Data Analysis.....	54
4.3. Results and Discussion	54
4.3.1 Mercury Pulse Injection Test.....	54
4.3.2 Mercury Loading	56

4.3.3 X-ray Fluorescence Spectroscopy.....	56
4.3.4 S K-edge XANES	57
4.3.5 Hg L _{III} -edge XANES	58
4.3.6 Hg EXAFS.....	60
4.3.7 Br K-edge XANES	63
4.3.8 Implications for Hg Capture	63
4.4. References.....	66
Chapter 5: Potential Hazards of Brominated Carbon Sorbents for Mercury Emission Control	
69	
5.1. Introduction.....	69
5.2. Experimental Procedure.....	71
5.2.1 Br Leaching in Ultra-Pure Water	71
5.2.2 Hg, Br Leaching by TCLP	72
5.2.3 Tests at Varying pH and Liquid to Solid Ratios	73
5.2.4 XPS Characterization.....	74
5.3. Results and Discussion	74
5.4. References.....	84
Chapter 6: Sulfur Loading on Brominated Carbon Sorbent for Improved Mercury Capture	
86	
6.1. Introduction:.....	86
6.2. Experimental Procedure.....	88
6.2.1 Synthesis of S-Ash and Br-Ash	88
6.2.2 Mercury Loading and Pulse Injection Tests	90
6.2.3 SEM and TEM Analysis:.....	91
6.2.4 XAS Analysis:	91

6.3. Results/Discussion:	92
6.4. References:.....	106
Chapter 7: Thesis Summary, Conclusions and Future Work	111
Bibliography	116
Appendix A: Additional Figures for Chapter 4	129
Appendix B: Additional Figures and Tables for Chapter 6.....	130

List of Tables

Table 3.1. Ultimate analysis of Raw Ash and Br-Ash.....	38
Table 3.2. XRF analysis of Raw Ash.....	39
Table 3.3. XPS results for Br-Ash treated at different temperatures.....	42
Table 3.4. XPS results for Br-Norit treated at different temperatures.....	42
Table 3.5. XPS results for Br-Ash treated at different temperatures (at.%).	43
Table 4.1. Mercury L _{III} -edge EXAFS fitting results for Hg mercury bound to carbon sorbents. ^a	63
Table 5.1. Results of bromine leaching tests.	75
Table 5.2. Results of mercury leaching tests using TCLP method.....	77
Table 5.3. Results of CaBr ₂ addition to leaching tests (W=Water).	80
Table 6.1. Elemental analysis results and BET data.....	93
Table 6.2. Mercury XANES and EXAFS results summary.....	102
Table B1. Hg leach test results using TCLP leaching method.	131
Table B2. Br leach test results TCLP leaching method.....	131

List of Figures

Figure 1.1. Mercury emissions from Canadian coal fired power plants. Plot drawn based on data obtained from the Canadian Council of Ministers of the Environment.....	3
Figure 1.2. Possible mercury transformations from coal combustion and flue gas species, reproduced from Galbreath et al. ¹⁴	4
Figure 2.1. Proposed mechanism of mercury capture by sulfide group by Yao et al. ³⁴	23
Figure 3.1. Chemical-mechanical bromination of biomass waste ash in a laboratory tumbler. ⁸ ..	35
Figure 3.2. Comparison of XPS surface mass concentrations of interesting elements in brominated ash (Br-Ash), brominated activated carbon (Br-Norit), and Raw Ash (Raw Ash). ⁸ .	38
Figure 3.3. SEM micrographs and BET surface area values of commercial brominated activated carbon and biomass ashes.	39
Figure 3.4. High resolution SEM micrographs of commercial brominated activated carbon and biomass ashes to show pore structures.....	40
Figure 3.5. TG heating curves for Br-Ash and Raw Ash.....	41
Figure 3.6. Isotherm curves of Br-Ash at two different temperatures.	42
Figure 3.7. XPS survey scan of Br-Ash.....	43
Figure 3.8. Results of mercury breakthrough as a function of capture temperature.....	44
Figure 3.9. Mercury uptake by sorbents exposed to real flue gases of an operating power plant. The numbers above the bars are actual value of mercury uptake by sorbents.....	45
Figure 4.1. Schematic for loading of elemental mercury onto sorbents.	53
Figure 4.2. Capture of Hg ⁰ by various sorbents in pulse injection tests.	55
Figure 4.3. Hg concentration of sorbents after exposure to elemental mercury, along with test duration and sorbent mass (*indicates second set of BA samples prepared for further analysis). 57	
Figure 4.4. Sulfur K-edge XANES spectra for the carbon sorbents. The black arrow denotes the reduced sulfur group (E ₀ = 2472 eV). Inset: Sulfur K-edge XANES spectra for the commercial	

activated carbon sorbent before (top) and after (bottom) exposure to Hg flue gas demonstrating a change in the bonding electronic structure of the reduced sulfur peaks with the addition of Hg. 59

Figure 4.5. (a) Mercury L_{III}-edge XANES spectra for the carbon sorbents ($E_0 = 12,284$ eV), (b) First derivative of the mercury L_{III}-edge XANES spectra for the carbon sorbents ($E_0 = 12,284$ eV)..... 60

Figure 4.6. (a) Mercury L_{III}-edge EXAFS chi spectra for the carbon sorbents. Black line is the sample spectra and red line is the best fit to the data. (b) Mercury L_{III}-edge EXAFS real-space Fourier transforms for the carbon sorbents. Black line is the sample spectra and red line is the best fit to the data..... 61

Figure 4.7. Illustration of proposed mechanism of Hg⁰ capture by Br-Norit commercial AC. Fused rings represent carbon in Br-Norit..... 64

Figure 4.8. Illustration of proposed mechanism of Hg⁰ capture by Br-Ash sorbent. Fused rings represent carbon in wood ash..... 65

Figure 5.1. Mercury loading schematic. 72

Figure 5.2. Br Leached (W=Water test; T=TCLP Test; Hg = Sorbents contained mercury). 75

Figure 5.3. Mercury pulse injection test results for water-leached Br-Ash and Br- Norit. 78

Figure 5.4. Mercury pulse injection test results for raw ash, Br-Ash⁵ and water-leached Br-Ash. 78

Figure 5.5. Amount of Hg and Br leached from Br-Ash as a function of pH in leachate after leach test. 0.2 mg/L line illustrates limit imposed by EPA¹¹ for amount of Hg in leachate. 79

Figure 5.6. Hg and Br leached from Br-Ash sorbent as a function of liquid to solid ratio. 0.2 mg/L line is shown as limit imposed by EPA¹¹ for Hg leaching..... 80

Figure 5.7. XPS survey scan of Br-Ash (top) and water-leached Br-Ash (bottom). 81

Figure 5.8. High resolution Br XPS scan of Br-Ash..... 82

Figure 5.9. High resolution Br XPS scan of water-leached Br-Ash. 83

Figure 6.1. Mercury Breakthrough of sulfur-loaded samples..... 94

Figure 6.2. High resolution SEM images of (a) Raw Ash; ⁴¹ (b) S-Ash; (c) High S-Ash.	95
Figure 6.3. TEM images mapped by EDS for (a) S-Ash and (b) High S-Ash.....	95
Figure 6.4. Mercury breakthrough of sulfur and low Br-Ash samples.	96
Figure 6.5. Mercury loading test results indicating the amount of Hg ⁰ the sorbents are able to capture during a 24 hour period of mercury exposure in air at 100 °C.	97
Figure 6.6. Sulfur K-edge results for varying sulfur contents. (a) FY Spectra; (b) S K-edge amplitude analysis providing speciation.	99
Figure 6.8. Mercury L _{III} -edge XANES spectra. Inset: First derivative of normalized XANES spectra.	103
Figure 6.9. Mercury EXAFS amplitude analysis for the samples.	103
Figure 6.10. Illustration of proposed mechanism of Hg ⁰ capture by 2D Br-S-Ash. Fused rings represent carbon in wood ash.....	104
Figure 6.11. Hg and Br leached from 2D Br-S-Ash compared to original Br-Ash Sorbent. 0.2 mg/L line shows the limit imposed by the EPA for Hg leaching. ⁴⁸	105
Figure A1. Bulk X-ray fluorescence spectra of each sample. Excitation energy at 2605 eV.....	129
Figure A2. Bromine K-edge XANES spectra for the activated carbon sorbents (E ₀ = 13,474 eV).	129
Figure B1. Schematic of sulfur loading setup.....	130
Figure B2. Hg ⁰ loading experimental setup.....	130
Figure B3. Mercury EXAFS fitting.	131

Chapter 1

Introduction

1.1. Background on Mercury Pollution Control

Air quality degradation is an environmental issue which has recently been receiving increased attention from the public. In particular, coal-fired power plants are a major source of air pollutants. For coal to be a long-term power solution, improvements on pollutant emission control must be made. Mercury (Hg) is a toxic trace element that is emitted from coal fired power plants. On average, a typical coal plant produces 170 pounds of mercury each year,¹ but this value is greatly dependant on the type of coal burned and the initial mercury content in the coal. After emission into the atmosphere, mercury pollutes rivers, lakes, oceans and land through deposition of contaminated rainwater.^{2,3} Once environmental contamination is complete, mercury is converted to methyl-mercury through biological processes and is bioaccumulated in the food chain. Humans are primarily exposed to mercury through consumption of contaminated fish,³ particularly the larger predatory fish. Mercury exposure has been linked to many neurological disorders such as memory loss, insomnia, impaired fetal brain development, behavioral issues, and cerebral palsy.^{3,4} The immune, gastrointestinal and cardiovascular systems can also be negatively impacted by mercury exposure.⁴ Humans are not the only species affected by mercury exposure. Many mammals, fish and birds have been impacted by the bioaccumulation of methyl-mercury. Some of the effects observed in other species have been reduced reproduction, impaired growth, behavioral abnormalities and death.³

Recently, the United Nations have recognized the hazardous nature of mercury, and have drawn attention to its detrimental effect on the environment as the emissions of mercury are transported globally. As a result, 97 countries have signed the Minamata Convention treaty in October 2013, which is a legally-binding commitment to prevent mercury emissions.⁵

In the USA, the 1990 Clean Air Act amendments have recently resulted in the Mercury and Air Toxics Standards (MATS). These standards have set limits on mercury emissions that require technological improvements in order to be achievable.⁶ Most mercury capture applications can guarantee 90% capture, but the MATS regulations would require greater than 99% capture for some coals.⁶ The following options (or a combination of them) are anticipated to be used to achieve this capture efficiency; switching fuel/coal or co-firing a combination of fuel/coal to reduce mercury content, adding additives to fuel before or during combustion, adding additives to fuel gas desulfurization units, using chemically promoted activated carbon and/or increasing injection rates, using chemical oxidants or oxidizing catalysts, addition of fabric filters (possible removal of electrostatic precipitators), and development of new technologies.

Mercury has long been recognized as a toxic substance by the Canadian government in the Canadian Environmental Protection Act.⁷ In 2006, the Canadian government endorsed Canada wide standards for mercury emissions from coal-fired power plants.⁸ In 2012, a progress report was issued for the provinces, which indicated a significant decrease in Canada's emissions from coal-fired power plants (Figure 1).⁹ In Alberta, mercury capture rates in 2012 varied between approximately 63-81%⁹ compared to a target of 80% put in place by the Alberta government.⁷ The sample of government regulations presented indicates the necessity to continue to improve mercury capture technologies. In addition, consideration of cost must also be taken into account in order to ensure the ability of power plants to apply the mercury capture technologies in their facilities.

1.1.1 Mercury in Coal and Flue Gases

Concentration of mercury in coal is highly variable, and depends on the source (location) and type of coal (ex: lignite, bituminous, sub-bituminous or anthracite).¹⁰ A typical range of mercury in coal is 0.01 to 0.48 mg/kg.¹⁰ Even though this content seems low, the high throughput of coal burned results in a larger amount of mercury emitted, which is substantial considering its toxicity.

Mercury in coal is often associated with cinnabar (HgS) and pyrite (FeS₂), but can also be organically bound.¹¹ The three main forms of mercury emitted from coal-fired power plants are particulate bound mercury, oxidized mercury (Hg²⁺), and elemental mercury (Hg⁰).^{12,13}

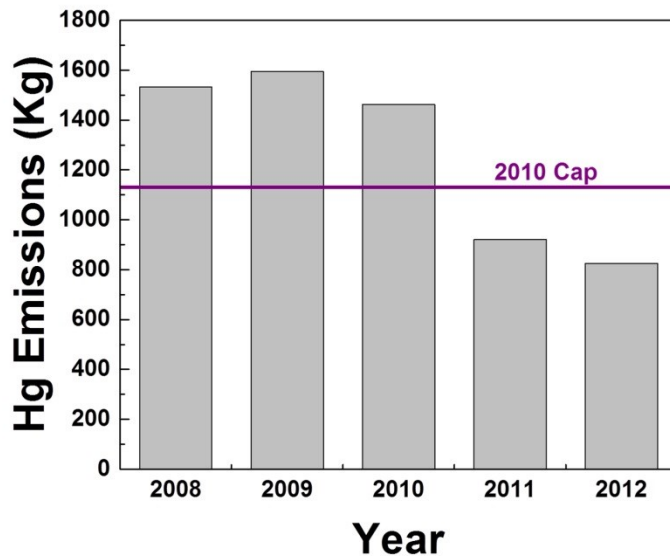


Figure 1.1. Mercury emissions from Canadian coal fired power plants. Plot drawn based on data obtained from the Canadian Council of Ministers of the Environment.⁹

Particulate bound mercury is considered easy to remove as it is generally trapped in the plant particulate control devices (e.g. fabric filters or electrostatic precipitators). Hg^{2+} is highly soluble in water and can be removed by the wet flue gas desulphurization unit. Hg^0 , however, is problematic since it is the most dominant form in the flue gas, is insoluble in water, and cannot be completely trapped by particulate control devices.¹² Hg^0 also has a long atmospheric lifetime, resulting in wide global dispersion.¹⁰ Possible mercury transformations during coal combustion are shown in Figure 1.2. Above 600 – 700 °C, Hg^0 is the stable form of mercury, and most of the mercury leaving the combustion zone is expected to be in the form of Hg^0 .¹⁰ Upon emission, the Hg^0 undergoes other transformations as shown in Figure 1.2.

The mercury species in combustion systems can be affected by coal type or composition, boiler design, heat transfer rates, cooling rates, combustion environment (gas composition), operating practices and any air pollution control devices employed.¹¹ In both high and low-rank coals, mercury has been found to be concentrated in finer fly ash fractions.¹¹

Mercury removal technologies have typically focused on removing mercury by treating the coal before burning, coal treatment during burning, or removing the Hg^0 from the flue gases after burning. Coal treatment has resulted in some success for Hg^0 reduction, but Hg^0 can still remain

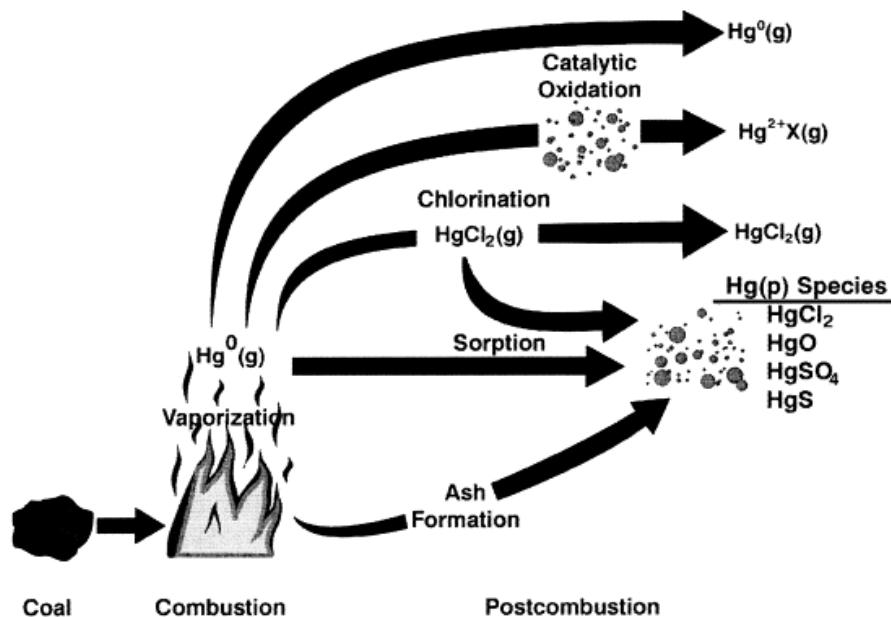


Figure 1.2. Possible mercury transformations from coal combustion and flue gas species, reproduced from Galbreath et al.¹⁴

after treatment and will transfer to flue gases.¹⁰ Flue gas treatment is therefore currently necessary. The most researched and technologically ready Hg^0 removal method is injection of powdered activated carbon (AC). AC is injected downstream of the air preheater and upstream of the particulate control device. The carbon mixes with flue gases, traps the Hg^0 through chemisorption or physisorption, and is removed in the particulate control device. This technology has already been demonstrated on many full scale systems and is the most widely adopted Hg^0 removal method to date.^{7,10,15}

The downside with mercury control options is the cost of removal creating higher operational costs for power plants. Activated carbon injection costs were estimated to range (depending on coal type) from \$39,000 - \$49,000 /lb of Hg removed in 2003 for a 500 MW boiler.¹⁶ In 2009, updated estimates by Feeley III et al.¹⁷ indicate a range of less than \$10,000 to \$30,000 /lb of Hg removed depending on the facility. The reduced costs of Hg^0 removal were attributed to the

improved efficiency in Hg capture by chemically impregnated AC sorbents. The increase in efficiency (and reduction in sorbent injection) offsets the higher cost of the impregnated AC.¹⁷

1.2. Objectives and Thesis Outline

Reducing the costs associated with AC injection continues to be attractive. The cost of AC could be further reduced by using a carbon source material available at a lower cost than coal. Recently, a bromination process has been developed to add bromine to a waste material (wood ash from biomass combustion).¹⁸ The ash is low cost, has high carbon content, and also has the environmental benefit of using a waste material that is typically sent to landfill, a concept of waste-treat-waste. The main objective of this research is to study the suitability of the brominated biomass ash sorbent for mercury capture and to improve the sorbent design, creating a low cost alternative to AC. Stability of mercury and bromine on the sorbent will be determined, and increased understanding of the binding mechanism of mercury on the brominated ash sorbent will lead to a creative design of the sorbent for mercury capture.

The following description outlines each chapter in this thesis:

Chapter 1 is a general introduction on the problem and thesis objectives, along with the outline of the thesis.

Chapter 2 contains a literature review on activated carbon sorbents for mercury capture. Several impregnation methods are reviewed, and particular focus is made to review the literature to date investigating the mechanism of mercury removal by activated carbon.

Chapter 3 investigates using waste biomass ash as an alternative material to activated carbon. A chemical-mechanical bromination procedure is presented and used to prepare the brominated biomass ash sorbent. Scanning electron microscopy, x-ray photoelectron spectroscopy and thermo gravimetric analysis are used to characterize the sorbents and test thermal stability. The bromine on the brominated biomass ash is found to be stable upon heating to high temperatures (up to 650 °C). Mercury pulse injection tests are used to determine mercury capture on the lab scale, and demonstrate that the brominated biomass ash has improved mercury capture compared to the raw biomass ash. In addition, the mercury removal performance is comparable to a commercial brominated activated carbon. Exposure of the sorbents to real flue gases in an operating plant also shows mercury

capture by brominated biomass ash in real flue gases. A version of this chapter has been published as “Chemical-mechanical bromination of biomass ash for mercury removal from flue gases” in *Fuel*. **2013**, *108*, 54-59.

Chapter 4 is a study on the binding of mercury on the brominated biomass sorbent and commercial brominated AC sorbent. The sorbents are loaded with mercury and analyzed by x-ray absorption spectroscopy to determine the bonding environment of mercury on the samples. The binding of Hg on a commercial brominated AC appears to follow the same mechanism reported by previous studies involving surface enhanced oxidation of the mercury, followed by binding of mercury to sulfide groups. In contrast, the brominated biomass ash sorbent mechanism is proposed to include surface enhanced oxidation, with subsequent binding to carbon near the Br species. A version of this chapter has been published as “Characterization of mercury binding onto a novel brominated biomass ash sorbent by x-ray absorption spectroscopy” in *Environ. Sci. Technol.* **2012**, *46*, 12186–12193.

Chapter 5 examines the stability of bromine and mercury on the brominated biomass ash sorbent compared to a commercial brominated AC commonly used for mercury control in industry. The standard leaching procedure for characterizing toxicity of waste materials is used to evaluate leaching of mercury and bromine from the sorbents, which shows low leaching of mercury and high leaching of Br. Leaching tests at varying pH and liquid to solid ratios show that possible variation in landfill conditions can increase the leaching of mercury. It is recommended that the applicable landfill condition should be considered prior to disposal of spent sorbents, particularly for high or low pH conditions, or low liquid to solid mass ratio conditions. The mercury captured by the sorbents after leaching is demonstrated by mercury pulse injection tests. X-ray photoelectron spectroscopy is used to investigate the binding of Br before and after leaching, indicating that less metal-bound Br is present after leaching.

Chapter 6 investigates the combination of both sulfur and bromine species on the biomass ash to improve the mercury capture and reduce the amount of bromine required on the sorbent. Mercury pulse injection tests showed that combining sulfur and bromine on the ash improves mercury removal. Sorbents are exposed continuously to mercury for 24

hours and the mercury-loaded sorbents are analyzed by x-ray absorption spectroscopy (XAS) to determine the binding of the mercury on the sorbents. Peak areas of the XAS spectra are analyzed to determine the contribution of different species to mercury binding in the sample. A mechanism of surface enhanced oxidation of mercury, with subsequent binding of the oxidized mercury to S, Br or C sites was proposed for the combined sulfur-bromine-ash sorbent. Standard leach tests showed lower concentrations of Br and Hg in the leachate for the sulfur-bromine-ash sorbent compared to the brominated ash sorbent.

Chapter 7 contains the summary of the thesis, conclusions and recommendations for future work.

1.3. References

- (1) Union of Concerned Citizens, Environmental impacts of coal power: air pollution. http://www.ucsusa.org/clean_energy/coalvswind/c02c.html (Accessed June 22, 2009).
- (2) Nugent, O., The Acid Rain Primer, 2-29, <http://www.pollutionprobe.org/Publications/ARP06dwnldpage.htm> (Accessed June 22, 2009).
- (3) Keating, M.H.; Mahaffey, K.R.; Schoeny, R.; Rice, G.R.; Bullock, O.R.; Ambrose, R.B.; Swartout, J.; Nichols, J.W., Mercury Study Report to Congress, Volume I: Executive Summary, <http://www.epa.gov/ttn/caaa/t3/reports/volume1.pdf> (Accessed August 24, 2009).
- (4) Berlin, M.; Zalups, R.K.; Fowler, B.A. Chapter 33: Mercury, Handbook on the Toxicology of Metals. In: 3rd Ed. ed.; Nordberg, G.F.; Fowler, B. A.; Nordberg, M.; Friberg, L. T., Eds.; Academic Press, Inc.: , 2007; pp.675-719.
- (5) United Nations Minamata Convention on Mercury. <http://www.mercuryconvention.org/> (Accessed May 23, 2014).
- (6) Johnson, D. W.; Brown, J. H.; Martin, M. J.; Rumble, A. Coal's triple challenge for air regulation compliance: technology, measurement, and commercial. In *Power Plant Air Pollution Control 'Mega' Symposium 2012*, Proceedings of the Power Plant Air Pollutant Control "MEGA" Symposium, Baltimore, Maryland, USA, August 20-23, 2012; Curan Associates: Red Hook, NY, 2013; p. 1-13.
- (7) Valupadas, P. Alberta mercury regulation for coal-fired power plants. *Fuel Process. Technol.* **2009**, *90*, 1339–1342.
- (8) Canadian Council of Ministers of the Environment. CANADA-WIDE STANDARDS for MERCURY EMISSIONS from COAL-FIRED ELECTRIC POWER GENERATION PLANTS http://www.ccme.ca/assets/pdf/hg_epg_cws_w_annex.pdf (Accessed July 1, 2014).
- (9) Canadian Council of Ministers of the Environment. 2012 PROGRESS REPORT. http://www.ccme.ca/assets/pdf/pn_1518_cws_hg_coal_prgrs_rpt_2012.pdf (Accessed July 1, 2014).

- (10) Reddy, B. M.; Durgasri, N.; Vinod Kumar, T.; Bhargava, S. K. Abatement of gas-phase mercury-recent developments. *Catal. Rev.- Sci. Eng.* **2012**, *54*, 344-398.
- (11) Pavlish, J. H.; Sondreal, E. A.; Mann, M. D.; Olson, E. S.; Galbreath, K. C.; Laudal, D. L.; Benson, S. A. Status review of mercury control options for coal-fired power plants. *Fuel Process. Technol.* **2003**, *82*, 89-165.
- (12) Y. Li, P.D. Murphy, C.Y. Wu, K.W. Powers, J.C.J. Bonzongo, Development of silica/vanadia/titania catalysts for removal of elemental mercury from coal-combustion flue gas. *Environ. Sci. Technol.* **2008**, *42*, 5304–5309.
- (13) Y. Li, P. Murphy, C.Y. Wu, Removal of elemental mercury from simulated coal combustion flue gas using a SiO₂–TiO₂ nanocomposite. *Fuel Process. Technol.* **2008**, *89*, 567–573.
- (14) Galbreath, K. C.; Zygarlicke, C. J. Mercury transformations in coal combustion flue gas. *Fuel Process. Technol.* **2000**, *65–66*, 289 – 310.
- (15) Brown, T.; Lissianski, V. First full-scale demonstration of mercury control in Alberta. *Fuel Process. Technol.* **2009**, *90*, 1412-1418.
- (16) Hoffman, J.; Ratafia-Brown, J. Preliminary cost estimate of activated carbon injection for controlling mercury emissions from an un-scrubbed 500 MW coal-fired power plant. http://www.alrc.doe.gov/technologies/coalpower/ewr/mercury/pubs/ACI_Cost_Final.pdf (Accessed August 4, 2014)
- (17) Feeley III, T. J.; Jones, A. P.; Brickett, L. A.; O’Palko, B. A.; Miller, C. E.; Murphy, J. T. An update on DOE’s phase II and phase III mercury control technology R&D program. *Fuel Process. Technol.* **2009**, *90*, 1388-1391.
- (18) Gupta, R. P.; Xu Z.; Clark, I.; Yang, H. Bromination process. United States Patent No. 20100126345, May 27, 2010.

Chapter 2

Literature Review

2.1. Introduction

Mercury (Hg) is a problematic air pollutant emitted from coal-fired power plants and is known to cause neurological disorders in humans and animals.^{1,2} The removal of mercury from flue gases is environmentally beneficial and has been legislated by governments worldwide. This chapter focuses on the removal of mercury by the most commonly applied mercury removal technology (powdered activated carbon sorbents) and reviews literature involving the development, improvement and capture mechanisms studied in this area to date. As activated carbon sorbents have been identified as the most developed and ready to use technology for mercury adsorption, this chapter will focus on reviewing the activated carbon sorbent preparation, modification and mercury capture mechanisms.

2.2. Activated Carbon Sorbents

Powdered activated carbon (AC) sorbents have been widely studied for removal of Hg^0 from flue gases.³ AC has a high amount of surface reactivity, large specific surface area and suitable pore size, which make it effective for mercury removal.³ AC is typically injected upstream of the air pollution control device (e.g. electrostatic precipitator or fabric filter), and after the air preheater, resulting in an operating temperature range of 121-221 °C.³ The AC mixes with the flue gases and removes the Hg^0 through adsorption. The particulate control device then removes the AC with trapped Hg^0 as well as the fly ash from the flue gas stream. AC sorbents are already manufactured commercially and are useful in removing both mercury as well as other pollutants.⁴⁻⁷

Flue gas composition (including mercury concentration), temperature, and contact time have all been found to influence the adsorption of Hg^0 on AC.³ Unburned carbon in the fly ash has

been linked to enhanced mercury oxidation, with an even greater impact than the chlorine content in the coal.⁸ The type of carbon was also found to be important, depending on the number of sites available on the carbon that are active to mercury. Increasing Hg concentration has shown to increase the adsorption rate of Hg on activated carbon.⁹

Activation of carbon can be achieved by a physical or chemical method. Physical activation can involve periods of heating, and steam or carbon dioxide exposure. Steam and carbon dioxide both led to similar creation of micropore volume, but steam activation creates more mesopores.¹⁰ The structural properties and surface functional groups of activated carbons depend on the available oxidizing agent, temperature, activation time and starting material. The activation temperature can cause more dehydrogenation and deoxygenation of the carbon species, which can lead to the formation of more micropores.¹¹ Compared to physical activation, chemical activation has some advantages. The temperature is lower in chemical activation and the procedure is less complex, usually involving one step. Chemicals such as zinc chloride, phosphoric acid, and alkaline metal compounds (e.g. potassium hydroxide) are used to activate the surface.¹⁰

Due to the high cost of activated carbon, many studies have focused on using less expensive materials, such as agricultural residue,¹² petroleum coke¹³ and biochar.¹⁴ Skodras et al.¹⁰ used olive seed biomass, pine wood, oak wood and waste tires as the carbon source. KOH activated olive seeds had a high specific surface area, beneficial micropore structure, and contained all of the types of oxygen groups found on the activated carbons tested (carboxyls, quinones, lactones, carbonyls, phenols and ethers), leading to the highest capture of Hg⁰. The mechanism of Hg⁰ removal by these materials appeared to be dependent on surface functional groups containing oxygen. The waste tires had the worst mercury capture ability, possibly due to the low amount of lactone groups. The overall amount of mercury capture by the materials tested increased from Tires < Oak Wood < Pine Wood < Olive Seed Waste.¹⁰ While these waste materials were available and low cost, KOH required for activation could raise the production costs. The price increase due to KOH should be considered when comparing the cost of these sorbents to other activated carbon materials.¹⁰

Zinc chloride was used to chemically activate soybean straw, rice straw and corn stalks.¹¹ An optimal point was found for the loading of zinc chloride, depending on the type of biomass used.

30% ZnCl₂ was the optimum concentration for soybean straw and corn stalk, while 40% was the optimum ZnCl₂ concentration for the rice straw. For ZnCl₂ concentrations above these values, the specific surface area would slightly decrease and the pore structure would be damaged, leading to less mercury capture. The activation temperature was also found to have a maximum point for each sorbent (500 °C for the rice straw and 600 °C for both of the soybean straw and corn stalk). At the optimum temperature and ZnCl₂ loading, the sorbents captured up to 95% of Hg⁰.¹¹

Activated carbons have poor performance at high temperatures due to the main capture mechanism by physisorption.¹⁵ Adding species to the AC, such as sulfur¹⁵ or halogens⁶ improves mercury capture performance at higher temperatures. If adequate gas-solid contact time is provided, unpromoted activated carbon sorbents were shown to have good capacity for Hg⁰ capture, even comparable with some bromine impregnated sorbents,¹⁶ but this effect is temperature dependent.

2.3. Sulfur Functionalized Sorbents

Sulfur functionalized sorbents were among the first tested for capture of mercury in flue gases.¹⁷ The addition of sulfur onto the activated carbon support greatly improves the efficiency of mercury capture, most likely due to chemisorption as the main mechanism of capture and formation of HgS.¹⁸ The majority of sulfur impregnation has been achieved by the following methods: impregnation via gas exchange of H₂S^{15,19-23} or heating the carbon in the presence of elemental sulfur.^{15,18,22,24-31} Other methods include impregnation in solution by other species such as Na₂S,^{30,32} CS₂,³³ and NaSH³⁴ followed by heating. Mercury has been found to adsorb on areas of the carbon sorbents that contain high sulfur concentration.³⁵ The next three sections review several studies involving sulfur impregnated activated carbon sorbents. Comparison of the studies shows that the sorbent specific surface area, pore characteristics, impregnation temperature and sulfur content are all important aspects to consider for design of the sulfur impregnated sorbent. In particular, elemental sulfur has shown to be quite effective for mercury capture, but even the form (long chain compared to short chain) of elemental sulfur is an important consideration.²² Continued research in this area should focus on finding lower cost

alternatives to activated carbons, increased efficiency for Hg^0 capture and/or creating recyclable materials to lower the application cost.

2.3.1 H_2S Oxidation

Morimoto et al.²³ studied Hg^0 removal by activated carbon sorbents with H_2S present in the simulated flue gas. Lower temperatures (80 – 125 °C) were most effective for Hg^0 removal with both H_2S and SO_2 present. In fact, the presence of H_2S greatly improved the Hg^0 removal efficiency compared to the cases where no H_2S was present. The presence of O_2 was also found to be essential for capture of Hg^0 , and elemental sulfur was formed on the activated carbon support as a result of the reactions between the sorbent, H_2S and SO_2 . NO present in the flue gas reduced the Hg^0 removal efficiency at 150 °C.²³

Impregnation of sulfur on activated carbon fibers (ACF) by H_2S oxidation was studied by Feng et al.²¹ Concentration of sulfur was varied on the ACF by modification of temperature (higher temperature produced higher sulfur content) and exposure time to the H_2S stream. Sulfur was found to deposit on the ACF predominantly in the elemental form, and was more evenly distributed at higher impregnation temperatures. Low temperature (80 °C) oxidation of H_2S did not achieve sufficient sulfur loading for Hg^0 capture. The sulfur predominantly deposited inside the ACF at low temperatures, and deposited both inside and on the outer surface of the ACF at higher temperatures. Calculations showed that the lost pore volume after impregnation was caused by pore blockage in addition to some pore filling by the impregnated sulfur. The impregnated sulfur was found to be stable on the ACF, with some of the sulfur remaining even after heating to 800 °C. The sulfur stable at high temperatures was possibly in the form of C-S complexes which would account for the high temperature stability. In comparison, the sulfur that was lost during heating to 800 °C likely was the sulfur which was bound to other sulfur atoms. Hg^0 uptake was improved with slightly higher sulfur loading, but was not directly correlated with sulfur concentration due to the blocking of pores by sulfur molecules at high sulfur loading conditions. A sulfur loading resulting in approximately 4 wt% sulfur concentration was found to have the highest mercury uptake capacity, and medium to large micropores were suggested to be the greatest contributor to uptake of Hg .²¹ The same group also studied the sulfur speciation of the H_2S sorbents as a function of temperature and H_2S exposure

during the heating and cooling stages of synthesis.²² Thiophene was the main form of sulfur found on the sorbents, with elemental sulfur also making up a large portion. The amount of sulfur increased with increasing loading temperatures, and at 800 °C, there was a dramatic increase in the metal sulfide content compared to the synthesis condition at 600 °C. At 600 °C, the effect of H₂S present during heating and cooling was determined. The samples with H₂S present during cooling increased the amount of thiophene and elemental sulfur in the sample. The mercury removal performance was also studied for the samples, with the sample synthesized at 600 °C outperforming the other samples synthesized at 200, 300, 400, and 800 °C. The reduction in mercury capture for the higher temperature sample indicates that the metal sulfides that were formed at 800 °C may not be as useful for mercury capture as the groups formed at lower temperatures. Presence of H₂S during the cooling portion of the sorbent synthesis was also found to be beneficial for mercury capture of the sorbent. This study considered the different forms of sulfur with similar surface pore structures. In this case, the form of sulfur appeared to be the most important aspect influencing mercury uptake. In particular, the authors concluded that elemental sulfur, thiophene and sulfate were responsible for mercury uptake,²² but it is difficult to separate the effect of these species as concentrations of all species increase as sulfur content increases.

2.3.2 Elemental Sulfur (S⁰) Impregnation

Saha et al.³⁶ tested two types of sulfur-impregnated activated carbons (one pellet, one fiber), as well as brominated AC pellets in a simulated flue gas atmosphere to determine the effect of NO_x and SO₂ on mercury uptake and mercury capture mechanism. The results showed that the activated carbon fiber containing reduced sulfur (S-ACF) had a higher initial mercury breakthrough (25%) compared to the Br impregnated pellet (10%), but had a higher capacity for the duration of the test. The Br and S-impregnated pellets (Br-ACP and S-ACP) had a much steeper breakthrough curve, while the S-ACF had a more constant breakthrough throughout the test. The S-ACF was found to have more reduced S species than Br-ACP and S-ACP, which had sulfur primarily in the form of SO₄. The reduced sulfur species appeared to play an essential role in mercury capture. In addition, the SO₄ concentration in both the Br-ACP and S-ACP increased significantly throughout the test, while the SO₄ concentration on the S-ACF increased only

slightly. This increase in SO_4 concentration indicates less SO_2 adsorption on the S-ACF, and less competition between the Hg and SO_2 species on the carbon surface containing more reduced S groups (note that the XPS study could not differentiate between carbon-bonded sulfur and other sulfur complexes such as thiols or thiophene, and all of these groups were referred to as “reduced sulfur.”).³⁶ The method for S impregnation for the S-ACF was physical mixing with elemental S followed by heat treatment in N_2 . Br and S impregnation methods were not given for the other two sorbent samples.

Hsi et al.²⁴⁻²⁷ have extensively studied sulfur addition to activated carbon sorbents by thermal treatment of a mixture of carbon and elemental sulfur to create sorbents for Hg removal from flue gases. Different types of coals were tested for creating AC sorbents with different types of sulfur present in the source coal.²⁴ The coals with higher concentrations of organic sulfur were found to produce sorbents which were very effective for Hg^0 capture. Thiols, thiophenes, sulfides and disulfides (i.e. divalent species of sulfur) are the type of organic sulfur species present in coal, and could be the precursors to the sulfur active sites formed for Hg^0 removal. In comparison, the concentration of pyritic sulfur was seen to have a minimal impact on Hg^0 adsorption. Addition of 12 wt% S to the AC by thermal treatment resulted in a small amount of specific surface area reduction. At a treatment temperature of 600 °C, smaller S_2 - S_4 molecules were formed, which reacted with the unsaturated carbon sites, carboxyl groups and carbon-hydrogen bonds in the AC matrix. The sulfur functional groups resulting from these reactions were sulfone organic sulfur groups, thiophene/S-S/S-O, and sulfoxide groups.²⁴ After impregnation at this temperature, the Hg^0 capture capacity increased by approximately 55-60% for the AC generated from the low organic-sulfur coal. For the AC prepared from the coal that contained higher organic sulfur, the Hg^0 capture capacity actually decreased slightly, showing that the addition of sulfur is more useful for coals with lower organic sulfur content. The group also studied the effect of sulfur impregnation temperature on the resulting sulfur species formed, by saturating the AC with sulfur at each temperature studied (250, 400, 600, 650°C).²⁵ As impregnation temperature increased, the amount of sulfur loaded onto the AC decreased. The amount of organic sulfur increased as temperature increased, while the amount of elemental sulfur decreased. The sulfur loaded at higher temperatures was found to form more stable sulfur functional groups. 400 °C was found to be the optimum impregnation temperature based on the

Hg⁰ capture capacity. In their study, initial rates of Hg⁰ capture by the various sorbents were not investigated. Temperatures below 250 °C were not investigated as the elemental sulfur at these temperatures has a large amount of sulfur in the form of S₆-S₈, which are large molecules and can block the entrance of small pores, reducing the specific surface area.²⁵ The amount of sulfur uptake depended on the sample used, and the reduction in specific surface area (and pore volume) was dependant on the sulfur loading.¹² Hsi et al.²⁵ also noted that increasing the amount of bulk sulfur in the AC does not always ensure improved Hg⁰ capture. A sulfur monolayer may be ideal, in order to avoid pore blocking by excess sulfur in the AC.^{21,25} Lower sulfur content is therefore desirable as the impact to physical properties is minimal. Higher temperature sample preparation (ex: 600 °C) was also determined to have less impact on physical properties.²⁵ Elemental sulfur remaining after impregnation, as well as organic sulfur (formed during impregnation) were both found to be important for Hg⁰ adsorption.¹²

Liu et al.¹⁸ tested the effect of varying temperature as well as the sulfur to carbon ratio of activated carbons impregnated with elemental sulfur. The sulfur impregnation setup involved heating two crucibles side by side in a tube furnace. The first crucible contained elemental sulfur, while the other was loaded with activated carbon. During heating to the desired temperature in nitrogen flow, the elemental sulfur vaporized and deposited onto the activated carbon. Impregnation temperature was found to have the greatest impact on the mercury capture performance of the sorbent, which increased as the temperature increased (up to 600 °C). The reason for the temperature dependence was proposed to be due to the varying elemental sulfur allotropes present. At lower temperatures (ex: 250 °C), the sulfur allotropes are in the form of S₆-S₈, while at 600 °C, approximately 16% of the sulfur is in the form of S₂, which is more reactive.¹⁸ The sulfur to carbon ratio was found to have a small effect on mercury capture (less sulfur during impregnation led to lower Hg⁰ capture capacity), in contrast to temperature (and sulfur form), which was found to be more critical.

The impregnation methods using H₂S and S⁰ were both studied and compared by Kwon and Vidic.¹⁵ The method involving reaction between carbon and elemental sulfur at 600 °C was found to be more effective for mercury removal (capacity) than the H₂S oxidation method at 150°C, even though the sulfur content was less. The authors suggested that the lower impregnation temperature of the H₂S loaded sorbent may have caused larger sulfur chains which

are not as reactive toward mercury and caused pore blockage. In light of new evidence by Feng et al.²² described above, the H₂S impregnated AC may have a more competitive Hg⁰ capacity if prepared at 600 °C. This higher temperature is not as ideal from the perspective of treating the waste stream, but would create a more efficient sorbent for Hg⁰ capture. A separate study was conducted²² to further compare these two methods of sulfur impregnation. The samples were analyzed for different forms of sulfur for each sample. The H₂S impregnated sample had sulfur mainly in the form of thiophene (approximately 60% of the sulfur species) and elemental sulfur (approximately 20%), with small amounts of sulfate, metal sulfide, sulfoxide and sulfone. The sample formed by heating with elemental sulfur at 600 °C was predominantly thiophene (approximately 43% of sulfur species) with a larger amount of elemental sulfur (approximately 40%) compared to the sample formed by H₂S. Since elemental sulfur is anticipated to be the more active form for mercury removal in this case,²² the elemental sulfur addition method may be more effective for creating sorbents for Hg⁰ removal.

2.3.3 Other Sulfur Addition Methods

While H₂S impregnation and elemental S impregnation are the most common methods studied, other sulfur addition methods have also been studied. Otani et al.³³ created sulfur-impregnated carbon, alumina and zeolite sorbents by impregnation in solutions of CS₂, followed by evaporation in nitrogen. Specific surface area and sulfur content of the samples were found to be important factors affecting mercury breakthrough of the sorbents. As sulfur loading increased on the samples, the mercury breakthrough time increased, indicating more sulfur was useful for mercury capture. In this case, the porosity was maintained for the high surface area samples, and increased sulfur loading did not have a negative effect. Calculations were made based on the mechanism of Hg and S forming HgS, which showed that all sulfur on the zeolite and alumina supports was participating in the reaction, while some of the sulfur on the activated carbon support was not participating. The authors suggested that the sulfur that did not participate in reaction was stable and chemically adsorbed on the AC surface. The main disadvantage of using the zeolite or alumina supports is that the breakthrough curve had a non-zero outlet concentration at the beginning of the test (room temperature) and took some time to decrease. The authors

suggested a system application linking the S-impregnated zeolite or alumina bed with the S-AC bed to utilize the benefits of both types of sorbents.

Another sulfur loading condition was studied by Ie and colleagues using a combination of Na_2S followed by S^0 impregnation.^{30,32} The sulfur content and specific surface area were both found to be important for adsorption of HgCl_2 (g), as well as the impregnation order of Na_2S before elemental S^0 . The study did not test the effectiveness of Na_2S impregnation without elemental sulfur addition.

Yao et al.³⁴ synthesized several sulfur-impregnated activated carbon fibers using 5 different treatments: dimethyl sulfoxide (DMSO), Na_2S_4 , NaSH, mixing with elemental S, and a two-step impregnation with $\text{Na}_2\text{S}_4/\text{HSO}_3$. All treatment methods contained a combination (mixing) step and a heating step to achieve sulfur groups on the surface. Only the treatments with elemental S and NaSH resulted in sorbents with good mercury capacity. A high ratio of sulfide to sulfate was found to be a good indicator of efficient mercury removal. However, high overall sulfide content in the sample was not found to guarantee effective mercury removal. Mercury removal was also influenced by the specific surface area of the sample. In some cases the sulfur addition reduced the specific surface area by pore blocking, which reduced the mercury uptake. In the case of the elemental S addition and heating, the specific surface area increased due to the S vapor acting as an activation gas, which etched the outer carbon surface, increasing pore volume.³⁴

Sulfur-chlorine compounds combined with AC is another Hg^0 removal method that has been investigated by Yan et al.^{3,37} Sulfur dichloride (SCl_2) and sulfur monochloride (S_2Cl_2) were tested for removal of Hg^0 , achieving Hg^0 removal of up to 75%. The reaction was found to accelerate by the addition of fly ash or AC in the flue gas stream.³⁷ Sulfur monobromide (S_2Br_2) was also tested by Qu et al.,³⁸ achieving Hg^0 removal of over 70% in air and over 65% in simulated flue gas in the presence of AC at 120 °C. When no AC was present, the removal of Hg^0 was greatly reduced. Gas phase reaction tests between S_2Br_2 and Hg^0 showed that the order of Hg^0 reactivity from the greatest to the least was $\text{Br}_2 > \text{S}_2\text{Br}_2 > \text{S}$, when comparing sorbents tested under similar gas compositions. After combination with S, the Br atom is less reactive with Hg^0 , but was still more reactive than Cl in previous tests.³⁸

2.4. Halogenated Activated Carbon Sorbents

Mercury capture is generally more efficient in power plants which burn bituminous coals compared to lignite or subbituminous coals. The higher mercury capture in the bituminous coal plants is usually attributed to the higher chlorine content in the coal.³⁹ This understanding has led to much work involving removal of Hg^0 through addition of Cl onto activated carbons prior to injection, particularly for applications for plants burning lignite or subbituminous coals.⁶ Several different methods of halogen impregnation have also been studied, including the use of HCl ,⁴⁰⁻⁴¹ CuCl_2 ,⁴² ZnCl_2 ,⁴³ KI ,⁴¹ KBr ⁴⁴ and Br_2 .⁴⁵ Impregnation of halide ions on powdered graphite sorbents indicated the efficiency of Hg^0 removal increased as ion size increased from $\text{Cl}^- < \text{Br}^- < \text{I}^-$.⁴⁶

Chlorine Impregnated Activated Carbon

Higher chlorine content in coals (and consequently in the flue gas) has been known to greatly improve the mercury capture of activated carbon sorbents.³⁹ This understanding led to the development of directly impregnating halides on the activated carbon sorbents to (a) improve efficiency in low chlorine content coals and (b) to reduce the amount of activated carbon required for injection. Lower injection amounts would decrease costs and impact of the unburned carbon in the fly ash (sold to concrete industry). Activated carbon impregnated with HCl ⁴⁰ has shown excellent Hg^0 removal efficiency (80-90%). Surface functional groups containing Cl appear to play a major role in the removal of mercury using the Cl-impregnated activated carbon. Another study found that the removal efficiency of HCl-impregnated AC decreased with increasing temperature from 80 °C to 160 °C.⁴¹ Zinc chloride has also been used to impregnate activated carbon, which was shown to enhance the Hg^0 uptake up to 800 $\mu\text{g/g}$ over 8 hours.⁴³

Cupric chloride is another substance used to impregnate Cl species onto activated carbon, which was a better substrate than clay as it could more easily capture the Hg^0 after oxidation.⁴⁷ XAFS analysis showed that the main mercury species on the CuCl-AC was oxidized mercury, and that chemisorption was the dominant Hg^0 capture mechanism. The bonding of Hg to Cl was found in the case of CuCl-AC as well as HCl-AC, with HgCl_2 being more likely to form than HgCl .⁴⁷ In addition, another study has shown that the removal of Hg^0 by CuCl – AC was not

limited by mass – transfer, and the interaction of Hg^0 and Cl was proposed to be the rate limiting step.⁴² An increase of chloride concentration from 1% to 5% resulted in higher mercury capture by CuCl – AC.

2.4.1 Brominated Activated Carbon

Hg^0 is highly polarizable with a large electron cloud (80 electrons). London dispersion forces should therefore be considered for the interaction of Hg^0 with neighboring molecules or atoms.^{39,48} Cl_2 and Br_2 have 34 and 70 electrons, respectively. With a much larger number of electrons, Br_2 is expected to have higher London dispersion forces and would be more effective for oxidation of Hg^0 .⁴⁶

Brominated graphite was synthesized and tested before and after Hg capture by X-ray photoelectron spectroscopy (XPS).⁴⁶ The $3d_{5/2}$ electron binding energy in KBr was found to be 69.3 eV, and was 68.4 eV in brominated graphite. The authors suggested that the lower binding energy in brominated graphite indicates that the electrons are drawn closer to the Br nucleus, which would induce a more positive charge on the graphite. Graphite is an electrical conductor, and can delocalize the positive charge across its surface, and attracts the Hg^0 molecule (containing a large number of electrons). Charge transfer from Hg^0 to the graphite would form oxidized mercury, which could be considered the cation, and the graphite lattice would be the counteranion.⁴⁶

KBr impregnation solutions have also been used to prepare brominated activated carbons.⁴⁴ The mercury removal efficiencies improved over raw activated carbon (42%) to 69% for 1 wt% Br concentration. However, higher Br concentration reduced the Hg^0 removal efficiency.⁴⁴ Bromine gas was also used to enhance the removal of Hg^0 in flue gases.³⁹ Addition of SO_2 , H_2O , HCl and CO into the gas did not have any effect on Hg^0 removal in an environment with no fly ash. At low concentrations of NO (<8ppm), the Hg^0 oxidation was improved by NO addition, however, high concentrations of NO (>10ppm) reduced Hg^0 oxidation. Increasing temperatures caused the Hg^0 gas phase oxidation rates to decrease. Oxidation of Hg^0 by Br_2 was greatly improved in the presence of fly ash, with the unburned carbon content in the ash being one of the main factors to determine Hg^0 removal. When testing fly ash that contained no unburned carbon,

the fly ash no longer improved Hg^0 removal. In the presence of fly ash, NO promoted Hg^0 removal, while SO_2 had an inhibitive effect.³⁹

In addition to these lab tests, brominated AC injection has also been demonstrated in full scale operations.⁴⁹

2.5. Flue Gas Effects:

Flue gases are known to impact Hg^0 removal, and interaction of flue gases with the activated carbon has been observed to cause the surface species (such as I, Cl or SO_x) to be gained or lost, which can influence Hg^0 capture.⁵⁰ Hsi et al.²⁶ studied the effect of various components in a simulated flue gas atmosphere with a sulfur impregnated activated carbon using factorial analysis. NO and HCl were both found to improve Hg^0 adsorption, while SO_2 (with O_2 also present) decreased Hg^0 adsorption. The results indicated that the mercury capture performance of the sulfur impregnated AC was poor if the flue gas did not have acidic or oxidizing components. The authors proposed an Eley-Rideal mechanism involving the acidic gas components adsorbing onto the carbon surface followed by covalent bonding with gaseous Hg^0 to those components. The Hg then bonds with an active site (possibly involving sulfur) on the carbon surface (S-Hg-X, with X being Cl, N, O, etc.).²⁶

Tests by Rupp and Wilcox⁴⁵ on activated carbon fibers impregnated with bromine indicated that the presence of SO_2 in the system hindered adsorption and oxidation of Hg^0 . The oxidation of Hg^0 was promoted by NO_x , but the interaction NO_x species with the surface could prevent oxidized Hg from binding to the surface. In comparison, Eswaran and Stenger found that addition of NO and SO_2 to unpromoted activated carbon showed an improvement in mercury capture at approximately 90 °C.⁹

Liu et al.⁵¹ tested the mercury uptake by activated carbon sorbents impregnated with sulfur under different flue gas conditions. Up to 15% CO_2 , 1600 ppm of SO_2 and 500 ppm of NO did not affect mercury adsorption. The presence of moisture in the system was found to decrease the uptake of mercury by up to 25%. Addition of oxygen in the simulated flue gas improved the adsorption of Hg^0 by the sulfur-impregnated activated carbon, increasing the sorbent's capacity up to 30%. The surface of the activated carbon was further modified (preoxidized) to contain more oxygen-acidic functional groups, but this modification did not improve mercury uptake.⁵¹

As SO_2 and NO_2 concentrations increased, the capture capacity of mercury by activated carbons decreased, even at the relatively low concentrations of 2.5 ppm NO_2 and 100 ppm SO_2 .⁵² It was noted that even though capacity for Hg^0 was reached, the sorbent continued to oxidize the Hg^0 and the oxidized Hg was reemitted into the gas stream. The researchers proposed a mechanism where NO_2 catalytically oxidizes Hg^0 at the surface of AC, forming $\text{Hg}(\text{NO}_3)_2$, which then binds to basic sites on the AC. As basic sites are used up, breakthrough occurs. SO_2 is said to compete for the basic sites, and speeds up breakthrough.⁵²

Presto et al.¹⁶ observed that SO_2 concentration in simulated flue gas did not affect the mercury uptake by activated carbon, but mercury capture was inhibited by even very low (20ppm) concentrations of SO_3 .¹⁶ With SO_3 addition the used activated carbon not only captured less mercury, but also had higher sulfur content (predominantly in the form of sulfate). These results suggested that the sulfur oxides were in competition with mercury for the binding sites available on the surface of the carbon. This effect was seen for both commercial AC and brominated AC.¹⁶

Based on the studies to date, it is difficult to make a wide statement summarizing the effects of flue gas components. The effect of the flue gas components is dependent on flue gas temperature, composition, and the type of sorbent used. This shows the importance of performing a test run with the sorbent in the actual flue gases of the power plant before implementation. One overall observation can be made from the simulated flue gas tests: in all cases, HCl appears to cause a promotive effect on Hg^0 oxidation.

2.6. Mechanisms of Hg^0 Removal by Activated Carbon Sorbents

Many studies have been conducted to try to better understand the mechanism of mercury capture by AC sorbents.^{4,6,46,48,52-64} Pavlish et al.⁵² summarized the possible steps in capturing Hg^0 by activated carbon sorbents as:

- Mercury diffusion from the bulk gas to the activated carbon surface.
- Weak attraction by van der Waals forces causing weak physical adsorption of Hg^0 on the activated carbon.

- Hg^0 oxidation (on the surface of the AC) on Lewis acid sites. Since oxidation continues even after capacity is reached, these sites are not likely to be the final binding sites of the oxidized Hg.
- Adsorption of acid gases (such as Cl^- , NO_2^- , SO_2^-) on Lewis base sites.
- Mobility of Hg ions to adjacent sites, allowing the Hg to move to the negatively charged sites.
- When all basic sites are occupied, the saturation capacity is reached.

Other studies have focused on impregnated AC sorbent mechanisms. After combined XPS and TGA study, it was found that the NaSH and elemental S treated sorbents had higher ratio of sulfide to sulfate in the sample.³⁴ Sulfate groups were expected to be less reactive to mercury as all of the electrons of sulfur are occupied in the sulfate matrix. Sulfide, on the other hand, is capable of reacting and binding elemental mercury due to the two available electron lone pairs.³⁴ Assuming the active site consisted of the electron lone pairs, the mercury removal mechanism was proposed to be oxidation followed by electron transfer and rearrangement as shown in Figure 2.1.

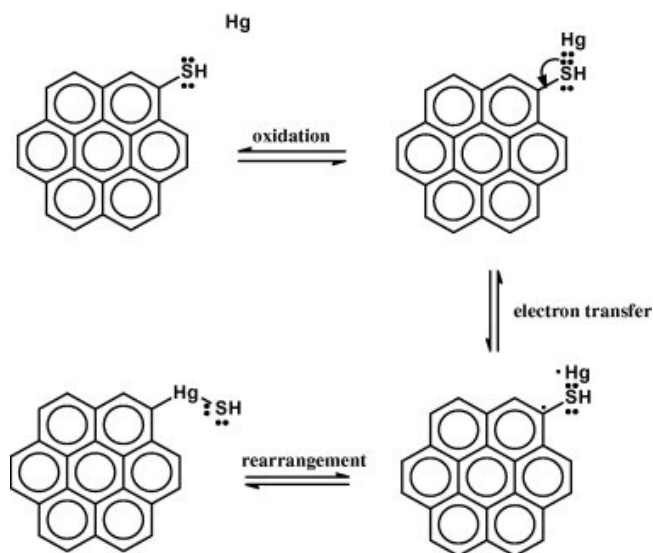


Figure 2.1. Proposed mechanism of mercury capture by sulfide group by Yao et al.³⁴

Sequential extraction was used to compare the mercury adsorption on chlorinated and brominated activated carbons, which were prepared with potassium chlorate solution and

bromine solution, respectively.⁶⁵ The extraction tests showed that mercury was present on the activated carbons as a highly stable compound, and also in elemental form. In the case of brominated activated carbon, the mercury was captured mainly as a stable compound (over 90%), while for the chlorinated activated carbon, mercury was mainly in the elemental form.⁶⁵

Another set of sequential extraction tests compared the stability of Hg on Br, Cl and S impregnated activated carbon materials.⁶⁶ The Hg on the Br and S impregnated AC was more stable than the Cl – impregnated AC. The authors suggested that the high stability in Br-AC was not due to HgBr₂ or Hg₂Br₂ formation due to the soluble nature of these compounds. Instead, another mechanism was suggested, consisting of Hg⁺ chelation with brominated sites on the activated carbon.

Kinetic modelling has shown that the interaction between Hg⁰ and gas phase Cl is not sufficient to account for the amount of Hg⁰ oxidized and captured in field tests.⁴⁶ Oxidation of Hg⁰ is catalyzed by the surface the halogen is impregnated on in addition to the halogen themselves. The type of activated carbon and halogen are both important for the oxidation mechanism.⁴⁶

Liu et al.⁴⁸ explored the adsorption of mercury species and mercury bromide species on activated carbon. Inclusion of Br on the surface of the activated carbon was found to increase the activity of the neighboring sites, which increases Hg⁰ adsorption capacity. The improvement in Hg⁰ capture was suggested to be due to the charge-transfer mechanism. In the charge transfer mechanism, electrons are drawn closer to the nucleus of Br, which in turn induces a positive charge on the carbon surface making it a strong electron acceptor. Hg⁰ is highly polarizable, and London dispersion forces could be responsible for its attraction to the brominated activated carbon.⁴⁸ In the case of HgBr, chemisorption is the predominant mechanism, and is thermally favorable. HgBr₂ was not stable on the surface, and is more likely to adsorb as HgBr.⁴⁸

Olson et al.⁵⁸ proposed that Hg⁰ acts as a Lewis base by donating its electrons to another gas-phase molecule or to the surface. The interaction of the Hg⁰ with an acidic site would create a strong covalent bond between the surface carbon and Hg⁰.⁶³ Sasmaz et al.⁶³ tested the capture of Hg⁰ in air by brominated activated carbon sorbents to investigate the mercury chemistry by EXAFS. At 30 and 140 °C, the Hg⁰ was found to be oxidized to Hg²⁺ on the brominated carbon surface. The Hg²⁺ was found to be coordinated with two atoms of Br, but no coordination was

observed between Hg^{2+} and O. These findings did not agree with the density functional theory calculations, which predicted that Hg is more stable by interaction with Br combined with binding to an edge C atom. However, the authors pointed out that carbon is considered a weak backscatterer, and Hg-C can be difficult by detection through EXAFS especially when other strong backscatters are present in the sample.

Hutson et al.⁴ studied the binding of Hg^0 on commercial activated carbon, chlorinated activated carbon and brominated activated carbon using both X-ray absorption spectroscopy (XAS) and X-ray photoelectron spectroscopy (XPS). The Hg^0 was captured in the oxidized form by all of the sorbents tested. Mercury was found to coordinate with mainly chlorinated sites on both the activated carbon and chlorinated activated carbon, but possibly bound to sulfate species (from adsorbed SO_2) as well. Mercury was bound to brominated sites in the case of the brominated activated carbon. The tests did not indicate any homogeneous reactions between flue gas components (e.g. HCl) and mercury, but did support the heterogeneous reaction mechanism between Hg and adsorbed species. The proposed mechanism was heterogeneous oxidation of Hg^0 by chlorine or bromine species on the sorbent, followed by binding to the chlorine, bromine or sulfur species on the surface.⁴

The binding of Hg has also been studied on iodine and sulfur impregnated activated carbons by Huggins et al.⁵⁵⁻⁵⁶ Mercury was found to be bound in the oxidized form in both the sulfur and iodine impregnated carbons. In addition, the Hg was bound to the chemically impregnated species on the surface (iodine, chlorine and sulfur), as well as oxygen. It should be noted that this study did not consider bromine species on the carbon surface. Mechanisms of mercury removal were dependent on mercury speciation, acidic species present in the flue gas (e.g. sulfur and chlorine), and the activating compounds (iodine and sulfur). Chemisorption was determined to be the most likely route of Hg^0 capture, but it was also possible that the oxidation of Hg^0 could occur in the flue gas followed by condensation onto the sorbent. However, mercury adsorption seemed dependent on the S/Cl ratio, which does favor chemisorption of the Hg^0 species rather than gas phase oxidation.⁵⁶ Overall, they proposed a mechanism for mercury capture by impregnated activated carbons to be surface enhanced oxidation, with binding of the oxidized mercury to the surface iodine, chlorine, sulfur or oxygen.⁵⁶ In addition, the adsorbed sulfur on the AC was found to be in the form of sulfate or bisulfate, depending on the binding sites

available on the carbon. The adsorption of HCl was also dependent on the AC, with some sorbents having high affinity for HCl and others having little.⁵⁶ Based on their findings, Huggins et al.⁵⁶ also mentioned that it is possible that each type of AC sorbent could have a different Hg⁰ capture mechanism.

2.7. Conclusion

Activated carbon injection has been shown to be effective for mercury capture, and many studies have been accomplished to understand mercury capture mechanisms in order to design more efficient and lower cost alternatives. Waste materials have been investigated as new lower cost alternatives to coal for producing activated carbon, but still require chemical or thermal treatment, which increases the production cost. Many studies have investigated sulfur addition to AC, but a limitation has been found regarding how much S can be loaded without blocking pores. In addition, speciation of sulfur is critical. Halogen addition to AC (in particular, bromide) has also proven to be effective for mercury capture, and has been proven at full scale operations. Flue gas composition has been shown to affect the mercury capture by most AC sorbents, but the gas effects appear to depend on the sorbent used. Many mechanisms have been suggested for mercury removal by activated carbons, but it is possible that differing types of mechanisms can be responsible for the Hg⁰ capture by the various AC sorbents.

2.8. References

- (1) Keating, M.H.; Mahaffey, K.R.; Schoeny, R.; Rice, G.R.; Bullock, O.R.; Ambrose, R.B.; Swartout, J.; Nichols, J.W., Mercury Study Report to Congress, Volume I: Executive Summary, <http://www.epa.gov/ttn/caaa/t3/reports/volume1.pdf> (Accessed August 24, 2009).
- (2) Berlin, M.; Zalups, R.K.; Fowler, B.A. Chapter 33: Mercury, Handbook on the Toxicology of Metals. In: 3rd Ed. ed.; Nordberg, G.F.; Fowler, B. A.; Nordberg, M.; Friberg, L. T., Eds.; Academic Press, Inc.: , 2007; pp.675-719.
- (3) Reddy, B. M.; Durgasri, N.; Vinod Kumar, T.; Bhargava, S. K. Abatement of gas-phase mercury-recent developments. *Catal. Rev. - Sci. Eng.* **2012**, *54*, 344-398
- (4) Hutson, N. D.; Attwood, B. C.; Scheckel, K. G. XAS and XPS characterization of mercury binding on brominated activated carbon. *Environ. Sci. Technol.* **2007**, *41*, 1747-1752.
- (5) Srivastava, R. K.; Hutson, N.; Martin, B.; Princiotta, F.; Staudt, J., Control of mercury emissions from coal-fired electric utility boilers, *Environ. Sci. Technol.* **2006**, *40*, 1385-1393.
- (6) Yang, H.; Xu, Z.; Fan, M.; Bland, A.E.; Judkins, R.R., Adsorbents for capturing mercury in coal-fired boiler flue gas, *J. Hazard. Mater.* **2007**, *146*, 1-11.
- (7) Ma, J.; Liu, Z.; Liu, Q.; Guo, S.; Huang, Z.; Xiao, Y., SO₂ and NO removal from flue gas over V₂O₅/AC at lower temperatures - role of V₂O₅ on SO₂ removal, *Fuel Process. Technol.* **2008**, *89*, 242-248.
- (8) Gale, T. K.; Lani, B. W.; Offen, G. R. Mechanisms governing the fate of mercury in coal-fired power systems. *Fuel Process. Technol.* **2008**, *89*, 139-151.
- (9) Eswaran, S.; Stenger, H. G. Gas-phase mercury adsorption rate studies. *Energy Fuels.* **2007**, *21*, 852-857.
- (10) Skodras, G.; Diamantopoulou, I.; Zabaniotou, A.; Stavropoulos, G.; Sakellaropoulos, G. P. Enhanced mercury adsorption in activated carbons from biomass materials and waste tires. *Fuel Process. Technol.* **2007**, *88*, 749-758.
- (11) Zhao, L.; Liu, Q.; Wu, J.; Zhang, C.; Wu, Y.; Zha, J.; Yang, S.; Hu, C. Study on the removal of mercury in the simulated flue gas by biomass activated carbon. *Adv. Mater. Res.* **2014**, *864-867*, 1519-1524.

- (12) Hsi, H. C.; Tsai, C. Y.; Kuo, T. H.; Chiang, C. S. Development of low-concentration mercury adsorbents from biohydrogen-generation agricultural residues using sulfur impregnation. *Bioresource Technol.* **2011**, *102*, 7470-7477.
- (13) Lee, S. H.; Rhim, Y. J.; Cho, S. P.; Baek, J. I. Carbon-based novel sorbent for removing gas-phase mercury. *Fuel.* **2006**, *85*, 219-226.
- (14) De, M.; Azargohar, R.; Dalai, A. K.; Shewchuk, S. R. Mercury removal by bio-char based modified activated carbons. *Fuel.* **2013**, *103*, 570-578.
- (15) Kwon, S.; Vidic, R. D. Evaluation of two sulfur impregnation methods on activated carbon and bentonite for the production of elemental mercury sorbents. *Environ. Eng. Sci.* **2000**, *17*, 303-313.
- (16) Presto, A. A.; Granite, E. J. Impact of sulfur oxides on mercury capture by activated carbon. *Environ. Sci. Technol.* **2007**, *41*, 6579-6584.
- (17) Vitolo, S.; Pini, R. Deposition of sulfur from H₂S on porous adsorbents and effect on their mercury adsorption capacity. *Geothermics.* **1999**, *28*, 341-354.
- (18) Liu, W.; Vidic, R. D.; Brown, T. D. Optimization of sulfur impregnation protocol for fixed-bed application of activated carbon-based sorbents for gas-phase mercury removal. *Environ. Sci. Technol.* **1998**, *32*, 531-538.
- (19) Sinha, R. K.; Walker Jr., P. L. Removal of mercury by sulfurized carbons. *Carbon.* **1972**, *10*, 754-756.
- (20) Daza, L.; Mendioroz, S.; Pajares, J. A. Mercury elimination from gaseous streams. *Appl. Catal. B. Environ.* **1993**, *2*, 277-287.
- (21) Feng, W.; Kwon, S.; Feng, X.; Borguet, E.; Vidic, R. D. Sulfur impregnation on activated carbon fibers through H₂S oxidation for vapor phase mercury removal. *J. Environ. Eng.* **2006**, *132*, 292-300.
- (22) Feng, W.; Borguet, E.; Vidic, R. D. Sulfurization of a carbon surface for vapor phase mercury removal – II: Sulfur forms and mercury uptake. *Carbon.* **2006**, *44*, 2998-3004.
- (23) Morimoto, T.; Wu, S.; Uddin, M. A.; Sasaoka, E. Characteristics of the mercury vapor removal from coal combustion flue gas by activated carbon using H₂S. *Fuel.* **2005**, *84*, 1968-1974.

- (24) Hsi, H. C.; Chen, S.; Rostam-Abadi, M.; Rood, M. J.; Richardson, C. F.; Carey, T. R.; Chang, R. Preparation and Evaluation of coal-derived activated carbons for removal of mercury vapor from simulated coal combustion flue gases. *Energy Fuels*. **1998**, *12*, 1061-1070.
- (25) Hsi, H. C.; Rood, M. J.; Rostam-Abadi, M.; Chang, Y. M. Effects of sulfur, nitric acid, and thermal treatments on the properties and mercury adsorption of activated carbons from bituminous coals. *Aerosol Air Qual. Res.* **2013**, *13*, 730-738.
- (26) Hsi, H. C.; Rood, M. J.; Rostam-Abadi, M.; Chen, S.; Chang, R. Effects of sulfur impregnation temperature on the properties and mercury adsorption capacities of activated carbon fibers (ACFs). *Environ. Sci. Technol.* **2001**, *35*, 2785-2791.
- (27) Hsi, H. C.; Chen, C. T. Influences of acidic/oxidizing gases on elemental mercury adsorption equilibrium and kinetics of sulfur-impregnated activated carbon. *Fuel*. **2012**, *98*, 229-235.
- (28) Steijns, M.; Peppelenbos, A.; Mars, P. Mercury chemisorption by sulfur adsorbed in porous materials. *J. Colloid Interface Sci.* **1976**, *57*, 181-186.
- (29) Suresh Kumar Reddy, K.; Al Shoaibi, A.; Srinivasakannan, C. Gas-phase mercury removal through sulfur impregnated porous carbon. *J. Ind. Eng. Chem.* **2014**, *20*, 2969-2974.
- (30) Ie, I.-R.; Shen, H. Z.; Yuan, C.-S.; Hung, C.-H.; Chen, W.-H.; Jen, Y.-H. Single and dual adsorption of vapor-phase Hg^0 and/or HgCl_2 by innovative composite activated carbons impregnated with both S^0 and Na_2S . *Aerosol Air Qual. Res.* **2014**, *14*, 376-385.
- (31) Korpiel, J. A.; Vidic, R. D. Effect of sulfur impregnation method on activated carbon uptake of gas-phase mercury. *Environ. Sci. Technol.* **1997**, *31*, 2319-2325.
- (32) Ie, I. R.; Chen, W. C.; Yuan, C. S.; Hung, C. H.; Lin, Y. C.; Tsai, H. H.; Jen, Y. S. Enhancing the adsorption of vapor-phase mercury chloride with an innovative composite sulfur-impregnated activated carbon. *J. Hazard. Mater.* **2012**, *217-218*, 43-50.
- (33) Otani, Y.; Emi, H.; Kanaoka, C.; Uchijima, I.; Nishino, H. Removal of mercury vapor from air with sulfur-impregnated adsorbents. *Environ. Sci. Technol.* **1988**, *22*, 708-711.
- (34) Yao, Y.; Velpari, V.; Economy, J.; Design of sulfur treated activated carbon fibers for gas phase elemental mercury removal. *Fuel*. **2014**, *116*, 560-565.

- (35) Karatza, D.; Lancia, A.; Musmarra, D.; Zucchini, C. Study of mercury absorption and desorption on sulfur impregnated carbon. *Exp. Therm. Fluid Sci.* **2000**, *21*, 150-155.
- (36) Saha, A.; Abram, D. N.; Kuhl, K. P.; Paradis, J.; Crawford, J. L.; Sasmaz, E.; Chang, R.; Jaramillo, T. F.; Wilcox, J. An X-ray photoelectron spectroscopy study of surface changes on brominated and sulfur-treated activated carbon sorbents during mercury capture: performance of pellet versus fiber sorbents. *Environ. Sci. Technol.* **2013**, *47*, 13695-13701.
- (37) Yan, N.; Qu, Z.; Chi, Y.; Qiao, S.; Dod, R.L.; Chang, S.; Miller, C. Enhanced elemental mercury removal from coal-fired flue gas by sulfur-chlorine compounds. *Environ. Sci. Technol.* **2009**, *43*, 5410–5415.
- (38) Qu, Z.; Yan, N.; Liu, P.; Guo, Y.; Jia, J. Oxidation and stabilization of elemental mercury from coal-fired flue gas by sulfur monobromide. *Environ. Sci. Technol.* **2010**, *44*, 3889-3894.
- (39) Liu, S.; Yan, N. ; Liu, Z.; Qu, Z.; Wang, H. P.; Chang, S.; Miller, C. Using bromine gas to enhance mercury removal from flue gas of coal-fired power plants. *Environ. Sci. Technol.* **2007**, *41*,1405-1412.
- (40) Behrooz Ghorishi, S.; Keeney, R. M.; Serre, S. D.; Gullett, B. K.; Jozewicz, W. S. Development of a Cl-impregnated activated carbon for entrained flow capture of elemental mercury. *Environ. Sci. Technol.* **2002**, *36*, 4454-4459.
- (41) Lee, S. J.; Seo, Y.; Jurng, J.; Lee, T. G. Removal of gas-phase elemental mercury by iodine- and chlorine-impregnated activated carbons. *Atmos. Environ.* **2004**, *38*, 4887-4893.
- (42) Vidic, R. D.; Siler, D. P. Vapor-phase elemental mercury adsorption by activated carbon impregnated with chloride and chelating agents. *Carbon.* **2001**, *39*, 3-14.
- (43) Zeng, H.; Jin, F.; Guo, J. Removal of elemental mercury from coal combustion flue gas by chloride-impregnated activated carbon. *Fuel.* **2004**, *83*, 143-146.
- (44) Wu, J.; Chen, J.; Zhang, S.; He, P.; Fang, J.; Wu, Y. Removal of gas-phase elemental mercury by bromine-impregnated activated carbon. *Adv. Mater. Res.* **2012**, *356-360*, 1660-1663.
- (45) Rupp, E. C.; Wilcox J. Mercury chemistry of brominated activated carbons – packed-bed breakthrough experiments. *Fuel.* **2014**, *117*, 351-353.

- (46) Qu, Z.; Chang, J. J.; Hsiung, T.; Yan, N.; Wang, H. P.; Dod, R.; Chang, S.; Miller, C. Halides on carbonaceous materials for enhanced capture of Hg^0 : mechanistic study. *Energy Fuels*, **2010**, *24*, 3534-3539.
- (47) Li, X.; Lee, J.; Heald, S. XAFS characterization of mercury captured on cupric chloride-impregnated sorbents. *Fuel*. **2012**, *93*, 618-624.
- (48) Liu, J.; Qu, W.; Zheng, C. Theoretical studies of mercury-bromine species adsorption mechanism on carbonaceous surface. *Proceedings of the Combustion Institute*. **2013**, *34*, 2811-2819.
- (49) Brown, T.; Lissianski, V. First full-scale demonstration of mercury control in Alberta. *Fuel Process. Technol.* **2009**, *90*, 1412-1418.
- (50) Huggins, F. E.; Dalai, A. K.; Wallace, K. W.; Smith, D.; Shewchuk, S. R. *Surface properties of two activated carbons before and after exposure to a Hg-containing power-plant flue-gas*. Proceedings of the Combined Power Plant Air Pollutant Control Mega Symposium. August 30-September 2, 2004, Washington DC.
- (51) Liu, W.; Vidic, R. D.; Brown, T. D. Impact of flue gas conditions on mercury uptake by sulfur-impregnated activated carbon. *Environ. Sci. Technol.* **2000**, *34*, 154-159.
- (52) Pavlish, J. H.; Sondreal, E. A.; Mann, M. D.; Olson, E. S.; Galbreath, K. C.; Laudal, D. L.; Benson, S. A. Status review of mercury control options for coal-fired power plants. *Fuel Process. Technol.* **2003**, *82*, 89-165.
- (53) Wilcox, J.; Sasmaz, E.; Kirchofer, A.; Lee, S.-S. Heterogeneous Mercury Reaction Chemistry on Activated Carbon. *J. Air Waste Manage. Assoc.* **2011**, *61*, 418-426.
- (54) Bisson, T. M.; MacLean, L. C. W.; Hu, Y.; Xu, Z. Characterization of mercury binding onto a novel brominated biomass ash sorbent by x-ray absorption spectroscopy. *Environ. Sci. Technol.* **2012**, *46*, 12186-12193.
- (55) Huggins, F. E.; Huffman, G. P. XAFS examination of mercury sorption on three activated carbons. *Energy Fuels*. **1999**, *13*, 114-121.
- (56) Huggins, F. E.; Yap, N.; Huffman, G. P.; Senior, C. L.; XAFS characterization of mercury captured from combustion gases on sorbents at low temperatures. *Fuel Proc. Technol.* **2003**, *82*, 167-196.

- (57) Uddin, M. A.; Ozaki, M.; Sasaoka, E.; Wu, S. Temperature-Programmed Decomposition Desorption of Mercury Species over Activated Carbon Sorbents for Mercury Removal from Coal-Derived Fuel Gas. *Energy Fuels*. **2009**, *23*, 4710–4716.
- (58) Olson E. S.; Azenkeng, A.; Laumb, J. D.; Jensen, R. R.; Benson, S. A.; Hoffman, M. R. New developments in the theory and modeling of mercury oxidation and binding on activated carbons in flue gas. *Fuel Process. Technol.* **2009**, *90*, 1360-1363.
- (59) Laumb, J. D.; Benson, S. A.; Olson, E. A. X-ray photoelectron spectroscopy analysis of mercury sorbent surface chemistry. *Fuel Process. Technol.* **2004**, *85*, 577– 585.
- (60) Padak, B.; Brunetti, M.; Lewis, A.; Wilcox, J. Mercury Binding on Activated Carbon. *Environ. Prog.* **2006**, *25*, 319-326.
- (61) Granite, E. J.; Pennline, H.W.; Hargis, R. A. Novel Sorbents for Mercury Removal from Flue Gas. *Ind. Eng. Chem. Res.* **2000**, *39*, 1020-1029.
- (62) Ho, T. C.; Ghai, A. R.; Guo, F.; Wang, K. S.; Hopper, J. R. Adsorption and Desorption of Mercury on Sorbents at Elevated Temperatures. *Combust. Sci. Tech.* **1998**, *134*, 263-289.
- (63) Sasmaz, E.; Kirchofer, A.; Jew, A. D.; Saha, A.; Abram, D.; Jaramillo, T. F.; Wilcox, J. Mercury chemistry on brominated activated carbon. *Fuel*. **2012**, *99*, 188-196.
- (64) Wilcox, J.; Rupp, E.; Ying, S. C.; Lim, D. –H.; a, Suarez Negreira, A.; Kirchofer, A.; Feng, F.; Lee, K. Mercury adsorption and oxidation in coal combustion and gasification processes. *Int. J. Coal Geol.* **2012**, *90-91*, 4–20.
- (65) Fan, M.; Tong, S.; Jia, C. Q.; Mao, L.; Li, Y.; Zhang, X. *Adsorption and stability of mercury on different types of impregnated activated carbon*. Proceedings of the 2011 International Conference on Computer Distributed Control and intelligent Environmental Monitoring. Feb 19-20, 2011. Changsha, Hunan, China. pp.1929-1932.
- (66) Tong, S.; Fan, M.; Mao, L.; Jia, C. Q. Sequential extraction study of stability of adsorbed mercury in chemically modified activated carbons. *Environ. Sci. Technol.* **2011**, *45*, 7416–7421.

Chapter 3

Chemical–Mechanical Bromination of Biomass Ash for Mercury Removal from Flue Gases

A version of this chapter has been published as:

Teresa M. Bisson, Zhenghe Xu, Rajender Gupta, Yadollah Maham, Yan Liu, Hongqun Yang, Ian Clark, Manoj Patel. *Fuel*. **2013**. *108*. p.54-59.

3.1. Introduction

Mercury is a toxic substance which is emitted to the atmosphere through many sources, including coal-fired power plants. Airborne mercury becomes deposited into rivers, lakes and oceans, and bioaccumulates in the form of methyl-mercury, moving up the food chain as it is consumed by various aquatic species.¹ The primary source of mercury exposure in humans is through eating contaminated fish, which can cause neurological disorders and is especially detrimental to fetal brain development.^{1,2} Some of the diseases which can be caused by mercury exposure are cerebral palsy, behavioural issues, memory loss and insomnia, along with problems with the immune, gastrointestinal and cardiovascular systems.¹ Bioaccumulation of methyl-mercury also impacts other animals such as fish, birds and mammals, causing impaired growth, behavioural abnormalities, lower reproductive success and even death.² The toxic effects of mercury have been largely realized in the last 20 years, leading to regulations at the state and federal levels of government. In Alberta, Canada, a regulation has been set in place to capture mercury at a minimum level of 70%, to be implemented in 2010 and proposals must be submitted by December 31, 2011 outlining the plan for continuous improvement (targeting a minimum of 80% capture).³

Injecting a powdered activated carbon-based sorbent into flue gases of coal-fired power plants is one technology which has been studied for reducing mercury emissions.⁴⁻⁶ For coals with sufficient chlorine content, a homogeneous reaction occurs between the gaseous chlorine and

mercury, producing HgCl_2 . This understanding has led to work involving the addition of halogens, such as chlorine or bromine, to the activated carbon sorbent. Impregnating the halogen components on the sorbent has been found to increase its effectiveness of mercury removal (with higher removal efficiency and lower injection rates), especially for coal containing low levels of chlorine.⁴⁻⁶ A review of various studies completed on brominated carbon sorbents by Yang et al.⁶ described a faster adsorption of elemental mercury (Hg^0) on brominated sorbents than on non-brominated carbon sorbents. The same study showed that the sorbent capacity was slightly reduced when the temperature increased, while the capacity of the carbon sorbent improved as the amount of bromine on the sorbents increased. Tests at various power plants showed that the brominated activated carbon is very efficient at removing mercury.⁶

In Alberta, at least one power plant has proposed to use the technology of injecting brominated activated carbon to meet the regulation requirements of 70% mercury removal, set in place by the government.³ However, use of activated carbons as source materials is costly.⁷ In biomass combustion based power plants, a large amount of ash with high carbon content up to 40-50% is produced as a solid waste. It would be attractive to use this waste as the source material to produce sorbents for mercury emission control. The objective of this study is to develop an environmentally benign and economically practical sorbent for mercury emission control of flue gases from coal-fired power plants using biomass combustion wastes and liquid bromine as source materials. This sorbent is prepared using a novel chemical-mechanical bromination procedure developed in our research laboratory, and intended to be used as an injectable powdered sorbent. The brominated biomass ash is characterized and exposed to real flue gases in an online coal-fired power plant.

3.2. Experimental

The received biomass ash had a broad size distribution, and was ball-milled to prepare samples for bromination and mercury breakthrough tests. The biomass ash was placed in a tumbler charged with 1" steel balls. The tumbler was then capped and rotated for 3 hours on a pair of mechanical rollers. The particle size distribution after tumbling was close to normal distribution with $d_{0.1} = 4.3 \mu\text{m}$, $d_{0.5} = 17.0 \mu\text{m}$, and $d_{0.9} = 53.4 \mu\text{m}$.⁸

3.2.1 Novel Bromination Procedure

Bromination was achieved through chemical-mechanical activation of biomass ash using a tumbler containing liquid bromine, biomass and glass beads, as shown schematically in Figure 3.1. This chemical-mechanical bromination process featured two major benefits: good contact was established between the bromine and ash particles; and the ash particles were ground to an appropriate size convenient for transportation and injection.

A 10-L carboy containing 6-mm glass beads and liquid bromine was used for the chemical-mechanical bromination. Biomass ash was placed in the carboy at a glass beads to biomass ash ratio of 7.⁸ The carboy was tightly sealed and rotated on a set of rollers for 30 min. The resulting brominated ash was separated from the mixture using a 3.35 mm sieve before thermal treatment in a vacuum oven at 200 °C to ensure the stability of loaded bromine on biomass ash for safe storage, transportation and applications.

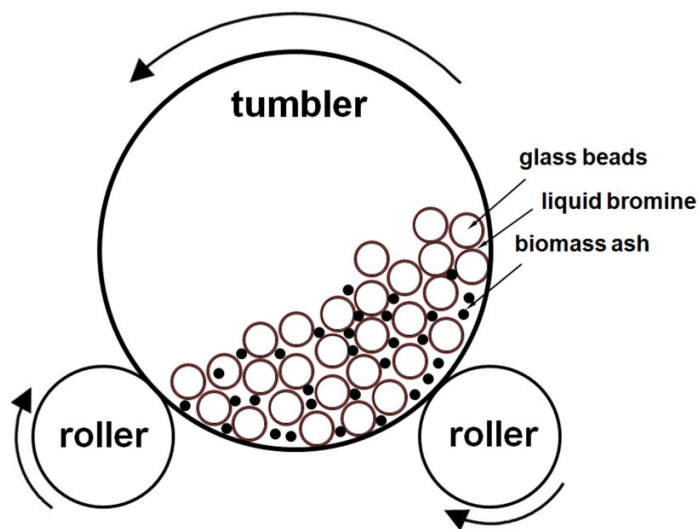


Figure 3.1. Chemical-mechanical bromination of biomass waste ash in a laboratory tumbler.⁸

3.2.2 Mercury Injection Tests

Mercury pulse injection tests were performed in an argon carrier gas stream running at 40 ml/min, with the experimental setup described elsewhere.⁷ A precisely weighed 40 mg of sample was placed in a borosilicate glass tube (4-mm i.d.) with quartz wool to keep the powdered sorbent from escaping the tube. The tube was then placed inside a GC oven to control

the mercury breakthrough tests at the desired temperatures from 20 to 400 °C. Once the oven reached the desired temperature for 5 min, the downstream GB trap was heated to remove any bromine or mercury liberated from the brominated biomass ash during heating. The GB trap consisted of gold-sputtered silica beads inside a quartz tube, and was used to preconcentrate trace amounts of mercury in the purge gas before its analysis. After cooling the GB trap, 200 µL of air saturated with Hg⁰ at room temperature between 16 and 22°C, corresponding an Hg⁰ concentration of 10.08 - 16.61 pg/µL,⁹ was injected upstream of the sorbent. Mercury that was not captured by the sorbent leaked through the sorbent and was captured in the GB trap by amalgamation with the sputtered gold. Five minutes after the initial injection, the GB Trap was quickly heated, using a voltage applied to a heating wire, to above 400°C to release the mercury from the GB trap to a Cold Vapour Atomic Fluorescence Spectrophotometry (CVAFS) detector (Tekran model-2500), where the amount of mercury passed through the sorbent was determined accurately. Mercury breakthrough for pulse injection tests has been previously defined⁷ as the amount of mercury which is not captured by the sorbent, usually described as a percentage of the mercury injected. The goal is to have a low mercury breakthrough (or high capture) value.

Calibrations were completed at each temperature by injecting a known volume of Hg⁰ saturated air, with a blank borosilicate glass tube containing quartz wool (no sorbent present). The test at each temperature was repeated several times to ensure repeatability of results. Three tubes (one blank, two samples) can be inserted into the GC oven for testing at each temperature. The materials used in constructing this experimental setup are all in Teflon, except the borosilicate glass tube.

3.2.3 Flue Gas Exposure Tests

The brominated biomass ash was exposed to real flue gases at a 375 MW Alberta power plant using the method described by Liu et al.⁷ The selected power plant was burning Alberta subbituminous coal, and the exposure point was upstream of the electrostatic precipitator (ESP). The duct gas temperature was approximately 130 °C at the time of analysis, with a velocity of 17.9 m/s. Raw biomass ash, brominated biomass ash, commercial activated carbon (Norit FGL) and commercial brominated activated carbon (Norit Darco HgLH) were all tested for mercury capture in the flue gases. A portion of each sorbent was separated into a sampling container

without being exposed to the field flue gases and used as the “field blank” sample. This “field blank” sample was tested for mercury content and compared with the sorbent exposed to mercury in the flue gases. The amount of mercury captured on the sorbent was determined by wet digestion of the samples followed by analysis using a PSA Millennium Merlin mercury analyzer based on the CVAFS principle.

3.2.4 Sorbent Characterization

Scanning Electron Microscope (SEM) and X-ray Photoelectron Spectroscopy (XPS) at the Alberta Centre for Surface Engineering and Science (ACSES) were used to characterize the sorbents. XPS analysis was conducted on the Br-Ash, Norit Darco HgLH and Raw Ash samples in order to compare bromine concentrations and carbon content in the sample. SEM analysis was also completed on the raw biomass ash before grinding, the brominated biomass ash and the commercial activated carbon sorbents. The sorbents were further characterized by measuring the BET surface area at the Integrated Nanosystems Research Facility (INRF) at the National Institute of Nanotechnology (NINT). Thermal Gravimetric (TG) analysis (also at INRF) was used to explore the stability of bromine loaded on the sorbents at high temperatures. X-ray Fluorescence (XRF) was conducted using an EDAX Orbis Micro-XRF to determine mineral content in the raw ash.

3.3. Results and Discussion

3.3.1 Surface Composition

Raw biomass ash as received (named Raw Ash), brominated ash (Br-Ash), and Norit Darco HgLH (Br-Norit) were analyzed by X-ray Photoelectron Spectroscopy at ACSES. The results in Figure 3.2 show a much higher surface concentration of bromine on the Br-Ash than on commercial brominated activated carbon. The concentration of bromine on Br-Ash was determined by XPS immediately after bromination and again after several months of storage. The results showed that the bromine on Br-Ash was very stable under storage conditions. The bromine on Raw Ash is below detection limit of XPS as anticipated. The oxygen content on these three samples is essentially the same, while the Br-Ash showed a slightly lower carbon content. The results of ultimate analysis in Table 3.1 show that the elemental composition of C,

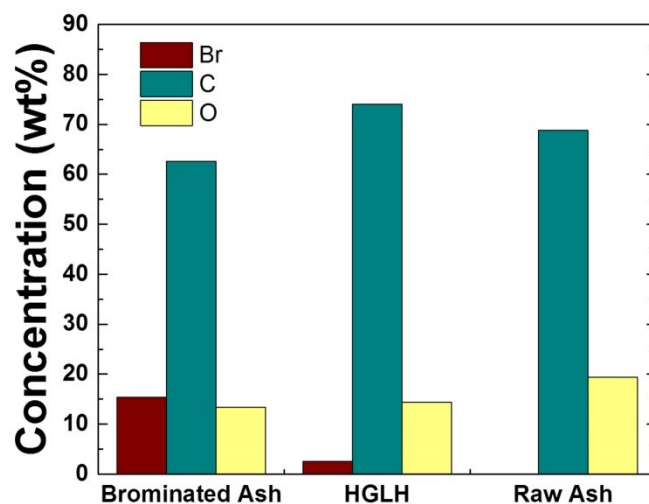


Figure 3.2. Comparison of XPS surface mass concentrations of interesting elements in brominated ash (Br-Ash), brominated activated carbon (Br-Norit), and Raw Ash (Raw Ash).⁸

Table 3.1. Ultimate analysis of Raw Ash and Br-Ash.

Sample	C (wt.%)	H (wt.%)	N (wt.%)	S (wt.%)
Raw-Ash	35.5 ± 2.4	0.4 ± 0.1	0.2 ± 0.2	1.0 ± 0.2
Br-Ash	29.7 ± 4.3	0.7 ± 0.1	0.2 ± 0.1	0.8 ± 0.2

H, N and S did not change significantly after bromination of the Raw Ash. XRF analysis on the raw ash (Table 3.2) indicated that in addition to the C, H, N, S, many other minerals including Ca, Fe, K, and Si are present in the sample.

3.3.2 Surface Morphology

BET surface area of the three sorbents were obtained after degassing at 200 °C and testing with equilibration time of 20 min. SEM images were also obtained to identify the role of surface morphology in mercury capture. Figure 3.3 shows surface morphology of all three samples at 2500× magnification. Compared with brominated and raw biomass ash, the surface of commercial Norit Darco HgLN appears to be rougher with many small particles, which likely contributes to a larger specific surface area. The particle size of the brominated ash appears to be

smaller than the Raw Ash, illustrating the reduction of particle size during the chemical-mechanical bromination process.

Table 3.2. XRF analysis of Raw Ash.

Element	wt.%	Element	wt.%
Mg	1.74 ± 0.04	Cr	0.10 ± 0.01
Al	1.72 ± 0.10	Mn	3.14 ± 0.11
Si	8.86 ± 0.27	Fe	13.12 ± 1.15
P	1.93 ± 0.06	Ni	0.05 ± 0.01
S	3.16 ± 0.15	Cu	0.11 ± 0.01
K	9.81 ± 0.09	Zn	0.61 ± 0.11
Ca	53.85 ± 0.91	Br	0.08 ± 0.02
Ti	1.38 ± 0.13	Sr	0.23 ± 0.08
V	0.08 ± 0.01	Total:	100

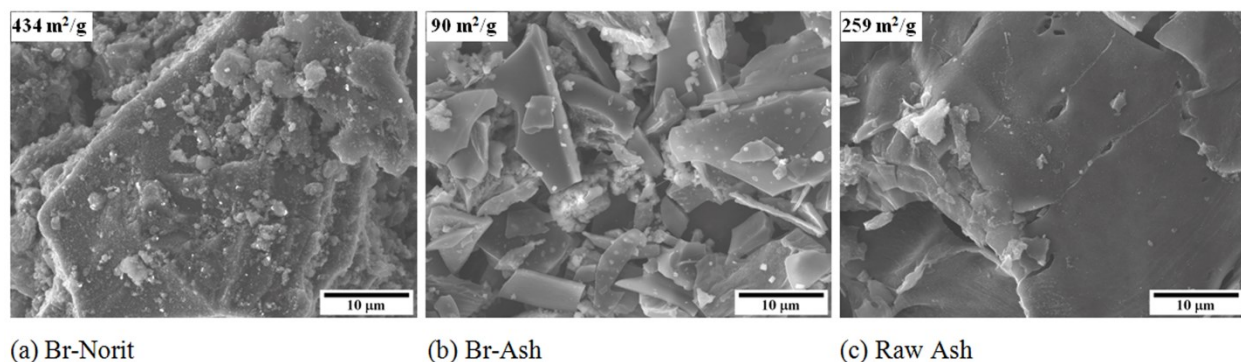


Figure 3.3. SEM micrographs and BET surface area values of commercial brominated activated carbon and biomass ashes.

At higher magnifications (90,000×), the images in Figure 3.4 show small pores of diameters ranging from 10 to 60 nm on the surface of both the Raw Ash and Br-Ash. According to the data provided by Norit, Darco HgLH contains pores of sizes ranging from 2 to 50 nm,¹⁰ which is in the similar range as pores of our biomass ashes. Comparison of images in Figure 3.4 reveals a different pore structure of the commercial Darco HgLH sorbent from that of the biomass ash.

The pores in Norit Darco Hg₂LH appear to be created by small cavities among the fine particles adhering on the large amorphous particles, while the pores in biomass ash are mainly in the form of pits.

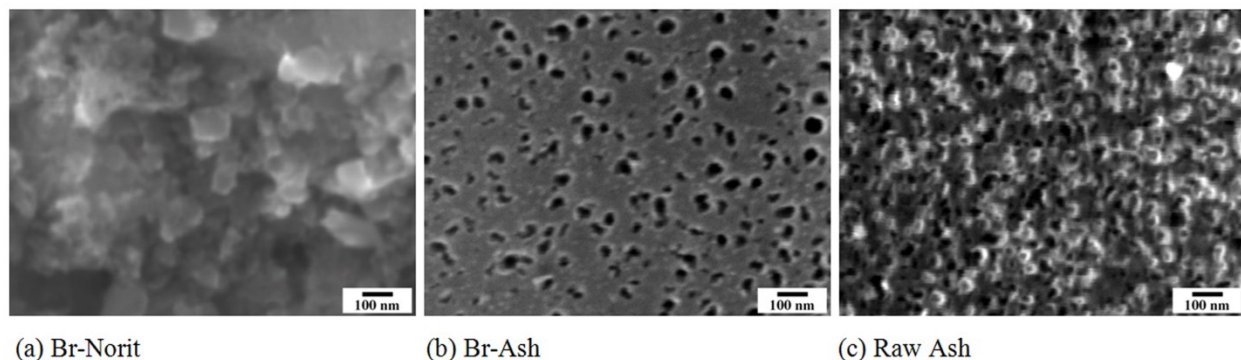


Figure 3.4. High resolution SEM micrographs of commercial brominated activated carbon and biomass ashes to show pore structures.

3.3.3 TG Analysis

TG analysis was completed for the Raw Ash and brominated ash (Br-Ash) samples by heating from room temperature up to 1000 °C at a heating rate of 10 °C/min with nitrogen as the neutral purge gas. The resulting weight loss and differential weight loss curves are shown in Figure 3.5. The differential curves in Figure 3.5 show a common peak for both the brominated ash and Raw Ash between 600 and 700 °C, indicating the release of some residual volatiles in and/or thermal decomposition product from the Raw Ash. It is interesting to note a difference in the slope change of TG profiles beginning at 750 °C between the raw and brominated biomass ashes, which appears as a peak on the differential TG curve of brominated biomass ash. This peak is attributed to the release of bromine from the brominated biomass ash, as the main difference between the two samples is that the Br-Ash is treated with bromine. The weight loss in this region was found to be approximately 17% for the Br-Ash, which is in an excellent agreement with the results of XPS analysis shown in Figure 3.2.

In order to investigate this further, TG isotherms were completed for the brominated ash sample at 650 °C and 800 °C in nitrogen purge gas. The samples were heated at a rate of 50 °C/min to and then held at the desired temperature for 5 h. Figure 3.6 shows the resulting TG isotherms at these two temperatures. The mass loss was much greater at 800 °C than at 650 °C

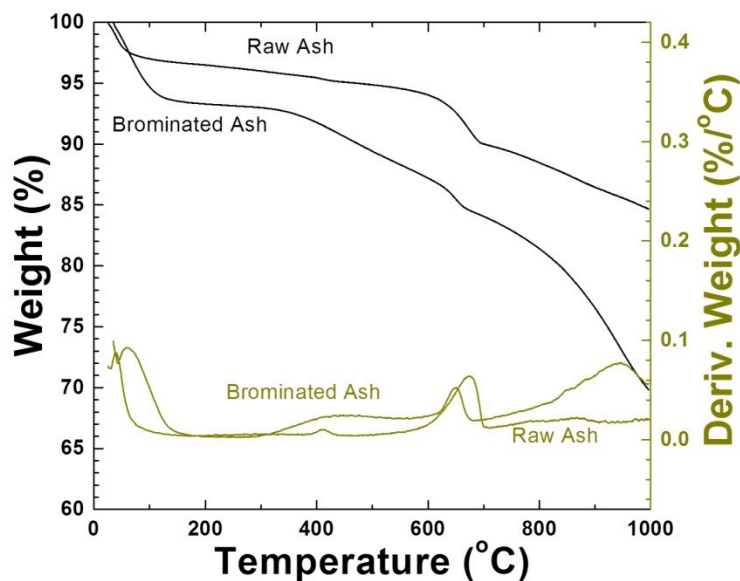


Figure 3.5. TG heating curves for Br-Ash and Raw Ash.

(approximately 12% more mass loss). The samples after the TG analysis were analyzed using XPS. The results in Table 3.3 show a limited loss of bromine (~20%) at 650°C, in contrast to an 80% bromine loss at 800°C. The XPS results support that the sharper slope change at 750°C seen on the TG curve of the brominated biomass ash in Figure 3.5 is due to the loss of bromine. The release of bromine from the brominated biomass ash at such high temperatures indicates that the bromine is tightly bound to the biomass ash surface and stable at high temperatures. Similar analysis was conducted on Br-Norit with the results shown in Table 3.4. The Br-Norit has 57% Br loss at 650 °C and 98% Br loss at 800 °C. The loss of bromine on Br-Norit is greater on a wt% basis than the Br-Ash indicating that the binding of Br on Br-Ash has a greater thermal stability.

The removal of Br at 750 °C found in the TG thermal profiles is likely not due to physisorption at such a high temperature. It is interesting to investigate further the binding of Br to the Br-Ash, causing a high thermal stability. Considering the wide XPS scan shown in Figure 3.7, calcium is one of the major elements in the Br-Ash along with C and O. The thermal decomposition of CaBr_2 has been studied in N_2 and O_2 atmospheres by Paulik et al.¹¹ In a N_2 atmosphere (the condition of the TG test in the current paper), CaBr_2 was found to melt at a

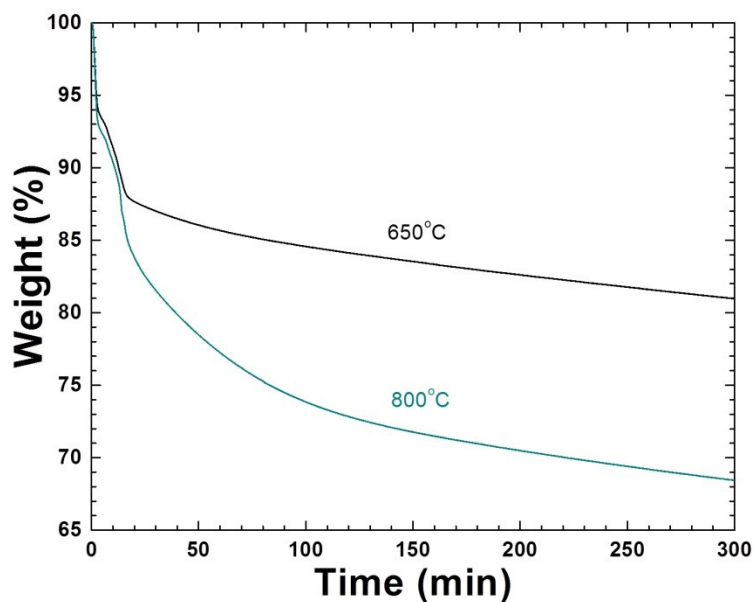


Figure 3.6. Isotherm curves of Br-Ash at two different temperatures.

Table 3.3. XPS results for Br-Ash treated at different temperatures.

Sample	Surface Bromine Concentration (wt.%)
Br-Ash (no heating)	13.0 ± 1.3
Br-Ash (heated at 650°C)	10.4 ± 1.0
Br-Ash (heated at 800°C)	3.0 ± 0.3

Table 3.4. XPS results for Br-Norit treated at different temperatures.

Sample	Surface Bromine Concentration (wt.%)
Br-Norit (no heating)	2.8 ± 0.3
Br-Norit (heated at 650°C)	1.2 ± 0.1
Br-Norit (heated at 800°C)	0.05 ± 0.01

temperature of 730°C then evaporate as $\text{CaBr}_{2(g)}$ at temperatures up to 1000°C, with no Br_2 liberation.¹¹ This temperature range is in excellent agreement with the peak seen in Figure 3.5 at 750 °C. Narrow scan XPS data were obtained to determine the calcium and bromine atomic concentrations, shown in Table 3.5. The difference between heating at 650 °C and 800 °C is 1.4 at.% Br and 0.9 at.% Ca, which, when considering experimental error can possibly show the removal of calcium bromide (CaBr_2) during the heating over this temperature range. Based on

the analysis by Paulik et al.¹¹ TG results in Figure 3.5 and XPS results in Table 3.5, some bromine appears to be bound on the biomass ash as CaBr_2 .

3.3.4 Mercury Capture Results

Laboratory mercury pulse injection tests were completed on the Raw Ash, brominated ash (Br-Ash) and commercial brominated activated carbon (Norit Darco Hg_{LH}, labelled Br-Norit). Capacity tests are considered less relevant to the application of powdered activated carbon

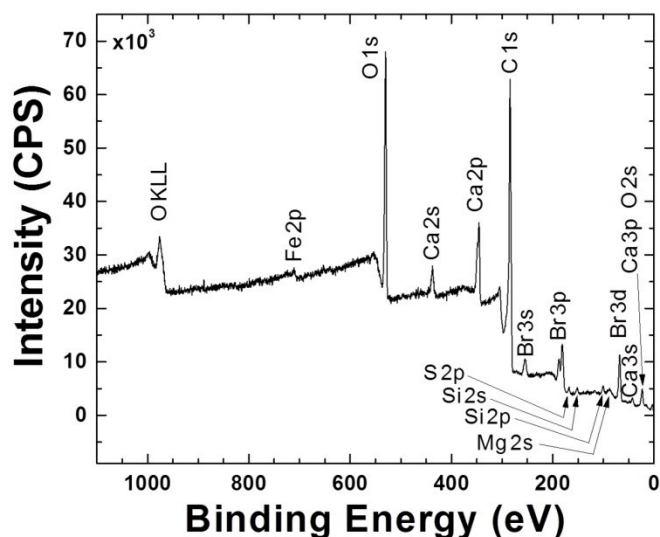


Figure 3.7. XPS survey scan of Br-Ash.

Table 3.5. XPS results for Br-Ash treated at different temperatures (at.%).

Sample	Surface bromine concentration (at.%)	Surface calcium concentration (at.%)
Br-Ash (no heating)	2.5 ± 0.3	3.7 ± 0.4
Br-Ash (heated at 650°C)	1.9 ± 0.2	3.0 ± 0.3
Br-Ash (heated at 800°C)	0.5 ± 0.1	2.1 ± 0.2

injection due to the short contact time available in the ESP and FF.¹² The short contact time in the mercury pulse injection tests should provide a better representation of the contact time for powdered sorbent injection. The results in Figure 3.8 show an almost complete capture of

mercury by the brominated biomass ash at temperatures as high as 390 °C. It is interesting to note that the brominated biomass ash performed as well as the commercial brominated activated carbon in mercury capture. In great contrast, the raw biomass ash shows very inefficient mercury capture at temperatures greater than 150 °C. The laboratory mercury capture tests indicate that brominated ash has a high potential as an effective sorbent for elemental mercury.

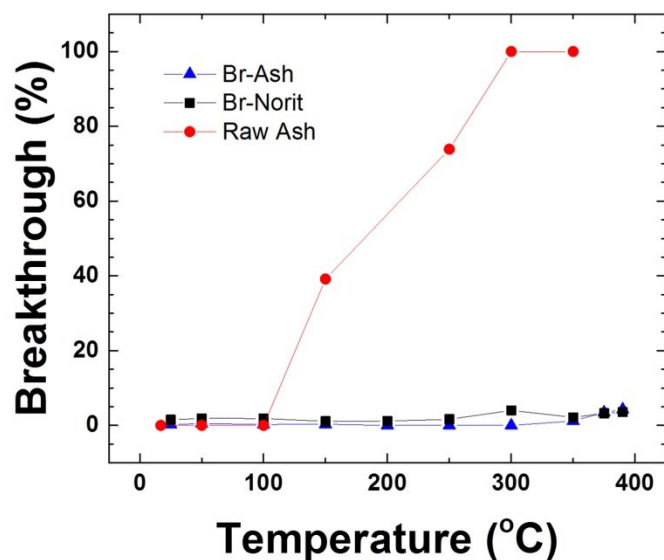


Figure 3.8. Results of mercury breakthrough as a function of capture temperature.

3.3.5 Flue Gas Exposure Results

Four different sorbents were exposed to flue gases for 5 min at a 375 MW power plant in Alberta, Canada. The sorbents tested included two commercially available sorbents: Norit FGD activated carbon (non-brominated, labelled ‘Norit’) and Norit HgLH (brominated activated carbon, labelled ‘Br-Norit’). The Raw Ash and brominated ash (Br-Ash) were also tested. The mercury content of these four sorbents before (“field blank” samples) and after the flue gas exposure is shown in Figure 3.9. After exposure to the real flue gases for 5 min, the brominated biomass ash gained much more mercury than the Raw Ash, showing effective capture of mercury from real flue gases of coal-fired power plants, confirming the results of laboratory tests. The overall Hg content in the brominated ash after the exposure was greater than that in the commercially available brominated activated carbon. However, the overall mercury gain on

sorbent mass basis was much greater for Norit Darco Hg_{LH} than for brominated biomass ash. It appears that the commercial brominated activated carbon is more effective in capturing mercury from flue gases. Such a difference is partially attributed to the lower initial content of mercury in the commercial brominated activated carbon than in the brominated biomass ash. The raw biomass ash has a high Hg content, most likely as a result of Hg adsorption during biomass combustion. The Br-Ash before flue gas exposure contains a higher Hg content, possibly as a result of mercury contained in liquid bromine that was used in bromination of biomass ash. The amount of mercury capture for each sorbent is therefore evaluated by the difference of mercury content on the sorbent before and after exposure of the sorbent to flue gases.

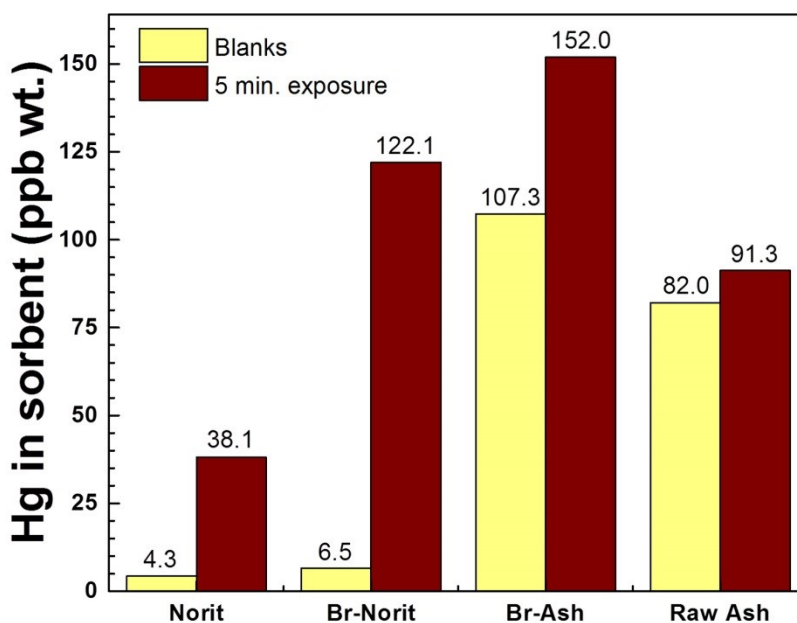


Figure 3.9. Mercury uptake by sorbents exposed to real flue gases of an operating power plant. The numbers above the bars are actual value of mercury uptake by sorbents.

It is interesting to note that considering more than four times of specific surface area of the commercial Br-Norit than Br-Ash (Figure 3.3), the amount of mercury gain by Br-Norit is rather comparable as by Br-Ash. Comparing the sorbents on a specific surface area basis, for example, the Br-Ash captured 2.0 ppb/m² surface area while the Br-Norit captured 0.27 ppb/m² surface area. Since a higher surface area of a sorbent is anticipated to capture a higher amount of mercury due to enhanced contact of the sorbent with the flue gases on surface area basis, it is

therefore more appropriate to compare the performance of mercury capture on specific surface area of sorbent rather than by total mercury capture capacity of the sorbent. Others have also observed that surface area alone cannot predict sorbent mercury capture performance.¹²

3.4. Conclusion

Mercury is a hazardous air pollutant present in high temperature flue gas streams. Powdered brominated activated carbon injection is one method of removing mercury from the hot flue gases. In this project, a novel procedure was introduced for bromination of biomass ash, which is normally considered a waste by-product of biomass combustion. With chemical-mechanical bromination, the bromine was found to be very stable on the biomass ash surface at high temperatures. The brominated biomass ash exhibited greatly improved mercury capture compared to the Raw Ash. Mercury capture of the brominated ash at high temperatures was found to be comparable to that of a commercially available brominated activated carbon sorbent. In a test with the exposure of the brominated biomass ash to flue gases in an operating power plant, the brominated ash captured much more mercury than the Raw Ash. On a specific surface area basis, the brominated biomass ash performed as well as the commercial brominated activated carbon. It remains to be resolved as to why high bromine loading on biomass ash does not contribute to high mercury capture. This raises a question as to how the larger amount of bromine is bound on biomass ash. TG tests in this paper have indicated the possibility that the bromine is bound as CaBr_2 . However, whether bromine bound on Br-ash as CaBr_2 plays a major role in mercury capture remains to be determined. The findings would be extremely valuable, as it would provide a scientific basis for calcium doping of biomass ash (with a low calcium content) during the bromination process to improve its ability to bind with bromine and enhance mercury capture. Further understanding the binding of bromine and mercury on brominated biomass ash would optimize bromination of biomass and lead to a commercial product applicable for high temperature mercury capture.

3.5. References

- (1) Berlin, M.; Zalups, R. K.; Fowler, B. A. Mercury. In: *Handbook on the Toxicology of Metals 3rd ed*; Nordberg, G. F, Fowler, B. A., Nordberg, M., Friberg, L. T., Eds.; Academic Press, Inc: USA, 2007, pp 675-719.
- (2) Keating, M. H.; Mahaffey, K. R.; Schoeny, R.; Rice, G. E.; Bullock, O. R.; Ambrose, R. B.; Swartout, J.; Nichols, J. W. Mercury Study Report to Congress, Volume I: Executive Summary, <http://www.epa.gov/ttn/caaa/t3/reports/volume1.pdf> (Accessed March 29, 2010).
- (3) Valupadas P. Alberta mercury regulation for coal-fired power plants. *Fuel Proc. Technol.* **2009**, *90*, 1339-1342.
- (4) Hutson, N. D.; Attwood, B. C; Scheckel, K. G. XAS and XPS characterization of mercury binding on brominated activated carbon. *Environ. Sci. Technol.* **2007**, *41*, 1747-1752.
- (5) Srivastava, R. K.; Hutson, N.; Martin, B.; Princiotta, F.; Staudt, J. Control of mercury emissions from coal-fired electric utility boilers. *Environ. Sci. Technol.* **2006**, *40*, 1385-1393.
- (6) Yang, H.; Xu, Z.; Fan, M.; Bland, A. E.; Judkins, R. R. Adsorbents for capturing mercury in coal-fired boiler flue gas. *J. Hazard. Mater.* **2007**, *146*, 1-11.
- (7) Liu Y.; Kelly, D. J. A.; Yang, H.; Lin, C. C. H.; Kuznicki, S. M.; Xu, Z. Novel regenerable sorbent for mercury capture from flue gases of coal-fired power plant. *Environ. Sci. Technol.* **2008**, *42*, 6205-6210.
- (8) Gupta, R. P.; Xu Z.; Clark, I.; Yang, H. Bromination process. United States Patent No. 20100126345, May 27, 2010.
- (9) Huber, M. L.; Laesecke, A.; Friend, D. G. The vapour pressure of mercury. National Institute of Standards and Technology <http://www.nist.gov/mml/properties/upload/NISTIR-6643.pdf> (Accessed February 3, 2012).
- (10) Norit. "Norit activated carbons for mercury removal from power plant flue gas", http://www.norit-america.com/pdf/Mercury_Removal_Power_Plants_rev5.pdf (Accessed March 29, 2010).

- (11) Paulik, F.; Paulik, J.; Buzágh-Gere, É.; Arnold, M. Examination of the decomposition of CaBr_2 with the method of simultaneous TG, DTG, DTA and EGA. *J. Therm. Anal.* **1979**, *15*, 271-277.
- (12) Pavlish, J. H.; Sondreal, E. A.; Mann, M. D.; Olson, E. S.; Galbreath, K. C.; Laudal, D. L.; Benson, S. A. Status review of mercury control options for coal-fired power plants. *Fuel Process. Technol.* **2003**. *82*, 89-165.

Chapter 4

Characterization of Mercury Binding onto a Novel Brominated Biomass Ash Sorbent by X-ray Absorption Spectroscopy

A version of this chapter has been published as:

Teresa M. Bisson, Lachlan C. W. MacLean, Yongfeng Hu, and Zhenghe Xu, *Environ. Sci. Technol.* 2012, 46, 12186–12193

4.1. Introduction

Mercury is a toxic substance that can be emitted to the environment through many natural and anthropogenic sources. A major source of airborne Hg in the environment is coal-fired power plants.¹ Mercury emitted from power plants by coal combustion could be in any form of elemental (Hg^0), oxidized and particulate-bound mercury.² Of these forms, Hg^0 is the most difficult to remove due to its insoluble nature in water. Once released to the environment, mercury can be transformed into methyl-mercury and bio-accumulated in the food-chain, resulting in human exposure.³ In humans, mercury poisoning causes significant neurological disorders and renal damage.³ Limiting release of mercury into the environment is therefore essential. Governments have recently established regulations to reduce the amount of mercury released in flue gases.^{1,4} In Alberta, Canada, for example, regulations developed to control industrial mercury emissions target desired mercury removal efficiencies up to 80%.⁴ To meet the strict government regulations, it is highly desirable to develop sorbents which can efficiently capture mercury while remaining economically feasible. Current approaches for Hg^0 removal mainly focus on the injection of activated carbon-based sorbents into the flue gas stream. High cost of activated carbon has led to a search for alternative sorbent materials,⁵ while continuing to

improve efficiency and reduce cost. In particular, brominated activated carbon has been proven to be effective at capturing mercury from coal-fired power plant flue gases.²

In searching for alternative materials to engineer low cost and highly efficient mercury sorbents, a novel chemical-mechanical bromination procedure was developed to impregnate biomass ash with liquid bromine.^{6,7} The biomass ash was chosen as it is a solid waste from biomass combustion with near zero value and wide availability. It also contains a significant portion of unburned carbon suitable for bromination, as practiced in engineering of brominated activated carbon. The resulting brominated biomass ash sorbent was shown to have good mercury capture efficiency, at a much lower cost due to the use of a waste product as the carbon material. Laboratory tests showed similar mercury capture performance by the brominated biomass ash (Br-Ash) as commercial brominated activated carbon (Norit Hg_{LH}, herein referred to as Br-NoritAC).⁶ A major difference between these two sorbents is much lower specific surface area and higher bromine content in Br-Ash than in Br-NoritAC, posing the question on the effectiveness and mechanism of mercury removal by Br-Ash. It is possible that the binding of bromine and mercury on the Br-Ash is different from that on Br-NoritAC, leading to different mercury capture mechanisms. Understanding the binding environment of Hg in the brominated biomass system will improve the design of more effective and lower cost mercury capture sorbents for abatement of mercury emissions from coal-fired power plants.

The binding mechanisms involved in Hg capture by a carbon sorbent are complex and depend on numerous factors, including the chemistry and temperature of flue gases, mercury speciation in the gas phase, and the type and concentration of active sites on the sorbent.⁸ In the case of Br-Ash, the effective capture of mercury is most likely associated with the oxidation of Hg⁰ by Br supported on carbon (up to 40%) in the ash. While Hg capture by carbon sorbents is recognized as a practical technique for mercury removal from flue gases, there have been few X-ray absorption spectroscopy (XAS) studies performed to elucidate the binding environment of Hg on carbon surfaces designed to adsorb mercury.⁸⁻¹⁰

X-ray absorption near edge spectroscopy (XANES) and Extended X-ray absorption fine structure (EXAFS) are powerful techniques in determining the oxidation state of mercury, the binding environment of mercury on the surface of a sorbent, and identifying its nearest atomic neighbours. Using XAS analysis, Huggins et al.^{9,10} showed that Hg⁰ was oxidized and bound to

anionic species (*e.g.* I, Cl, S or O) on the surface of various activated carbons. In addition, reaction temperature was found to play a key role in the mechanism and rate of mercury adsorption.⁹ Hutson et al.⁸ combined XAS with X-ray photoelectron spectroscopy (XPS) to determine the binding environment of Hg with both chlorinated and brominated activated carbons. They concluded that the elemental mercury in the flue gas was oxidized by surface-bound halide species, followed by the binding of the oxidized Hg to the surface halides. Reaction temperature was found to play a key role in the mechanism and rate of mercury adsorption on activated carbons.⁹ While these previous studies examined the mechanisms of Hg⁰ removal by Br-AC, the mechanism of Hg⁰ removal by Br-Ash has not been investigated, and the difference in Hg⁰ removal by Br-AC and Br-Ash has not been explained.

In this study, Hg L_{III}-edge XANES and EXAFS, along with Br K-edge XANES and S K-edge XANES are used to elucidate the bonding mechanisms involved in the capture of mercury by brominated biomass ash at two different temperatures. In addition, the results are compared with the bonding environment of Hg on a commercial activated carbon (brominated and non-brominated) to explain the difference in their Hg⁰ capture, enhancing our understanding of the binding mechanisms involved in mercury sorption on the brominated biomass ash sorbent.

4.2. Experimental Section

4.2.1 Sample Preparation

Raw biomass ash with a high carbon content (35.5 wt%) and high specific surface area (259 m²/g) was ball-milled prior to bromination, resulting in a close to normal particle size distribution of $d_{0.1} = 4.3 \mu\text{m}$, $d_{0.5} = 17.0 \mu\text{m}$, and $d_{0.9} = 53.4 \mu\text{m}$ ⁶. The raw ash was brominated using a novel chemical-mechanical bromination process described elsewhere.^{6,7} Commercial activated carbon, “Norit Darco Hg” (herein referred to as NoritAC) and brominated activated carbon, “Norit Darco Hg-LH” (herein referred to as Br-NoritAC) were purchased from NORIT Americas, Inc., Marshall, TX, and were used for comparison in this study. Elemental analyses of the Br-NoritAC and Br-Ash samples show a bromine content of 5% and 8%, respectively.

Further characterization of the Raw Ash, Br-Ash, and Br-NoritAC has been described elsewhere.⁶ Briefly, the ash was characterized by scanning electron microscopy (SEM) which showed the difference in surface morphology and pore structure of the ash samples compared to

activated carbon. Thermogravimetric (TG) analysis showed that the Br was stable on the Br-Ash at high temperatures up to 650°C. Combined with the results of x-ray photoelectron spectroscopy (XPS) analysis on surface compositions, it was suggested that the Br may be bound on the surface as CaBr_2 . Hg^0 pulse injection tests showed the improvement in Hg^0 capture by bromination of raw wood ash. The Br-Ash was able to capture a pulse of Hg^0 (2.0-3.3 ng) up to 390°C, with performance similar to the commercial sorbent Norit Darco Hg-LH.⁶ The present work aims at identifying binding mechanisms of mercury on various types of sorbents for the purpose of optimizing design of mercury capture sorbent.

4.2.2 Mercury Pulse Injection Test

Mercury pulse injection tests (also known as breakthrough tests) are useful for simulating the short contact time between the powdered injected carbon sorbent and the Hg^0 in a flue gas.⁵ The procedure for mercury pulse injection tests has been described in detail elsewhere.⁶ In summary, 40 mg of sorbent was placed in a borosilicate u-tube of 4-mm id. The u-tube was situated in a GC oven used to control the temperature at 100°C or 200°C. Downstream of the sorbent was a gold trap, which was used to pre-concentrate the Hg^0 by amalgamation. Two hundred μL of Hg^0 -saturated air at room temperature was injected upstream of the sorbent. After capture of Hg^0 by the sorbent, any remaining Hg^0 that passed through the sorbent was pre-concentrated on the gold trap. After 5 min, voltage was again applied to the heating coil to rapidly heat the gold trap and release the Hg^0 which was detected by a Tekran model-2500 cold vapor atomic fluorescence spectrophotometer (CVAFS). The amount of Hg^0 capture was reported as a percentage of the mercury injected, based on calibrations performed on a blank u-tube using the same procedure.⁶

4.2.3 Mercury Loading Test.

The Br-Ash (BA), was exposed to elemental mercury along with NoritAC (NAC) and Br-NoritAC (BNAC) using the experimental setup shown in Figure 4.1. A peristaltic pump was used to move air at a flow-rate of 6 L/h. The air, after contacting the mercury ball, carried the elemental mercury to the sorbent, which was placed inside a GC oven in order to control the mercury capture temperature. Each sorbent was tested at 100°C (BA100, BNAC100, NAC100). For comparison, the brominated ash was also tested at 200°C (BA200). A sample was taken

from each tested sorbent for mercury concentration analysis using a Milestone Direct Mercury Analyzer (DMA-80). After exposure, each sample was collected and transported to the Canadian Light Source (CLS) for analysis.

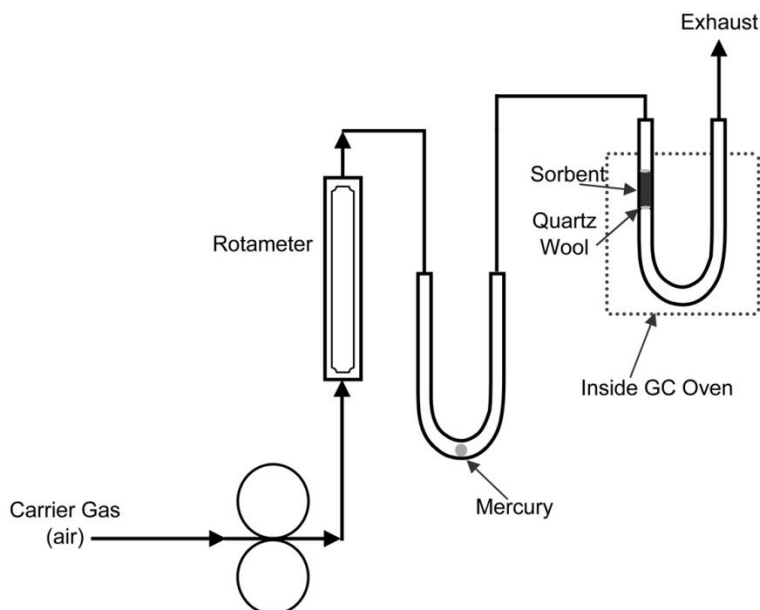


Figure 4.1. Schematic for loading of elemental mercury onto sorbents.

4.2.4 X-ray Fluorescence (XRF) Spectroscopy

Elemental fluorescence spectra were collected on the Soft X-ray Micro-Characterization Beamline (SXRMB) at the Canadian Light Source, Saskatoon, Canada, which has an energy resolution ($E/\Delta E$) of 10^4 .¹¹ An energy-resolved Si(Li) drift detector (Princeton Gamma-Tech) was used to collect XRF spectra at an excitation energy of 2605 eV. Each powder sample was spread evenly (several micrometers thick) onto a carbon tape, mounted onto a copper substrate and placed inside the sample chamber under vacuum.

4.2.5 X-ray Absorption Spectroscopy (XAS).

All XAS measurements were performed at room temperature at the Canadian Light Source synchrotron facility in Saskatoon, Canada, under standard operating conditions of 2.9 GeV and 250 mA beam current. The Br K-edge XANES and Hg L-edge XANES and EXAFS were performed on the Hard X-ray Micro-Analysis (HXMA) beamline using a Si(111) double-crystal

monochromator with Rh coated mirror and an unfocused beam size of ~ 1.0 mm x 3.0 mm, detuned by $\sim 50\%$ to eliminate higher-order harmonics. The dry sorbent samples were loaded into sample holders with Kapton windows and analyzed in both transmission and fluorescence modes. The transmission spectra were collected using 1 atm nitrogen gas-filled ionization chambers. Fluorescence spectra were obtained with a Canberra 32 element array Ge solid-state detector. Multiple scans were collected to monitor radiation induced chemical effects, but none were found in any sample.

The S K-edge XANES was performed on the SXRMB using a Si(111) double-crystal monochromator with the higher-order harmonics rejected with Pt-coated mirrors. Samples were spread onto a carbon tape, attached to a copper sample holder and placed under vacuum for analysis with total electron yield (TEY).

4.2.6 XAS Data Analysis.

All XANES data were processed in the Athena program^{12,13} except for sulfur, which was processed in OriginPro 8.1 (OriginLab Corporation). Each spectrum was normalized and averaged over the multiple scans of each particular element.

The EXAFS data were processed with the ATHENA program^{12,13} using standard procedures. Briefly, the EXAFS spectra were extracted from the measured data using the AUTOBK algorithm.¹⁴ This isolated $\chi(k)$ data was analyzed using the ARTEMIS program.^{12,13} Theoretical standards were computed from crystallographic data using Feff6,¹⁵ parameterized using ARTEMIS and fitted to the data using a Levenburg-Marquardt non-linear minimization.

4.3. Results and Discussion

4.3.1 Mercury Pulse Injection Test

The Hg⁰ pulse injection test allows evaluation of mercury capture by an adsorbent over a short contact time⁵. These tests do not measure the absolute capacity of mercury capture, but provide a sensitive method to evaluate the effect of temperature on Hg⁰ capture under the conditions close to practical application scenario. As shown in Figure 4.2, all four sorbents had good performance at 100°C, with almost all of the mercury being captured. At 200°C both sorbents containing bromine (Br-Ash and BNAC) continued to show excellent mercury capture

efficiency, while the mercury capture by NAC was slightly reduced to 88%. The mercury capture by the Raw Ash at 200°C was significantly reduced to only 16%. The presence of Br in the Br-Ash seems to play an integral role in the capture of Hg^0 , especially at elevated temperatures. One possible explanation for this difference is a physisorption mechanism for the Raw Ash compared to chemisorption for the Br-Ash due to the oxidation of the Hg by Br.¹⁶ It should be noted that the complete mercury capture by NAC determined at 100°C in this study agrees well with the results reported by Seneviratne et al.³² for the case after continuous exposure at 100°C for 1 hr in an inert atmosphere. In contrast to a 90% capture at 200°C in our study, a much lower mercury capture of 10% by NAC was reported by Seneviratne et al. This significant difference is attributed to very different test method used in the work by Seneviratne et al. from our pulse injection method which is more representative to the contact time of sorbent with flue gases in real sorbent injection practice. The continuous injection of mercury in the study by Seneviratne et al. leads to a total exposure of approximately 240 ng of Hg^0 , as compared to a much lower value of approximately 2-3ng in our tests. The prolonged exposure over 1 hr of the sorbent to a higher amount of mercury as in the study by Seneviratne et al. would result in a lower overall mercury capture efficiency.

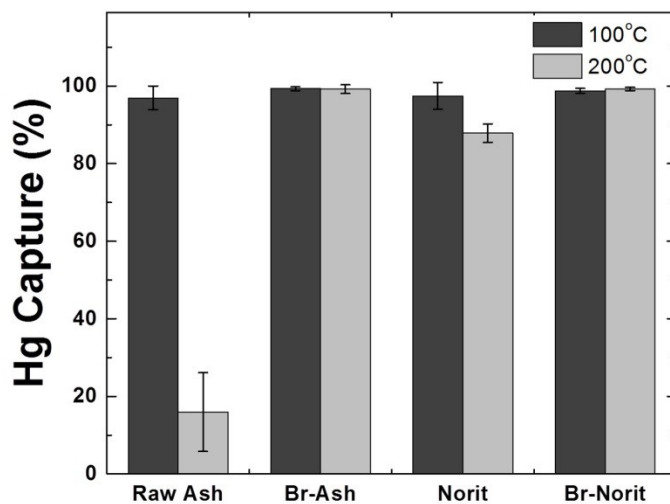


Figure 4.2. Capture of Hg^0 by various sorbents in pulse injection tests.

4.3.2 Mercury Loading

To investigate Hg^0 capture mechanisms by various sorbents, Hg^0 was loaded onto each sorbent at 100°C and also at 200°C for Br-Ash. This range of temperatures covers the typical operating range upstream of particulate control devices, which can range from approximately 150-175°C.¹ The resulting sorbents were measured for total mercury concentration, with the results shown in Figure 4.3. In the first test, the Br-Ash at 200°C (BA200) captured much less mercury over the 40-h time period than the Br-Ash at 100°C (BA100), showing the negative impact of increased temperature on mercury capture by Br-Ash, possibly due to a different mercury capture mechanism. The Raw Ash data are not shown in Figure 4.3, as it became saturated (100% breakthrough) after only 1 h at 100°C, with Hg concentration too low to obtain good XAS spectra (116 ppm Hg). The Brominated NoritAC (BNAC100) exhibited a much higher amount of mercury captured than the non-brominated NoritAC (NAC100). When considering the results of the Hg^0 loading test, it should be noted that this is an idealized system in regard to gaseous constituents to simplify the interpretation of the results for the purpose of studying binding mechanisms of mercury and the role of bromine in mercury capture. In the actual flue gas atmosphere, the amount of mercury capture by the adsorbents can be affected by the presence of other flue gas constituents such as SO_2 , NO, HCl and H_2S .

As the initial loading test did not produce sufficient sample for the subsequent analysis, a second set of Br-Ash with loaded mercury at 100°C and 200°C was produced and is labeled in Figure 4.3 as BA100* and BA200*, respectively. The mercury concentration of the second set of Br-Ash samples differed from the first set as the Hg^0 exposure time was reduced, *i.e.* it had less Hg in the sample. However, when analyzing the sorbents using XANES it was determined that the Hg XANES structure remained the same although the Hg^0 concentration had changed which suggests the same capture mechanism.

4.3.3 X-ray Fluorescence Spectroscopy

X-ray fluorescence (XRF) spectra were collected on each of the four samples (BA100, BA200, NAC and BNAC) in order to determine the relative abundances of sulfur, bromine, and any other elements present in each sample. Each XRF spectrum was normalized to the elastic scattering peak at 2605 eV. The X-ray fluorescence spectra in Figure A1 in Appendix A show a

much higher phosphorous and bromine species on the BA samples than on both the NAC and BNAC samples. In addition, BA100 seems to have more Br than BA200, indicating some loss of Br at 200°C during the mercury loading test. Both BA samples had similar concentrations of sulfur, indicating negligible loss of sulfur at higher temperature of 200°C. Overall, the Norit activated carbon (NAC and BNAC) samples contained significantly more sulfur species than Br-Ash (BA100 and BA200) samples. It is also interesting to note that the NAC contained more sulfur than the BNAC.

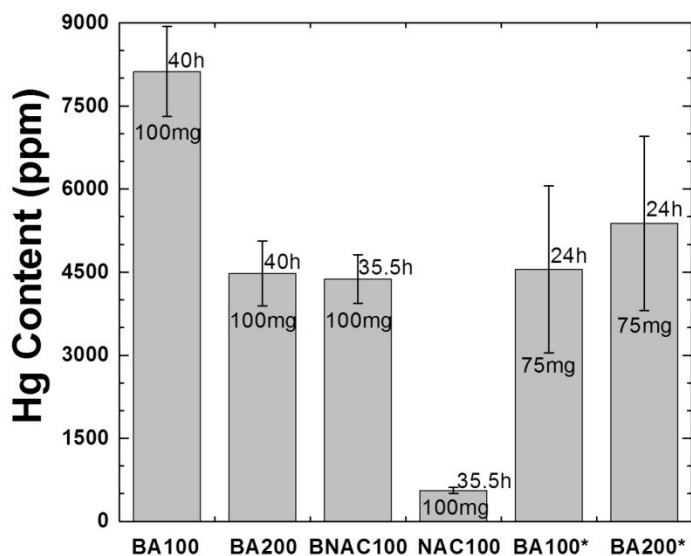


Figure 4.3. Hg concentration of sorbents after exposure to elemental mercury, along with test duration and sorbent mass (*indicates second set of BA samples prepared for further analysis).

4.3.4 S K-edge XANES

The amount and type of sulfur on the sorbents may have a substantial effect on mercury sorption chemistry. For example, studies examining mercury binding to organic matter have shown that mercury prefers to bind first to reduced sulfur species, and then to oxygen groups only after the reduced sulfur groups become saturated.^{17,18} Thus, understanding the sulfur speciation on the carbon samples is an important step in understanding the mercury binding to these samples. The results of the S K-edge XANES measurements in Figure 4.4 show the differences in the S species among the four samples. Both Ash samples contain only oxidized

sulfur species (sulfur in sulfate, SO_4^{2-} at ~ 2481.5 eV). In contrast, the NAC and BNAC samples contain both sulfate and a reduced sulfur species (S^{2-} at ~ 2472 eV) which may be inorganic sulfide or a reduced organosulfur species.

The inset in Figure 4.4 shows a comparison between S K-edge XANES spectra of the Br-NoritAC sample before and after the exposure of Hg, and the NoritAC sample with Hg exposure (NAC). There are two distinct reduced sulfur peaks in this energy region: 2472 eV and 2473 eV. We can see that the peak at 2472 eV is of a higher intensity in the spectrum of the brominated samples (BNAC) than in the spectrum of the nonbrominated sample, likely due to a Br-S coordination as suggested by Cotte et al.¹⁹ As expected, the nonbrominated sample (NAC) had a lower Br-S peak than the brominated samples (BNAC). Interestingly, the brominated sample with Hg (BNAC) has a lower intensity peak at 2472 eV than the BNAC sample without Hg loading. This finding suggests that mercury is outcompeting the Br for that particular reduced sulfur species and thus reducing the intensity of the peak at 2472 eV. The peak at 2473 eV in all three samples appears to be of the same intensity and thus not influenced by Hg addition. The presence of reduced sulfur groups in the NoritAC samples and the observed reduction in the intensity of the Br-S peak at 2472 eV in the presence of Hg suggests that Hg is bound to a reduced sulfur group in the NoritAC samples, although whether the reduced S is an organic or inorganic species cannot be discerned. The Norit AC samples are derived from a Texas lignite coal^{29,30} which is also likely the main source of the sulfur species on the AC. The sulfur content in Texas lignite coal has been shown to be in the form of pyrite, sulfide, thiophene, sulfone and sulfate³¹.

4.3.5 Hg L_{III} -edge XANES

The Hg L_{III} -edge XANES spectra and the first derivative ($d(\text{Abs})/dE$) of the XANES spectra for each Hg-adsorbed sample are shown in Figure 4.5 (a) and (b), respectively. BA100 and BA200 show similar XANES spectra, indicating similar bonding geometry of Hg on Br-Ash at two different temperatures of 100°C and 200°C. However, there is a clear difference in the XANES spectra between the BA and NAC/BNAC samples. Both the NAC and BNAC samples exhibit a clearly visible shoulder on the rising edge of the XANES spectra, which is not present on the spectrum of the BA samples, suggesting different mercury bonding environments between

the Br-Ash, NoritAC and Br-NoritAC samples. Interestingly, the XANES spectra of the NAC and BNAC are similar, suggesting a similar Hg bonding environment, even though the Hg^0 uptake was significantly different (Figure 4.3).

The derivative of the Hg L_{III}-edge XANES spectra has been used by many researchers to interpret Hg bonding,²⁰ including Hg binding with activated carbon.⁸⁻¹⁰ In Figure 4.5 (b), each spectrum of bound mercury has two main inflection points, which is indicative of oxidized Hg species, in contrast to only one peak for Hg^0 .²⁰ This finding suggests that the elemental mercury

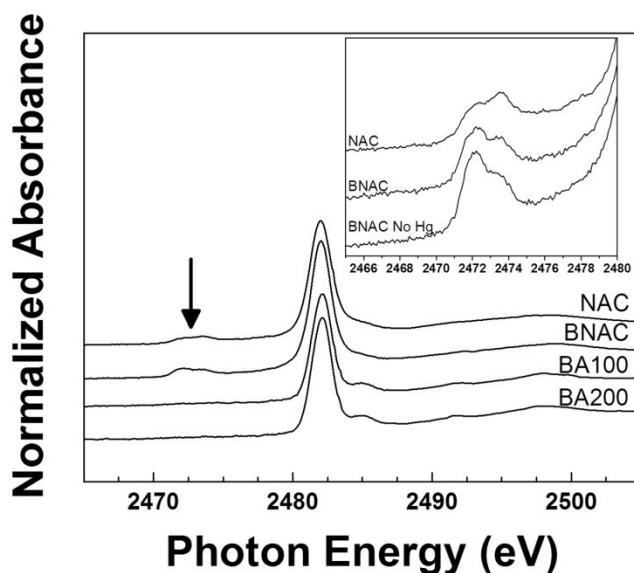


Figure 4.4. Sulfur K-edge XANES spectra for the carbon sorbents. The black arrow denotes the reduced sulfur group ($E_0 = 2472$ eV). Inset: Sulfur K-edge XANES spectra for the commercial activated carbon sorbent before (top) and after (bottom) exposure to Hg flue gas demonstrating a change in the bonding electronic structure of the reduced sulfur peaks with the addition of Hg.

has been oxidized during the experiment, most likely by the addition of Bromine on the sorbents.⁸

The energy difference ΔE (eV) between the two inflection peaks, termed by Huggins et al.¹⁰ as the inflection point difference (IPD) has been shown to provide a good approximation of the relative contributions of ionic or covalent bonds present in the Hg coordination environment.^{8-10,21} A large difference in energy between the two inflection points is indicative of

a more ionic contribution in the bond. Conversely, a small energy difference between the two derivative peaks is indicative of a more covalent bonding character.²⁰ In this study, IPD values are used only qualitatively as a guide to support our EXAFS models.

Figure 4.5 (b) shows that the NAC and BNAC samples have IPD values of 7.5 eV and 7.4 eV, respectively, correlating well with an ionic Hg-S bond seen by others.^{10,21} The two main peaks in the Br-Ash spectra have lower IPD values of 5.6 eV and 6.6 eV for BA100 and BA200, respectively. The lower IPD values, which are closer to the values of Hg-C, Hg-I and Hg-Se bonds reported by Huggins et al.,¹⁰ indicate more covalent bonding of Hg with Br-Ash. While additional factors may contribute to the observed IPDs²⁰ in the Hg derivative XANES data, this information can be used qualitatively to help constrain our EXAFS models (below) in order to determine the local geometry around the Hg atoms in each bonding environment.

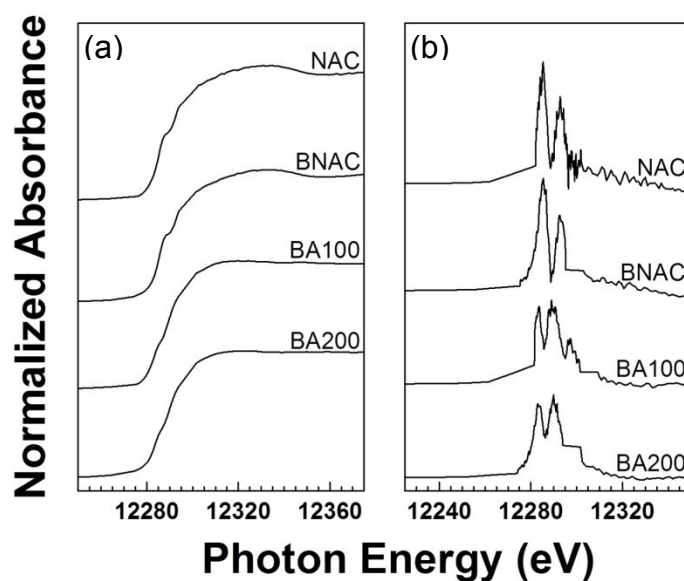


Figure 4.5. (a) Mercury L_{III} -edge XANES spectra for the carbon sorbents ($E_0 = 12,284$ eV), (b) First derivative of the mercury L_{III} -edge XANES spectra for the carbon sorbents ($E_0 = 12,284$ eV).

4.3.6 Hg EXAFS

Mercury L_{III} -edge EXAFS spectra (k_2 -weighted chi data) are shown in Figure 4.6 (a), with the real part of the Fourier transforms shown in Figure 4.6 (b). To better understand the bonding

environment around the Hg atom in both the BA, NAC and BNAC samples, least-square fitting analysis was performed between model data and theoretical spectra using the software program Artemis.^{12,13} The results of the Hg EXAFS measurements are shown in Table 4.1 and the fits to the data are shown in Figure 4.6. The nonbrominated ash sample (not shown) had little Hg associated and was below the detection limit of XAFS.

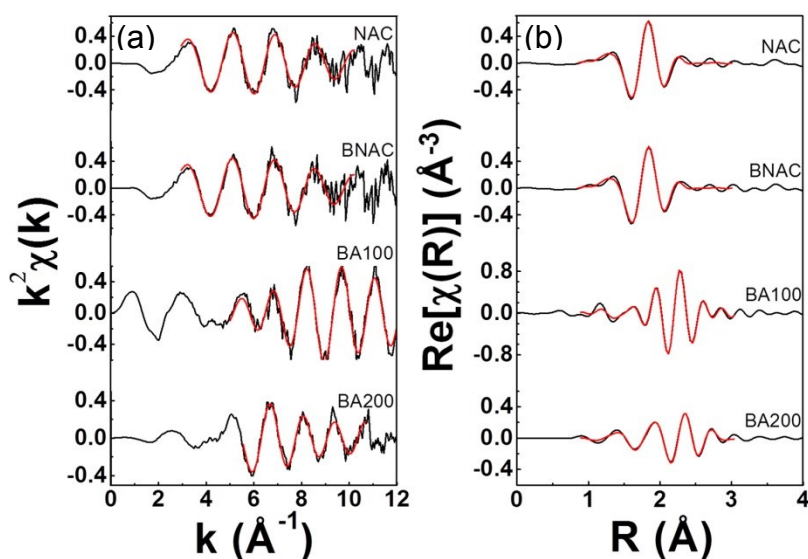


Figure 4.6. (a) Mercury L_{III}-edge EXAFS chi spectra for the carbon sorbents. Black line is the sample spectra and red line is the best fit to the data. (b) Mercury L_{III}-edge EXAFS real-space Fourier transforms for the carbon sorbents. Black line is the sample spectra and red line is the best fit to the data.

The best fit models for the EXAFS data of both Br-Ash samples are an Hg-C/O/N species and also an Hg-Br coordination environment (Table 4.1; Figure 4.6). EXAFS cannot distinguish between two elements within ~3-5 atomic numbers. As a result, we cannot determine from the EXAFS data whether the first shell is C, O or N. However, we can use complementary data to identify the scatterer. The smaller IPD values observed in the derivative XANES spectra (Figure 4.5 (b)) suggest that Hg is likely bound covalently to carbon not to oxygen. The coordination number of both Hg-C and Hg-Br paths was restrained in order to achieve the best fit to the data, based on comparison of the reduced χ^2 between EXAFS fits. The differences between the Hg-C

distances between the BA100 and BA200 (Table 4.1) suggest that the higher-temperature exposure of BA200 may have induced structural changes to the BA that resulted in changes to the Hg binding environment. This change is also reflected by the differences in IPD between BA100 and BA200 (5.6 eV and 6.6 eV, respectively)

The presence of Hg coordination with Br suggests that for the BA samples, the Br is intimately associated with the sorption of Hg to the ash sample – possibly as a separate Hg-Br species. This speculation would be in agreement with the data shown in Figure 4.2 and also in the earlier sorption tests using nonbrominated and brominated activated carbon.⁸ In their study, Hutson et al.⁸ suggested that mercury was bound to the carbon at the bromine sites through surface-enhanced oxidation of the Hg⁰ and subsequent binding with either surface bromine or sulfate species. In our model we have Hg-Br coordination but no subsequent binding with sulfur in either our EXAFS fitting of the Hg L_{III}-edge nor in our S K-edge XANES experiments (Figure 4.4). However, we do see binding of Hg-C, which makes up a good portion of the Br-Ash sample. This finding in combination with the differences in energy of the two inflection peaks of the XANES derivative data (Figure 4.5 (b)) suggests that Hg is bound to a carbon species and associated with surface-bound Br.

The least-square fitting results of the EXAFS data give the best fit for mercury to bind with the sulfide in the NAC and BNAC systems (Table 4.1; Figure 4.6). The Fourier transform of the EXAFS data shows only one peak indicative of Hg-S bond. This fit is supported by the presence of reduced sulfur species present in the S K-edge XANES data shown in Figure 4.4 and by the difference in the reduced sulfur peaks in the pre- and post- mercury exposure (Figure 4.4 – inset). Since only one atomic coordination shell is present in the Fourier transform, it is too difficult in EXAFS modeling to determine the type of reduced sulfur species bound to the Hg.²⁴ The Hg-S distance of 2.29 Å compares favorably with the results by Lennie et al.²⁵ who found Hg-S bond distances in the range of 2.28 to 2.31 Å in their study of inorganic HgS complexes in solution by EXAFS analysis. In addition, the coordination numbers for sulfur are both approximately equal to 2, as reported for Hg-S complexes seen by others.^{17,24,25}

4.3.7 Br K-edge XANES

Br K-edge XANES data were collected at the Br K-edge in order to determine whether the interaction modes between Br and the carbon samples and/or Br-Hg signal can be determined. The Br XANES data in Appendix A (Figure A2) show little variation between each spectrum. These results suggest that the bonding environment for Br in all these three samples is similar. No evidence of Hg-Br bonding can be seen from the Br absorption edge, most likely due to the fact that majority of Br is not associated with Hg, similar to the result found by Hutson et al.⁸

4.3.8 Implications for Hg Capture

Hard/Soft Acid-Base (HSAB) theory has been generally accepted in chemistry for determining the preference of species to bond together.^{26,27} This theory states that soft acids such as mercury will have a high affinity for soft bases such as reduced sulfur ligands and therefore

Table 4.1. Mercury L_{III}-edge EXAFS fitting results for Hg mercury bound to carbon sorbents.^a

Sample	k range (Å)	Path	CN	R(Å)	$\sigma^2(\text{Å}^2)$	ΔE (eV)	R-Factor
BA100	5.0 – 12	Hg-C	2.0 ^{b,c}	1.947 ± 0.013	0.007	6.866	0.0056
		Hg-Br	2.0 ^{b,d}	2.539 ± 0.007	0.002		
BA200	5.5 – 10.5	Hg-C	2.0 ^{b,c}	2.204 ± 0.07	0.005	6.16	0.0185
		Hg-Br	2.0 ^{b,d}	2.608 ± 0.04	0.006		
BNAC	3 – 10	Hg-S	2.376 ± 0.40	2.296 ± 0.013	0.0049	-3.197	0.0174
NAC	3 – 10	Hg-S	2.471 ± 0.47	2.293 ± 0.015	0.0050	-2.862	0.0207

^a CN is the coordination number, R is the Hg-X bond length, σ^2 is the Debye-Waller factor, and ΔE is the energy shift, ^bCoordination number constrained to crystallographic values, ^cCrystal structure model from HgC₂, ²² ^dCrystal structure model from HgBr₂.²³

preferentially bind with them.^{26,27,28} The relative hardness or softness of the species will give an indication whether or not the other species will preferentially bond. In the case of Br⁻ as compared with S²⁻ and SO₄²⁻, the order of increasing hardness is S²⁻ < Br⁻ < SO₄²⁻, where S²⁻ is a

soft base, Br^- is a borderline base and SO_4^{2-} is a hard base.^{26,27} As mercury is a soft acid, it will preferentially bond to the reduced sulfur, then the bromide, with little affinity to SO_4^{2-} . This is the reason why no coordination of mercury with S was seen in the Br-Ash samples, as they contained S only in the form of SO_4^{2-} . Without reduced S, the mercury preferred to coordinate with the Br^- in the Br-Ash samples. Based on the current study, adding reduced sulfur species to the Br-Ash samples may help improve their mercury capture capability, and potentially reduce the amount of Br required on the Br-Ash surface.

The capture mechanism of Hg has recently been studied by Wilcox et al.¹⁶ who applied XPS analysis and density functional theory calculations on the same NoritAC samples used in this study. Their study concluded that Hg^0 was removed from the gas stream most likely by oxidation of Hg^0 by surface bound Br (similar to the mechanism proposed by Hutson et al.⁸) and subsequent binding of the oxidized Hg species on the carbon surface. In the current study, the oxidized Hg species were determined to be associated with reduced sulfur on both the Norit activated carbon and Br-Norit activated carbon. Considering our findings in light of the results from the study by Wilcox et al.¹⁶, it appears that the mechanism of Hg removal by the Br-Norit activated carbon involves oxidation of the Hg species by Br on the AC surface, followed by binding of the oxidized Hg to the reduced sulfur species, as opposed to Hg binding to halide or sulfate species proposed by Hutson et al.⁸ and Huggins et al.⁹ Compared with Norit nonbrominated activated carbon, adding Br resulted in an improved Hg^0 removal, and a higher Hg loading on the sorbent as was seen in Figures 4.2 and 4.3. The proposed mechanism for Br-Norit is illustrated in Figure 4.7.

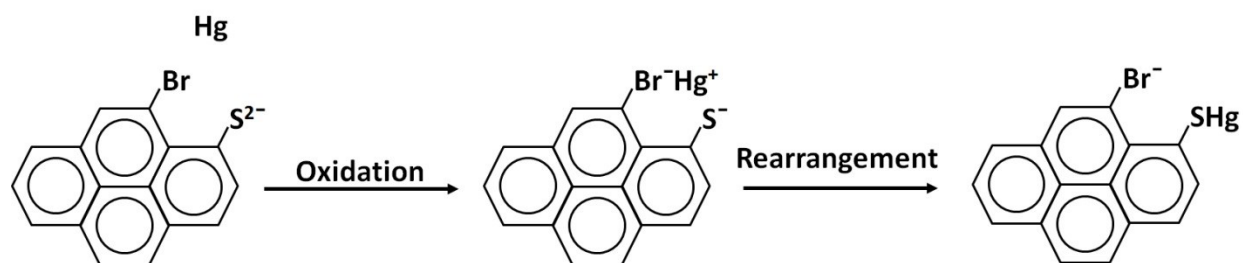


Figure 4.7. Illustration of proposed mechanism of Hg^0 capture by Br-Norit commercial AC. Fused rings represent carbon in Br-Norit.

In contrast, Hg found on the brominated biomass sorbents (BA100 and BA200) was bound to carbon and bromine sites. The difference in Hg^0 removal efficiency between Br-Ash and Raw Ash can be explained in a fashion similar to the Br-Norit and Norit activated carbons. The Hg capture mechanism appears to be enhanced oxidation of mercury by Br on the surface with subsequent binding of oxidized mercury to carbon near the Br, and is illustrated in Figure 4.8. Other studies have used Density Functional Theory to determine mercury removal mechanisms, and predicted that interaction between Br bonded to an edge C atom improves the stability of Hg.³³ Liu et al.³⁴ also found that Hg^0 adsorption was preferred on C atoms neighboring Br on the activated carbon due to a charge transfer mechanism. Both of these theoretical studies further support our findings and the mechanism suggested for Br-Ash. The differences seen in the first shell distances of Hg-C for the Br-Ash samples suggest a structural rearrangement in the carbon sorbent as the temperature of the experiment increased from 100°C to 200°C, which may influence the amount of Hg taken up by each of the biomass ash sorbents at different temperatures. HSAB theory analysis provides a direction for further improving mercury capture by incorporating soft base S^{2-} on Br-Ash.

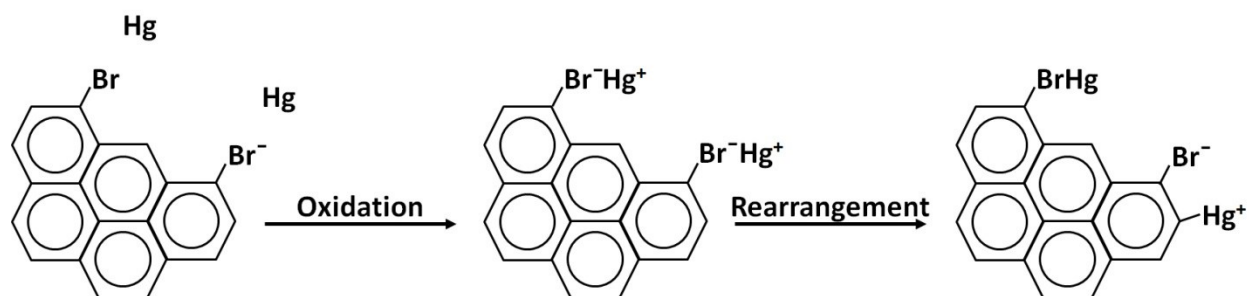


Figure 4.8. Illustration of proposed mechanism of Hg^0 capture by Br-Ash sorbent. Fused rings represent carbon in wood ash.

4.4. References

- (1) Srivastava, R. K.; Hutson, N.; Martin, B.; Princiotta, F.; Staudt, J. Control of mercury emissions from coal-fired electric utility boilers. *Environ. Sci. Technol.*, **2006**, *40*, 1385-1393.
- (2) Yang, H.; Xu, Z.; Fan, M.; Bland, A.E.; Judkins, R.R. Adsorbents for capturing mercury in coal-fired boiler flue gas. *J. Hazard. Mater.*, **2007**, *146*, 1-11.
- (3) Berlin, M.; Zalups, R. K.; Fowler, B. A. Mercury. In *Handbook on the Toxicology of Metals*, 3rd ed; Nordberg G. F.; Fowler B. A.; Nordberg M.; Friberg, L. T., Ed.; Academic Press, Inc: USA, **2007**; pp 675-719.
- (4) Valupadas, P. Alberta mercury regulation for coal-fired power plants. *Fuel. Proc. Technol.* **2009**, *90*, 1339-1342.
- (5) Liu, Y.; Kelly, D. J. A; Yang, H.; Lin, C. C. H; Kuznicki, S. M.; Xu, Z. Novel regenerable sorbent for mercury capture from flue gases of coal-fired power plant. *Environ. Sci. Technol.* **2008**; *42*, 6205-6210.
- (6) Bisson, T. M.; Xu, Z.; Gupta, R.; Maham, Y.; Liu, Y.; Yang, H.; Clark, M.; Patel, M. Chemical-mechanical bromination of biomass ash for mercury removal from flue gases. *Fuel.* **2013**, *108*, 54-59.
- (7) Gupta R. P.; Xu Z.; Clark I.; Yang H. Bromination process. United States Patent No. 20100126345.
- (8) Hutson, N. D.; Attwood, B. C.; Scheckel, K.G. XAS and XPS characterization of mercury binding on brominated activated carbon. *Environ. Sci. Technol.* **2007**, *41*, 1747-1752.
- (9) Huggins, F. E.; Huffman, G. P.; Dunham, G. E.; Senior, C. L. XAFS examination of mercury sorption on three activated carbons. *Energy Fuels* **1999**, *13*, 114-121.
- (10) Huggins, F. E.; Yap, N.; Huffman, G. P.; Senior, C. L. XAFS characterization of mercury captured from combustion gases on sorbents at low temperatures. *Fuel Proc. Tech.* **2003**, *82*, 167-196.
- (11) Hu, Y. F.; Coulthard, I.; Chevrier, D.; Wright, G.; Igarashi, R.; Sitnikov, A.; Yates, B. W.; Hallin, E. L.; Sham, T. K.; Reininger, R. Preliminary Commissioning and Performance of the Soft X-ray Micro-characterization Beamline at the Canadian Light

- Source in: *SRI 2009: The 10th International Conference On Synchrotron Radiation Instrumentation Sep 27-Oct 02, 2009*, AIP Conference Proceedings, Melbourne: Australia, 2010, vol. 1234, pp. 343-346.
- (12) Newville, M. EXAFS analysis using FEFF and FEFFIT. *Journal of Synchrotron Radiation*. **2001**, 8, 96-100.
 - (13) Ravel, B.; Newville, M. ATHENA, ARTEMIS, HEPHAESTUS: Data analysis for X-ray absorption spectroscopy using IFEFFIT. *Journal of Synchrotron Radiation*. **2005**, 12, 537-541.
 - (14) Newville, M.; Livins, Y.; Yacoby, Y.; Rehr, J. J.; Stern, E.A. An improved background removal method for XAFS. *Jpn. J. Appl. Phys. Pt1*. **1993**, 32, 125-127.
 - (15) Zabinsky, S. I.; Rehr, J. J.; Ankudinov, A.; Albers, R.C. Multiple-scattering calculations of X-ray absorption spectra. *Phys. Rev. B: Condens. Mater. Phys.* **1995**, 52, 2995-3009.
 - (16) Wilcox, J.; Sasmaz, E.; Kirchofer, A.; Lee, S-S. Heterogeneous Mercury Reaction Chemistry on Activated Carbon. *Journal of the Air & Waste Management Association*. **2011**, 61, 418-426.
 - (17) Hesterberg, D.; Chou, J. W.; Hutchison, K. J.; Sayers, D.E. Bonding of Hg(II) to reduced organic sulfur in humic acid as affected by S/Hg ratio. *Environ. Sci. Technol.* **2001**, 35, 2741-2745.
 - (18) Haitzer, M.; Aiken, G. R.; Ryan, J. N. Binding of mercury(II) to dissolved organic matter: The role of the mercury-to-DOM concentration ratio. *Environ. Sci. Technol.* **2002**, 36, 3564-3570.
 - (19) Cotte, M.; Susini, J.; Metrich, N.; Moscato, A.; Gratziau, C.; Bertagnini, A.; Pagano, M. Blackening of Pompeian cinnabar paintings: X-ray microspectroscopy analysis. *Anal.Chem.* **2006**, 78, 7484-7492.
 - (20) Andrews, J.C. Mercury speciation in the environment using X-ray absorption spectroscopy. *Structure & Bonding*. **2006**, 120, 1-35.
 - (21) Riddle, S. G.; Tran, H.H.; DeWitt, J. G.; Andrews, J. C. Field, laboratory, and X-ray absorption spectroscopic studies of mercury accumulation by water hyacinths. *Environ. Sci. Technol.* **2002**, 36, 1965-1970.

- (22) Wang, S.; Fackler, J. P. Mercury complexes with one-dimensional chain structures. Syntheses and crystal structures of $[\text{Hg}(\text{C}_5\text{H}_4\text{NS})(\text{CH}_3\text{CO}_2)]_n$, $\text{Hg}(\text{C}_5\text{H}_4\text{NS})_2$, and $\text{Hg}(\text{CH}_2\text{P}(\text{S})\text{Ph})_2$. *Inorg. Chem.*, **1989**, 28, 2615-2619.
- (23) Braekken, H. The crystal structure of HgBr_2 . *Z. Kristallogr.* **1932**, 81, 152-154.
- (24) Yoon, S. J.; Diener, L. M.; Bloom, P. R.; Nater, E. A.; Bleam, W. F. X-ray absorption studies of CH_3Hg^+ -binding sites in humic substances. *Geochim. Cosmochim. Acta.* **2005**, 69, 1111-1121.
- (25) Lennie, A. R.; Charnock, J. M.; Patrick, R. A. D. Structure of mercury(II)-sulfur complexes by EXAFS spectroscopic measurements. *Chem. Geol.* **2003**, 199, 199-207.
- (26) Douglas, B; McDaniel, D.; Alexander, J. Concepts and Models of Inorganic Chemistry, 3rd ed., John Wiley & Sons, Inc.: New York, U.S.A., **1994**
- (27) Pearson, R. G. Hard and Soft Acids and Bases. *Survey of Progress in Chemistry.* **1969**, 5, 1-52.
- (28) Greenwood, N. N.; Earnshaw, A. Chemistry of the Elements, Pergamon Press: Oxford, U.K., **1984**.
- (29) Norit. Norit activated carbon datasheet – DARCO Hg.
<http://www.norit-americas.com/product/darco-hg> Accessed June 6, 2012
- (30) Norit. Norit activated carbon datasheet – DARCO Hg-LH.
<http://www.norit-americas.com/product/darco-hg-lh> Accessed June 6, 2012
- (31) Huffman, G. P.; Mitra, S.; Huggins, F. E.; Shah, N.; Vaidya, S.; Lu, F. Quantitative analysis of all major forms of sulfur in coal by x-ray absorption fine structure spectroscopy. *Energy Fuels.* **1991**, 5, 574-581.
- (32) Seneviratne, H. R.; Charpentreau, C.; George, A.; Millan, M.; Dugwell, D. R.; Kandiyoti, R. Ranking low cost sorbents for mercury capture from simulated flue gases. *Energy Fuels*, **2007**, 21, 3249-3258.
- (33) Sasmaz, E.; Kirchofer, A.; Jew, A. D.; Saha, A.; Abram, D.; Jaramillo, T. F.; Wilcox, J. Mercury chemistry on brominated activated carbon. *Fuel.* **2012**, 99, 188-196.
- (34) Liu, J.; Qu, W.; Zheng, C. Theoretical studies of mercury-bromine species adsorption mechanism on carbonaceous surface. *Proceedings of the Combustion Institute.* **2013**, 34, 2811-2819.

Chapter 5

Potential Hazards of Brominated Carbon Sorbents for Mercury Emission Control

Teresa M. Bisson and Zhenghe Xu, To be submitted

5.1. Introduction

Mercury is a recognized air pollutant which is emitted in trace quantities from coal combustion. The mercury can return to the earth with rainfall, contaminating water bodies, and leading to bio-accumulation of mercury in aquatic species and subsequently up the food chain.¹ In order to reduce the emission of mercury, control systems must be applied at the source. The most promising technology to date for mercury emission control from a power plant involves injection of powdered activated carbon.² In this technology, activated carbon is injected into the flue gases to make contact with the mercury. Mercury is trapped on the activated carbon, which is then removed along with the fly ash in the electrostatic precipitator or baghouse filter. The ultimate fate of the activated carbon is the same as the fly ash, which is sent to landfill or is used in the concrete manufacturing industry. The effectiveness of AC to capture mercury has been improved through impregnating the sorbents with halogen or sulfur species.² The bromination of AC has been found to be particularly effective in capturing the elemental mercury from flue gases of power plants. Several different types of activated carbon materials have been investigated and much research has been focusing on reducing the cost of the activated carbon material by using inexpensive source materials.²⁻⁴ In particular, a novel low cost sorbent was developed by bromination of a waste by-product of biomass combustion (called brominated ash or Br-Ash).^{4,5} This Br-Ash, a low-cost alternative to Br-AC, was shown to be effective in mercury capture.^{4,5}

As the ultimate fate of the activated carbon sorbent (or Br-Ash) is most likely the landfill, it is prudent to investigate the stability of the mercury and bromine on the sorbent under prolonged

landfill conditions. Several studies investigated the stability of mercury on fly ash from coal combustion⁶⁻⁹ and on activated carbons^{6,10} using leaching test procedures. Graydon et al.⁶ exposed several activated carbon sorbents to an elemental mercury atmosphere. The toxicity characteristic leaching procedure (TCLP) was used to determine the stability of mercury on the AC. The Environmental Protection Agency (EPA) imposes a limit of Hg in the leachate to be 0.2 mg/L.¹¹ The results showed that the mercury was very stable on the AC sorbents and the leaching of mercury was not anticipated to be a concern. Graydon et al.⁶ also conducted a sequential leaching test that uses increasingly more acidic conditions. Depending on the steps during which the Hg was found to be leached out, the leaching tests allow the type of Hg species present on the sorbent to be inferred. Most of the mercury was found to be very stable and did not leach out until the last two steps, which may indicate elemental mercury (second last step) and very stable mercury sulfide (final extraction step). Luo et al.¹⁰ exposed three types of ACs to a simulated flue gas atmosphere (containing Hg⁰) before conducting TCLP analysis. Their results indicated that the mercury in the leachate was well below the TCLP limit, indicating extremely high stability of captured mercury with respect to standard leaching. While these studies showed very promising results for AC sorbents with varying sulfur concentrations, as well as FeCl₃ and MnO₂ impregnation, none of the ACs studied contained bromine. Tong et al.¹² investigated Hg⁰ leaching from several AC sorbents, including one brominated AC, through a sequential leaching procedure similar to the procedures used by Graydon et al.⁶ The majority of the mercury on the brominated AC was found to be very stable. The most extreme acidic leaching conditions were required in the final leaching step in order to remove mercury. These extreme conditions were not expected to be present in a landfill environment. From their study, Tong et al.¹² hypothesized that a TCLP test on the brominated AC would not leach a substantial amount of Hg⁰.

Although many studies have investigated the stability of mercury on AC, few studies investigated the leachability of brominated ACs and no studies could be found that investigated the amount of Br leached from the sorbent. In particular, no leach tests have yet been conducted on the novel Br-Ash sorbent. The purpose of this study is to investigate the leachability of both mercury and bromine from the Br-Ash sorbent, in comparison to that from a commercial brominated activated carbon.

5.2. Experimental Procedure

Samples of Br-Ash were prepared following the chemical-mechanical bromination procedure previously reported by Bisson et al.⁵ For comparison, a commercial brominated activated carbon (Norit Darco Hg_{LH}) was also tested. The bromine concentration was determined by elemental analysis at the Analytical and Instrumentation Laboratory of the University of Alberta. The Schöniger oxygen flask combustion method was used with 10 mL of 2% hydrazine sulfate solution to trap the bromide combustion gases. After combustion was complete, the solution was acidified with nitric acid and diluted to 80 mL with isopropanol. The resulting solution was titrated with 0.01 N silver nitrate using a Mettler-Toledo T70 autotitrator. Elemental analysis was conducted on each of the fresh samples to determine initial bromine content.

Mercury was loaded onto each of the sorbents by spreading approximately 1.25 g on bottom of a sealed borosilicate glass vessel, with a mercury source contained inside, as shown in Figure 5.1. The setup was left at room temperature for 1 week. Each sample was collected and mixed thoroughly using a mortar and pestle. To ensure repeatability of the samples, three tests were performed for the Br-Ash and Br-Norit samples. A Milestone DMA-80 was used to determine Hg content of the sample. As the Hg content was too high for direct detection on the DMA-80, the sorbent was first diluted with a blank activated carbon (Calgon Fluepac A) by homogenizing 10 mg mercury-loaded sorbent sample with 600 mg blank carbon using a mortar and pestle for 15 min. The blank activated carbon was also analyzed by DMA-80 for mercury content in order to subtract the mercury contribution of the blank carbon from the overall mercury content of the mixture. Two mixtures were made for each sample, and three samples were analyzed on each mixture using the DMA-80. The average and standard deviation are reported. A standard reference material with high mercury content (NIST 2451) was also diluted using the same procedure to ensure the accuracy of mercury measurement.

5.2.1 Br Leaching in Ultra-Pure Water

Br-Ash and Br-Norit sorbents with no mercury addition (1.5 g) were immersed in 30 mL of ultra-pure water in glass containers. The containers were tightly sealed and held at 40°C for 48 hours, with occasional swirling to ensure complete mixing. The sorbent/water mixture was

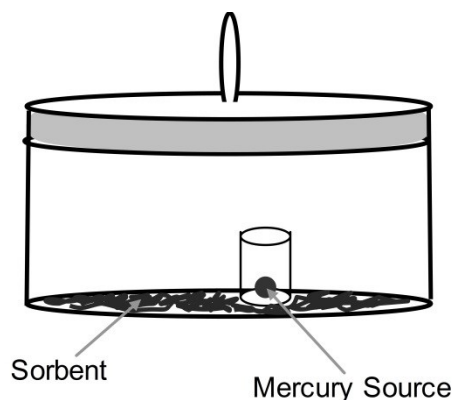


Figure 5.1. Mercury loading schematic.

filtered and the filtrate transferred to a 100 mL volumetric flask. After adding the ultra-pure water to make the 100 mL solution, the resulting solution was analyzed by ion chromatography (Dionex ICS-2500 with Dionex AS14A column and 8.0 mM Na_2CO_3 & 1.0 mM NaHCO_3 Eluent) to determine Br concentration. Solids from the leaching tests were dried at room temperature. Mercury pulse injection tests were used to determine whether the solids were still able to capture the mercury. The detailed description of the mercury pulse injection test can be found elsewhere.⁵ Briefly, 200 μL of air saturated with mercury was injected upstream of 40 mg of sorbent contained in a borosilicate u-tube. The u-tube was contained inside a GC oven which controlled the temperature of the sorbent. The mercury was captured on the sorbent and any non-captured mercury passed through to a gold trap, which pre-concentrated the mercury pulse. After 5 minutes, the gold trap was quickly heated to release the mercury which was detected as a peak on a Tekran 2500 CVAFS. The amount of Hg^0 that was not captured by the sorbent was termed “ Hg^0 breakthrough” and reported as a percentage of the Hg^0 injected. Each sample was tested 3 times to ensure repeatability. The average was reported with standard deviation indicating the sample error.

5.2.2 Hg, Br Leaching by TCLP

The Br-Ash and Br-Norit sorbents loaded with mercury were subjected to the TCLP¹³ in order to determine leachability of mercury from the sorbents. The TCLP was modified slightly, by using 1 g of sample instead of the 100 g samples as recommended, with the 20:1 liquid to solid

ratio being maintained. This change has also been used by others.⁶ All glassware and filter paper used in the leach tests were acid washed with 10% HNO₃ solution. The TCLP requires an appropriate extraction medium to be selected based on the acidity of the solid to be tested. The extraction fluid was chosen by the following procedure: 5 g of Br-Ash was weighed into a beaker, followed by the addition of 96.5 mL ultra-pure water. The Br-Ash/water mixture was stirred for 5 min with the natural pH of 8.94 (> 5.0). To the mixture, 3.7 mL of 10% HCl was added, and then heated to 50°C for 10 minutes. After cooling to room temperature, the pH was measured to be 6.97 (still > 5.0). As per the TCLP procedure, 5.7 mL/L glacial acetic acid (pH = 2.86) was chosen to be the extraction fluid for the TCLP test. 1g of mercury – loaded sample was transferred to a 250 mL extraction bottle, and 20 g of extraction fluid was added. The bottle was tightly sealed and transferred to a mechanical shaker for 18±2 h at room temperature. The resulting mixture was filtered into a 100mL volumetric flask and acidified with 5mL of 10% HNO₃ to ensure a pH <2. A PSA Millennium Merlin mercury analyzer was used to determine total Hg content of the filtrate. The filtrate was checked for bromide content by ion chromatography (Dionex 600 with Dionex IonPac AS9-HC column and 9 mM Na₂CO₃ Eluent) at the Biogeochemical Analytical Service Laboratory at the University of Alberta.

5.2.3 Tests at Varying pH and Liquid to Solid Ratios

Br-Ash samples loaded with mercury were also tested for leaching at different pH and liquid to solid ratios. For the pH adjustment tests, a sample of Br-Ash was combined with HNO₃ or KOH and ultra pure water to determine the amount of acid or base required to obtain the desired pH. Once the desired volume was known, 1 g of mercury loaded Br-Ash was weighed into the 250 mL extraction bottle. Ultra pure water was added to the bottle, and 10% HNO₃ or 1M KOH was added to adjust the pH and accomplish a total volume of 10 mL (10:1 liquid to solid ratio). For the variation in liquid to solid ratio test, 2 mL (2:1), 5 mL (5:1) or 10 mL (10:1) of ultra pure water was added to the extraction bottle. The rest of the procedure was the same as above for TCLP, except that the KOH samples were not acidified but were tested immediately to preserve sample integrity. Sample pH was recorded after shaking on the mechanical shaker and before filtration. This measured pH is recorded on the X-axis of the leach test results.

5.2.4 XPS Characterization

Samples of Br-Ash before and after leaching were analyzed by x-ray photoelectron spectroscopy (XPS) at the Alberta Centre for Surface Engineering and Science (ACES), University of Alberta. The Axis Ultra Spectrometer (Kratos Analytical) of a monochromatic Al K α source ($h\nu = 1486.6$ eV) powered at 210 W was used in this study. The spot size of sampling was set at 400 x 700 μm . Samples were loaded on double sided insulating tape prior to their analysis. Electronic flooding was used to compensate for charging of the powdered samples. Survey scans were collected, along with high resolution spectra for the Br and C species. The high resolution scan of the C species was used to calibrate the spectra of C_{1s} binding energy at 284.5 eV.¹⁴ Casa XPS software was used for peak modeling of the high resolution scans to better understand Br binding on the sorbents before and after their leaching.

5.3. Results and Discussion

Figure 5.2 and Table 5.1 show the results of the Br leach test for the sorbents. The amount of Br in Br-Ash varied between the two tests as each test was conducted on a fresh batch of Br-Ash. The original Br concentration on commercial Br-Norit was found to be substantially lower than that on Br-Ash as determined previously.^{5,15} In ultra pure water at 40°C, approximately 88% of the Br was leached into the filtrate for the commercial Br-Norit (As shown in Figure 5.2), while the Br-Ash had a slightly lower leachability at approximately 78%, indicating that a fraction of bromine present on the biomass ash is in a more stable form. The TCLP tests also show (Figure 5.2) that the leaching of bromine is lower on the Br-Ash than the Br-Norit. Exposure to mercury had a low impact on the Br leaching as shown by comparing the TCLP case of Br-Ash with and without Hg, indicating that mercury loading does not seem to affect the stability of Br. Table 5.1 shows the concentration of Br in the leachate of the samples. In both cases, the concentration of Br in the leachate of Br-Ash was higher than Br-Norit due to higher initial Br content of the sample. The Br leached in the Br-Norit case was slightly lower in ultra pure water than in the TCLP test, but was within experimental error (also seen in Figure 5.2). The higher temperature (40 °C in the water test) and lower pH (TCLP test) did not seem to affect the Br-leaching from Br-Norit. In the case of Br-Ash, more Br was found in the leachate in the water test, indicating that the higher pH or higher temperature in the water test resulted in more Br leaching.

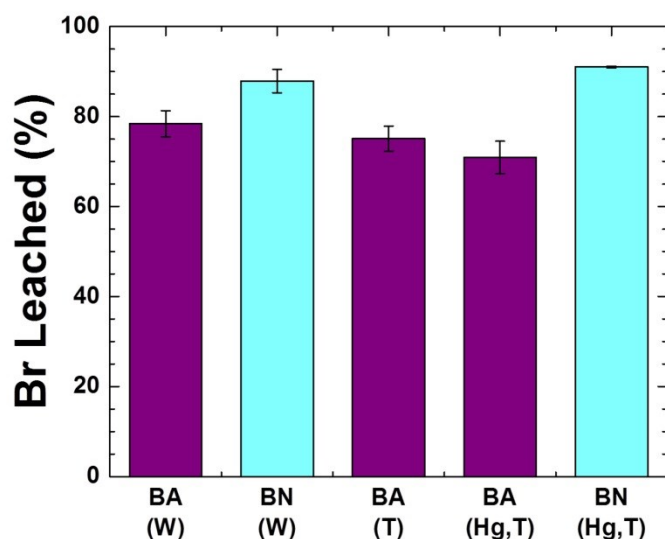


Figure 5.2. Br Leached (W=Water test; T=TCLP Test; Hg = Sorbents contained mercury).

The high concentration of Br leached from both the Br-Ash and Br-Norit samples suggests that the landfill of spent Br-Ash or Br-Norit may not be the proper disposal option. Water quality limits for Br may need to be taken into consideration prior to disposal of spent brominated mercury sorbent. For example, the World Health Organization (WHO) has recommended an upper limit of 6 mg/L Br in drinking water for adults and 2 mg/L for children.¹⁶

Table 5.1. Results of bromine leaching tests.

Sorbent	Initial Br Content (wt %)	Leachate Br Concentration (mg/L)
Br-Ash no Hg (Water)	8.7 ± 0.3	3424 ± 146
Br-Ash no Hg (TCLP)	7.4 ± 0.3	2792 ± 21
Br-Ash (TCLP)	7.4 ± 0.3	2630 ± 37
Br-Norit no Hg (Water)	4.3 ± 0.3	1909 ± 57
Br-Norit (TCLP)	4.3 ± 0.3	1967 ± 17

The current study is considering leaching from brominated carbon sorbents only. The Br from the Br-Ash (or Br-AC) is only a small portion of the Br contained in the power plant waste materials, especially if CaBr_2 is injected with the coal prior to combustion. Other leach tests for bromine should be conducted on the waste material from baghouse filters or electrostatic precipitators where powdered brominated activated carbons are injected to confirm the amount of bromine leached from the combined materials.

The initial mercury content of the samples and the results of TCLP leaching tests are given in Table 5.2. Both samples captured a similar amount of mercury at room temperature, in the order of approximately 550 ppm. Even under high mercury loading conditions, only a small amount of mercury was leached out from both Br-Ash and Br-Norit. Mercury concentrations in the leachate are well below the 0.2 mg/L limit as imposed by the EPA¹¹ for classifying a material as hazardous waste. It is interesting to note that even though a large proportion of Br is removed from the samples, the mercury is not leached away from the sorbents. This finding suggests that either the mercury was bound to only the small fraction of Br remaining on the spent sorbents or the mercury is actually bound to species other than (or in addition to) Br. Based on our findings in a previous paper investigating the binding mechanisms of mercury on the Br-Ash and Br-Norit carbons,¹⁵ the Hg is likely bound to C or S. The previous results supported the mechanism of surface enhanced oxidation of the Hg^0 by Br, and binding of the oxidized Hg on the carbon linked to S.¹⁵ Such mercury binding mechanisms would explain the removal of Br in the leaching test, with negligible impact on mercury leachability. However, the amount of Br left on the samples after leaching in water was approximately 1.9 wt% for the Br-Ash and 0.5 wt% for the Br-Norit, which is enough to still be bonded with all of the mercury captured by the sorbents. As the Br-Ash with Hg present did have slightly less Br leach in the TCLP test (Table 5.1), it is possible that Hg could be stabilizing part of the Br. Unfortunately, the amount of Hg on the sorbent is so low it is uncertain if it is stabilizing the Br or simply coordinated with other species on the sorbent.

Table 5.2. Results of mercury leaching tests using TCLP method.

Sorbent	Initial Hg ⁰ Content (ppm)	Hg ⁰ in Leachate (mg/L)	Hg ⁰ Leached (%)
Br-Ash	532 ± 95	0.0123 ± 0.0032	0.046 ± 0.012
Br-Norit	554 ± 15	0.0002 ± 0.0002	0.001 ± 0.001

Hg⁰ pulse injection tests were conducted for the sorbents of Br-Ash and Br-Norit after their leaching tests in water. The results in Figure 5.3 show a negligible mercury breakthrough up to 250 °C for both Br-Ash and Br-Norit, indicating excellent Hg⁰ capture even with the reduced Br content. However, above 250 °C, the sorbents quickly lose their effectiveness, indicating the importance of the leached bromine (or higher bromine concentration) for mercury capture at high temperatures. Figure 5.4 shows a comparison of mercury capture by the leached Br-Ash sample to the fresh Br-Ash sample and raw ash sample (which contains no Br). It is interesting to note that up to 250 °C, the Hg⁰ removal performance of leached Br-Ash is comparable to fresh Br-Ash, much higher than that by the raw wood ash which has little mercury capture above 150 °C. Above 250 °C, the Br-Ash shows slightly better Hg⁰ removal performance than the leached Br-Ash. The mercury capture capability of the leached sorbents further aligns with the results above indicating very low leaching of mercury by the TCLP leach test. The Hg⁰ retention and capture results suggest that one may consider the post treatment of Br-Ash by water washing as an alternative to produce more robust Br-Ash or Br-Norit that could be safely disposed in landfills after its utilization of mercury capture. The water washing would remove excess Br, while retaining the Br on the sorbent that is essential for Hg⁰ capture.

The low leachability of Hg⁰ by TCLP suggests that the mercury on the Br-Ash and Br-Norit sorbents is stable, and does not need to be classified as hazardous waste for disposal according to EPA regulations.¹¹ The TCLP, however, does not consider the wide variety of conditions that could be experienced by the fly ash and carbon in a landfill.¹⁷ Testing other parameters such as varying pH and liquid to solid ratios could give a better indication of leaching potential in landfill conditions.¹⁷ Figure 5.5 shows the amount of Hg leached from Br-Ash as a function of pH. Hg concentrations do not follow the same trend as Br concentration in the leachate. At low and high pH conditions, mercury leaches from the Br-Ash more considerably with greater than

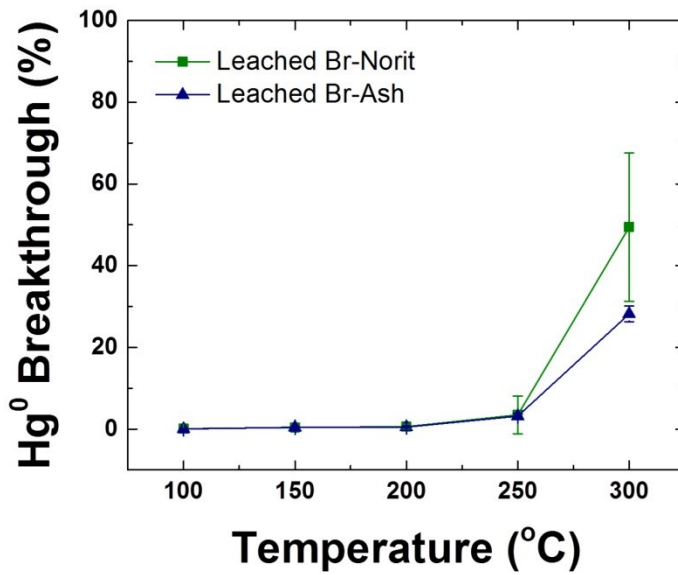


Figure 5.3. Mercury pulse injection test results for water-leached Br-Ash and Br- Norit.

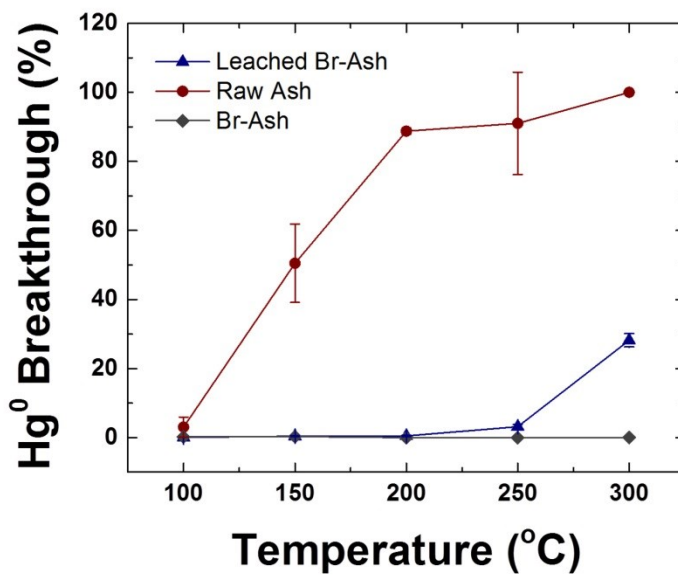


Figure 5.4. Mercury pulse injection test results for raw ash, Br-Ash⁵ and water-leached Br-Ash.

the 0.2 mg/L limit imposed by the EPA. However, an important consideration is that this study is conducted on sorbents with much higher concentrations of mercury than would be seen in flyash containing the carbon sorbents. In fact, still less than 2% of the mercury is leached in the worst case of low pH. Further tests should be completed with fly ash containing the brominated

carbon sorbents to determine if the leachate would still be greater than 0.2 mg/L at high and low pH values. Figure 5.5 also shows that the amount of Br leached does not seem to be a function of pH. However, highly acidic conditions do seem to result in a lower concentration of Br in the leachate.

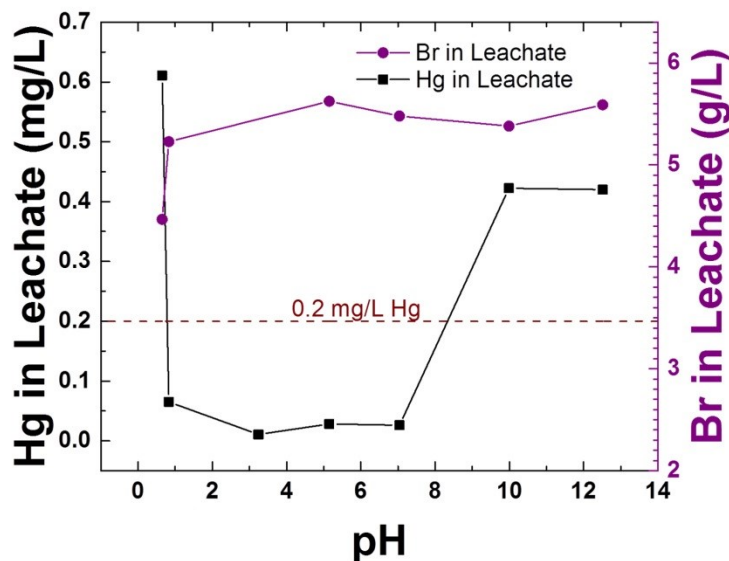


Figure 5.5. Amount of Hg and Br leached from Br-Ash as a function of pH in leachate after leach test. 0.2 mg/L line illustrates limit imposed by EPA¹¹ for amount of Hg in leachate.

The amount of mercury leached was also determined to be a function of the liquid to solid ratio (Figure 5.6). The pH of these tests was the natural pH of the Br-Ash samples, ranging from pH 9-10, except for the liquid to solid ratio of 20, which was the result from the TCLP test at pH 6.8. The mercury in the leachate in the case of natural pH tends to follow the same trend as Br for varying liquid to solid ratios. In particular, the amount of Hg and Br in the leachate increases dramatically at low liquid to solid ratios. The high Br concentration in the solution is likely causing the mercury to leach. In order to test the ability of high Br concentration to leach mercury, the 10:1 liquid to solid test (which initially had low amount of Hg in the leachate) was repeated. In this repeat test, CaBr₂ was added prior to placing the sample on the shaker in order to artificially increase the Br concentration in solution. The leach test results (Table 5.3) show that the addition of Br greatly increased the Hg concentration in the leach test. Others have also

noted low liquid to solid ratios can cause higher concentration of species in the leachate (higher ionic strength).¹⁷ The results of these additional leach tests indicate that landfill conditions should be considered before sorbent disposal. Water washing the Br-Ash prior to disposal could reduce the possible effect of high Br concentration for low liquid to solid conditions. Another option is to redesign the Br-Ash sorbent to contain less Br but still have high mercury capture capacity.

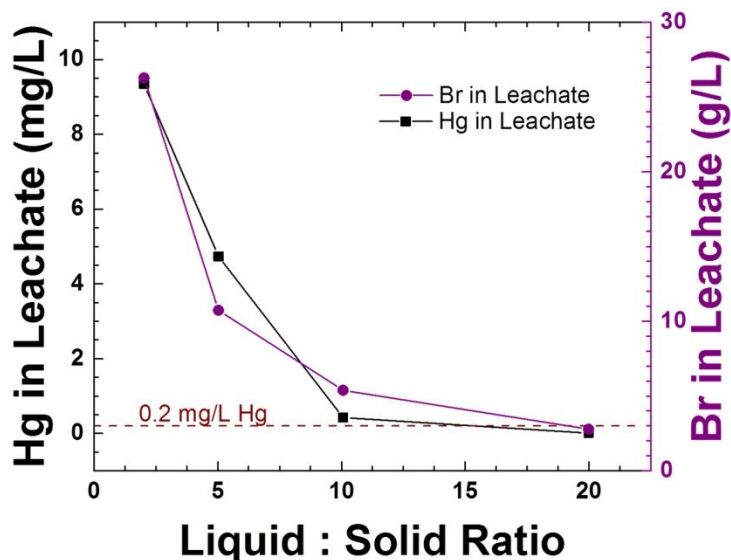


Figure 5.6. Hg and Br leached from Br-Ash sorbent as a function of liquid to solid ratio. 0.2 mg/L line is shown as limit imposed by EPA¹¹ for Hg leaching.

Table 5.3. Results of CaBr₂ addition to leaching tests (W=Water).

	Liquid : Solid Ratio	Hg Leached (µg)	Leachate Br Concentration (mg/L)
Br-Ash (W)	2	18.9	26276
Br-Ash (W)	10	4.3	5381
Br-Ash (W+CaBr ₂)	10	11.2	23985

XPS full survey scan spectra are shown in Figure 5.7 for Br-Ash and Water-Leached Br-Ash. Major elements detected in both samples include Carbon (C), Oxygen (O), Calcium (Ca), Bromine (Br), Magnesium (Mg), Sulfur (S). Silicon (Si) was seen in the leached Br-Ash but not in the original, likely due to non-homogeneous samples. It can be seen that the bromine content is much lower in the leached Br-Ash sample, which is in agreement with the results determined by Ion Chromatography.

The high resolution XPS scans for Br 3d are shown in Figures 5.8 and 5.9 for Br-Ash and water leached Br-Ash, respectively. Both figures show a broad asymmetrical band, indicating overlap of a number of characteristic bands. Considering two types of Br photoelectrons ($\text{Br}_{3d\ 3/2}$ and $\text{Br}_{3d\ 5/2}$) occurring over the similar binding energy regions, the asymmetrical bands of high resolution scans were modeled using Casa XPS software. Deconvolution of the Br peaks was

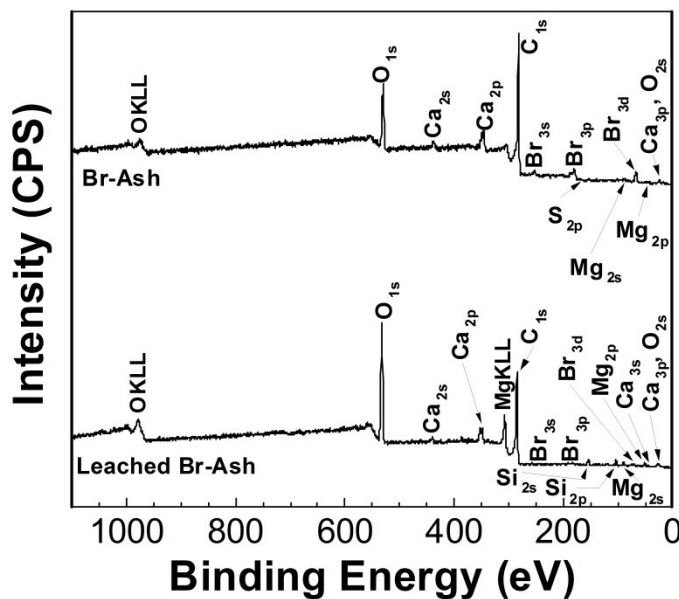


Figure 5.7. XPS survey scan of Br-Ash (top) and water-leached Br-Ash (bottom).

accomplished by setting the following constraints: equal peak width of $\text{Br}_{3d\ 3/2}$ and $\text{Br}_{3d\ 5/2}$ peaks, setting $\text{Br}_{3d\ 3/2}$ peak area = $0.67 \times \text{Br}_{3d\ 5/2}$ peak area, and Δ between $\text{Br}_{3d\ 3/2}$ and $\text{Br}_{3d\ 5/2}$ peaks = 1.05 eV.¹⁴ In both figures, the model shows two separate pairs of peaks (labeled “A” and “B”), indicating two Br bonding environments in the sample. Each pair of peaks consists of a $\text{Br}_{3d\ 3/2}$ and $\text{Br}_{3d\ 5/2}$ peak. The $\text{Br}_{3d\ 5/2}$ peaks for the Br-Ash were at 68.3 and 70.3 eV. After leaching, the

Br_{3d 5/2} peaks were at 68.3 and 70.1 eV. The difference in the binding energies of these two peaks before and after leaching tests is so minimal that the bonding environment of Br doesn't seem to have changed during the leaching process. However, it can be seen that after leaching, the area ratio of lower (A) to higher (B) binding energy peaks of Br_{3d 5/2} decreased from 1.8 of the unleached sample to 0.2, indicating preferential leaching of the lower binding energy Br labeled as A than higher binding energy Br labeled as B. To identify binding elements of Br featuring these two different binding energies, the Br_{3d 5/2} binding energies from the high resolution scans were compared to the spectra of NIST XPS database.¹⁸ Unfortunately, there is quite a bit of overlap of possible binding environments, making it difficult to identify the precise species attached to the Br. Nevertheless, the NIST database shows that the Br of Br_{3d 5/2} binding energies in the range of 65.7 – 70.0 eV tends to be bound to metals, while Br of binding energies higher than 70 eV tends to be bound to organic complexes.¹⁸ In this case, the decreasing A/B ratio would indicate less metal-bound Br than organically bound Br on leached Br-Ash complexes than on unleached Br-Ash. A sample of Br-Norit (before leaching) was also analyzed by XPS, and had an A/B ratio of approximately 3.5. The high A/B ratio indicates that the Br on the Br-Norit is primarily metal-bound Br, which could explain why slightly more Br leached from the Br-Norit than the Br-Ash (Figure 5.2).

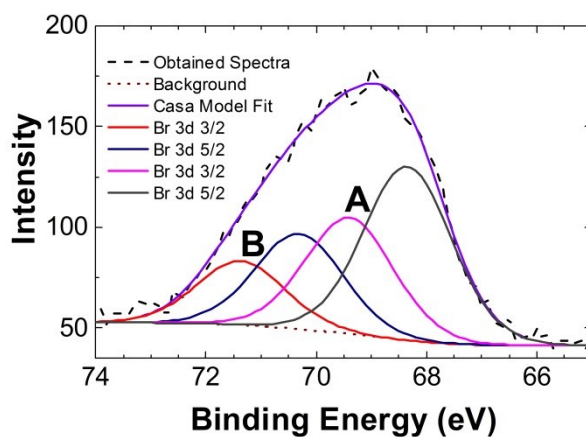


Figure 5.8. High resolution Br XPS scan of Br-Ash.

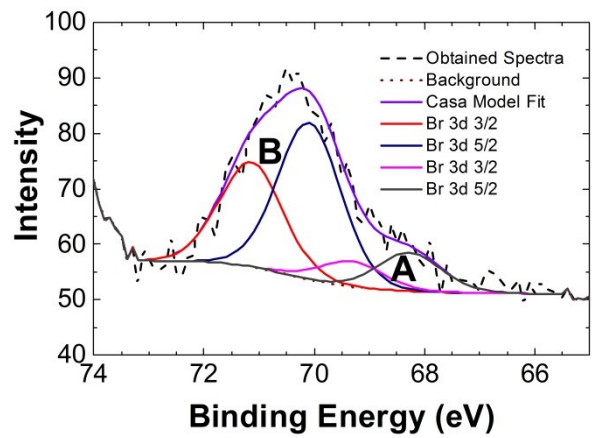


Figure 5.9. High resolution Br XPS scan of water-leached Br-Ash.

5.4. References

- (1) M. Berlin, R.K. Zalups, B.A. Fowler. Mercury. In: *Handbook on the toxicology of metals*. Nordberg, G. F., Fowler, B. A., Nordberg, M., Friberg, L.T., Eds.; Academic Press: USA 2007; pp. 675–729.
- (2) Yang, H.; Xu, Z.; Fan, M.; Bland, A. E.; Judkins, R. R. Adsorbents for capturing mercury in coal-fired boiler flue gas. *J. Hazard. Mater.* **2007**, *146*, 1-11.
- (3) Arvelakis, S.; Crocker, C.; Folkedahl, B.; Pavlish, J.; Spliethoff, H. Activated carbon from biomass for mercury capture: effect of the leaching pretreatment on the capture efficiency. *Energy Fuels*. **2010**, *24*, 4445-4453.
- (4) Gupta R. P.; Xu Z.; Clark I.; Yang H. Bromination process. U.S. Patent 20100126345.
- (5) Bisson, T. M.; Xu, Z.; Gupta, R.; Maham, Y.; Liu, Y.; Yang, H.; Clark, M.; Patel, M. Chemical-mechanical bromination of biomass ash for mercury removal from flue gases. *Fuel*. **2013**, *108*, 54-59.
- (6) Graydon, J. W.; Zhang, X.; Kirk, D. W.; Jia, C.Q. Sorption and stability of mercury on activated carbon for emission control. *J. Hazard. Mater.* **2009**, *168*, 978-982.
- (7) Srivastava, R. K.; Hutson, N.; Martin, B.; Princiotta, F.; Staudt, J. Control of mercury emissions from coal-fired electric utility boilers. *Environ. Sci. Technol.* **2006**, *40*, 1385-1393.
- (8) Pavlish, J. H.; Sondreal, E. A.; Mann, M. D.; Olson, E. S.; Galbreath, K. C.; Laudal, D. L.; Benson, S. A. Status review of mercury control options for coal-fired power plants. *Fuel Process. Technol.* **2003**, *82*, 89-165.
- (9) Cho, J. H.; Eom, Y.; Park, J.-M.; Lee, S.-B.; Hong, J.-H.; Lee, T. G. Mercury leaching characteristics of waste treatment residues generated from various sources in Korea. *Waste Management*. **2013**, *33*, 1675-1681.
- (10) Luo, Z.; Hu, C.; Zhou, J.; Cen, K. Stability of mercury on three activated carbon sorbents. *Fuel Process. Technol.* **2006**, *87*, 679-685.
- (11) Environmental Protection Agency. Hazardous waste characteristics, a user-friendly reference document. (2009)
<http://www.epa.gov/osw/hazard/wastetypes/wasteid/char/hw-char.pdf>
(Accessed April 14, 2014).

- (12) Tong, S.; Fan, M.; Mao, L.; Jia, C. Q. Sequential extraction study of stability of adsorbed mercury in chemically modified activated carbons. *Environ. Sci. Technol.* **2011**, *45*, 7416–7421.
- (13) US EPA Method 1311 toxicity characteristic leaching procedure. Fed. Regist. 55 (1992) 11798–11877
www.epa.gov/osw/hazard/testmethods/sw846/pdfs/1311.pdf
(Accessed December 5, 2013).
- (14) Moulder, J. F.; Stickle, W. F.; Sobol, P. E.; Bomben, K. D. *Handbook of X-ray Photoelectron Spectroscopy*; Physical Electronics USA, Inc., Chanhassen, MN, 1995.
- (15) Bisson, T. M.; MacLean, L. C. W.; Hu, Y.; Xu, Z. Characterization of mercury binding onto a novel brominated biomass ash sorbent by x-ray absorption spectroscopy. *Environ. Sci. Technol.* **2012**, *46*, 12186–12193.
- (16) World Health Organization, Bromide in drinking-water: Background document for development of WHO Guidelines for Drinking-water Quality (2009) http://www.who.int/water_sanitation_health/dwq/chemicals/Fourth_Edition_Bromide_Final_January_2010.pdf (Accessed April 14, 2014).
- (17) Environmental Protection Agency. Characterization of Mercury-Enriched Coal Combustion Residues from Electric Utilities Using Enhanced Sorbents for Mercury Control. (2006) <http://www.epa.gov/nrmrl/pubs/600r06008.html> (Accessed August 9, 2014)
- (18) Naumkin, A. V.; Kraut-Vass, A.; Gaarenstroom, S. W.; Powell, C. J. NIST X-ray Photoelectron Spectroscopy Database: NIST Standard Reference Database Version 4.1, 2012. <http://srdata.nist.gov/xps/Default.aspx> (Accessed February 1, 2014).

Chapter 6

Sulfur Loading on Brominated Carbon Sorbent for Improved Mercury Capture

Teresa M. Bisson, Zong Qian Ong, Aimee MacLennan, Yongfeng Hu, Zhenghe Xu,
To be submitted

6.1. Introduction:

Mercury is one of the toxic air pollutant emissions from coal fired power plants. Throughout the past several years, much work has been done to develop more efficient and cost effective methods to remove mercury from coal power plant flue gases. A very promising technology, which has been proven on the lab scale, pilot scale, and full scale, involves powdered activated carbon (AC) injection.¹ The powdered carbon is often impregnated with additional species, such as halogens or sulfur. These species improve the mercury capture efficiency, particularly when burning coals with low chlorine content. AC is generally injected into the flue gas upstream of the particulate removal device. Once the AC comes in contact with the flue gases, the mercury is bound to the sorbent material, which is removed in the particulate control device along with the fly ash. In order to synthesize more effective sorbents, several studies have been performed to understand the mechanism of mercury removal on the AC sorbents.¹⁻¹⁷

Recently, a novel brominated carbon (Br-Ash) sorbent has been developed using a waste by-product from biomass combustion (wood ash) as the carbon source. The sorbent was found to have good mercury capture, and was stable during mercury leach tests (Chapter 5). The mercury binding of the Br-Ash sorbent was studied by X-ray absorption near edge spectroscopy (XANES) and extended X-ray absorption fine structure (EXAFS) in comparison to a commercial brominated carbon sorbent.³ The mechanism of mercury binding to Br-Ash was proposed to be surface enhanced oxidation by the Br, with subsequent binding of the oxidized mercury on the carbon surface. In the case of the commercial brominated activated carbon, the surface enhanced

oxidation was followed by binding to the sulfide species present on the surface of the commercial sorbent. This finding suggested the possibility of a synergetic effect by combining both sulfur and bromine onto the carbon surface for mercury removal. Quite possibly, adding similar sulfur species to the Br-Ash sorbent could provide another site for mercury binding after oxidation by the Br. The addition of sulfur could also reduce the amount of bromine required for sorbent synthesis while maintaining adequate mercury removal capacity. Previous tests in Chapter 5 have shown that the bromine from brominated carbon has been found to leach, so reducing the bromine content of the sorbents is therefore desirable in order to reduce any potential environmental impact of bromine leaching.

Many previous studies have investigated the effect of sulfur addition to activated carbon on mercury capture. The main methods of sulfur addition include adsorption of H_2S ,¹⁸⁻²³ vapor impregnation by heating the carbon sorbent with elemental sulfur (S^0),^{21-22,24-32} or liquid impregnation using other sulfur species^{31,33,34,35} with subsequent heating to remove moisture. In addition, Qu and colleagues have conducted experiments of injecting sulfur chlorides (SCl_2 and S_2Cl_2)³⁶ and sulfur monobromide (S_2Br_2)³⁷ into flue gases for Hg^0 removal. SCl_2 and S_2Cl_2 injection achieved up to 75% Hg^0 removal at 100 °C, and Hg^0 removal was found to improve with the addition of activated carbon in the system (or impregnating the SCl_2 onto the activated carbon). With the injection of S_2Br_2 , over 70% of Hg^0 was removed in air at 120 °C, and over 65% was removed at 120 °C in a simulated flue gas atmosphere in the presence of activated carbon. The order of reactivity (mercury removal) was found to be $\text{Br}_2 > \text{S}_2\text{Br}_2 > \text{S}$. It was also found that when Br is bonded to S (as in S_2Br_2), the Br becomes less reactive with Hg^0 than Br not bonded to S.³⁷ Speciation of sulfur on the S-impregnated sorbent was found to be a key parameter for mercury removal.^{22,24,38} Feng et al.²² compared the loading of H_2S and S^0 and found that the sorbent impregnated with S^0 had a higher amount of elemental sulfur and sulfide content than that with H_2S . Our previous study also showed that the sulfide content on a commercial brominated activated carbon is an important factor for Hg^0 capture,³ and elemental sulfur has been found by others to be the effective component.²² With the current knowledge, the physical impregnation of S^0 was chosen for this study. Maximum sulfur loading had been reported to take place at 600 °C,³⁹ and at this temperature, approximately 16% of the sulfur consists of the S_2 allotrope.²⁹ Taking advantage of the results from these early studies,

impregnation temperature of 600 °C was chosen for this study for sulfur-impregnation on biomass ash (normally a waste product of biomass combustion). One incentive of adding sulfur to the brominated biomass ash is to reduce the loading of bromine that could cause potential environmental hazards from landfill disposal of the spent sorbent.

Another important feature of sulfur impregnation is its low cost. Based on publicly available commodity pricing information, the cost of elemental sulfur could be 14x lower than bromine⁴⁰ (depending on market fluctuation). As mentioned above, adding sulfur on its own to AC can result in a significant improvement in mercury capture of the resulting sorbent. However, continuous addition of sulfur does not always add to additional capacity of mercury capture. Excess sulfur could clog the pores, which could actually reduce mercury capture.^{20,25} Addition of a small amount of Br to the sulfur-impregnated sorbent is anticipated to improve mercury capture capacity of the sorbent. To our best knowledge, no previous studies were devoted to this approach. This paper is to fill this gap by investigating the combined loading of S and Br on a biomass ash and the role of these species on mercury capture. Possible binding mechanisms of Hg with the S and Br on the sorbents will be investigated using S K-edge and Hg L-edge XANES and EXAFS.

6.2. Experimental Procedure

6.2.1 Synthesis of S-Ash and Br-Ash

Biomass ash was obtained from a power station burning waste wood chips. The as-received ash was ball milled using the same procedure reported by Bisson et al.⁴¹ The ground ash is called "Raw Ash". The appropriate amount of elemental sulfur (S^0) (99% purity from Sigma Aldrich) was weighed into a ceramic crucible followed by Raw Ash, which was placed on the top of the sulfur. S-Ash (sulfur loaded Raw Ash) was prepared using a 20:1 Raw Ash to Sulfur mass ratio (that is, 2g Raw Ash with 100 mg S^0). In order to determine the optimal sulfur concentration on the wood ash for mercury removal, two other samples at a 100:1 Raw Ash to Sulfur mass ratio (5g Raw Ash and 50 mg S^0) and 4:1 mass ratio (750mg Raw Ash and 187.6 mg Sulfur) were also prepared and tested. The crucible containing ash and sulfur was placed in a custom made holder and inserted into a tube furnace (see schematic in Figure B1 in Appendix B). High purity nitrogen (99.998%) was used to purge the tube furnace throughout the

experiment at a flow rate of 500 mL/min. After 15 minutes, the air was purged out of the system, and the tube furnace was heated from room temperature to 100°C over a period of 30 minutes. The furnace was held at this temperature for 1 hour in order to remove any moisture from the sample. The furnace was then heated at a rate of 10°C/min to 200°C (just past the melting point of sulfur), and held at this temperature for 1 hour to allow liquid sulfur to mix with the Raw Ash. After this time, the furnace was heated at a rate of 5°C/min to 600°C, and held at this temperature for 2 hours before cooling to room temperature. The sulfur-loaded sample was removed and mixed with mortar and pestle for 5 minutes to ensure homogeneous distribution of the sulfur. Carbon-Nitrogen-Hydrogen-Sulfur (CHNS) content of the sample was analyzed by CHNS elemental analysis using a Thermo Carlo Erba EA 1108 analyzer at the Analytical and Instrumentation Laboratory of the University of Alberta. The CHNS analysis is based on the combustion of the sample in a Helium/Oxygen environment at 1000°C, and analysis of combustion gases by chromatography using a Porapak QS column (4 mm ID, 2 m long) and a thermal conductivity detector. The data were processed using Eager Xperience software.

In this study, lower bromine loading was used to reduce the cost and possible environmental issues with Br release from spent sorbent in landfill. Similar bromination procedures described by Bisson et al.⁴¹ were used. Briefly, 2D Br-Ash and 2D S-Ash sorbents were prepared by placing 9.0 g of Raw Ash (for 2D Br-Ash) or S-Ash (for 2D S-Ash) on top of 63g of 6-mm glass beads contained in a 250 mL gas-tight FEP jar. After addition of 2 drops of liquid Br₂ (liquid) on top of the ash, the jars were quickly capped and sealed. The jars were then packed tightly into a 10 L carboy and rolled for 30 minutes on a set of mechanical rollers. After the chemical-mechanical bromination was complete, the mixture was poured onto a tray inside a fumehood, and rested for 30 minutes. The mixture was then transferred into a vacuum oven at 200 °C for 30 minutes to remove any loosely bound bromine. Two sets of each brominated sorbent sample were prepared to ensure synthesis repeatability. The Br content of the sample was analyzed using Schöniger oxygen flask combustion method at the Analytical and Instrumentation Laboratory at the University of Alberta. During the combustion of the sample, the flue gases were captured inside a flask containing by 10 mL of 2% hydrazine sulfate solution. The solution was then acidified by nitric acid, followed by dilution with isopropanol to 80 mL. A Mettler-Toledo T70 autotitrator was used to titrate the solution with 0.01 N silver nitrate.

6.2.2 Mercury Loading and Pulse Injection Tests

Mercury pulse injection tests are a convenient way to determine if a sorbent is capable of removing mercury from gases. The test is designed to simulate the short contact time between the powdered sorbents and mercury in flue gases during powdered sorbent injection. A detailed description of the pulse injection test can be found elsewhere.⁴¹ Briefly, 40 mg of sample was loaded into a borosilicate u-tube, which was heated to the desired temperature using a GC oven. A mercury standard consisting of a pure Hg^0 ball in equilibrium with air was kept in a tightly sealed glass vessel with a syringe port, and was kept at room temperature. An accurately measured sample of 200 μl of Hg^0 in air was taken and injected into 40 ml/min Argon flow, upstream of the u-tube. The sorbent adsorbed the Hg^0 , and any portion that was not adsorbed and remained in the gas stream was preconcentrated on a gold trap downstream of the sorbent. After 5 minutes of collection, the gold trap was quickly heated to release the mercury which was detected on a Tekran 2500 CVAFS (Cold Vapor Atomic Fluorescence Spectrophotometer). The mercury that was not adsorbed or captured by the sample is divided by the amount of mercury injected, which is defined as “ Hg^0 Breakthrough” in this paper. Each sample was repeated 3 times to ensure repeatability, with the average and standard deviation being reported.

To investigate the binding mechanism of mercury on the sorbent, a sufficient amount of Hg^0 was loaded onto the sorbent samples using the procedure shown in Figure B2 in Appendix B. 75 mg of sample was weighed into a borosilicate u-tube containing quartz wool to keep the sorbent in place. The tube was placed into a GC oven and heated to 100°C. After heating the tube for 5 minutes, 100 mL/min of air was introduced, flowing over the top of a ball of mercury (Figure B2) and contacting the sorbent. The setup was left for 24 hours to achieve high mercury loading on the sample. After 24 hours the air flow was stopped, and the sample cooled down to room temperature. The sample was then removed from the u-tube and mixed for 5 minutes with mortar and pestle to ensure sample homogeneity. The mercury content of the sample was measured using a Milestone DMA-80 mercury analyzer. The mercury content in the sample was too high to directly measure by the DMA-80. To reduce mercury concentration for analysis, the sample was diluted by mixing 10 mg of the mercury loaded sorbent with 600 mg of raw activated carbon for 15 minutes using a mortar and pestle. The mercury content of the raw activated carbon was also determined using the DMA-80 in order to subtract the contribution of

mercury from the raw carbon from the diluted mixture. To ensure the validity of the method, a similar dilution procedure was applied to a standard sample (NIST 2451) containing a high mercury loading (certified value of 688 mg/kg \pm 28 mg/kg). The measured value of the standard was always within 10% of the reported value, within the known accuracy of the DMA-80 instrument. To further ensure the reliability of the data, two mixtures were made for each sample (and repeat sample), and mercury concentration was measured 3 times for each mixture. The results reported are the average and standard deviation of these measurements.

6.2.3 SEM and TEM Analysis:

Scanning Electron Microscope (SEM) and Transmission Electron Microscope (TEM) imaging was conducted by the Alberta Centre for Surface Engineering and Science (ACES). A JEOL JAMP 9500F Auger Microprobe was used for SEM images. TEM images and mapping was carried out using a CM20 FEG/STEM, which was equipped with an Oxford EDS detector. INCA software was used as an interface to the detector.

6.2.4 XAS Analysis:

Samples with and without Hg⁰ loading were sent to Canadian Light Source (CLS) for XAS analysis. Details regarding testing procedure and data analysis can be found elsewhere.³ Briefly, S K-edge XANES measurements were performed at the SXRMB beamline. Both surface sensitive total electron yield (TEY) and bulk sensitive fluorescence yield (FY) were recorded. Some surface oxidation (in the form of sulfate peak) could be observed in the TEY spectra, thus FY data of all testing samples were used for data fitting. Selected sulfur model compounds, including elemental sulfur, sulfides, sulfoxide, thiophene and sulfate, were also analyzed as reference. TEY data of model compounds were used for spectral fitting, as the FY spectrum of concentrated sample is known to suffer the self-absorption problem. Hg L_{III}-edge XANES and EXAFS were acquired using the HXMA beamline at the CLS. A 32 element Ge detector was used for fluorescence measurements, similar to our previous study.³

IFEFFIT^{42,43} software was used for all XAS data analysis. All spectra were normalized and multiple scans of each sample/element were merged using the ATHENA^{42,43} program. The data was normalized by fitting the pre-edge with a straight line and the post edge with cubic spline

function. The EXAFS function, χ , was calculated by subtracting the post edge background from the overall absorption, then normalizing with respect to the edge jump step. Peak fitting of the S K-edge was also performed using the ATHENA program. Each spectrum was fit between -20 to 20 eV from the excitation edge. The background was fit with an arctangent lineshape and the major peaks in the spectrum were fit with Gaussian lineshapes. The calculated peak areas from the fitted spectra were summed and the percent peak area was calculated for each of the sulfate, intermediate, and sulfite sulfur species.

EXAFS fitting of the Hg L-edge was performed using methods stated previously³ in the ARTEMIS program.^{42,43} Theoretical standards were generated from crystallographic data using Feff6⁴⁴ and fitted to the data using a Levenberg-Marquardt nonlinear minimization in order to extract chemical information for each sample.

6.3. Results/Discussion:

Elemental analysis results for all the samples are shown in Table 6.1. The sulfur concentration for Low S-Ash is 1.7%, while for the S-Ash sample it is 4.1%, which is similar to the optimum sulfur loading found by others.²⁰ It is interesting to note that the High S-Ash had twice the amount of elemental sulfur during impregnation compared to S-Ash, but resulted in similar final sulfur content. This result indicates a diminishing return of adding more elemental sulfur during the sample preparation. In particular, it does not seem to be possible to continue increasing mercury uptake capacity by adding more sulfur into the sorbent. Others have seen a detrimental effect of too much sulfur addition due to blockage of micropores, which restricts mercury removal.^{20,25} Table 6.1 also shows the low Br concentration on the two brominated sorbents (2D Br-S-Ash and 2D Br-Ash), ranging from 0.7-0.9%, which is much lower than the bromine content in the samples studied previously (5% for commercial brominated carbon and 8% for brominated biomass ash³). As shown in Table 6.1, the untreated raw ash sample has the highest specific BET surface area. For the sulfur-loaded samples, the specific surface area decreases in the order of Raw Ash > Low S-Ash > High S-Ash > S-Ash. The slightly higher specific surface area of High S-Ash than that of the S-Ash is possibly due to the higher sulfur concentration during impregnation of High S-Ash. The high sulfur concentration may have partially damaged the physical structure of the ash, creating a larger surface area even for similar

sulfur content. Yao et al.³⁵ suggested that sulfur vapor could act as an activating gas that etched the outer carbon surface causing an increase in pore volume and specific surface area.

Table 6.1. Elemental analysis results and BET data.

Sample	C (wt %)	H (wt %)	N (wt %)	S (wt %)	Br (wt %)	BET (m ² /g)
Raw Ash	37.9 ± 4.9	0.5 ± 0.1	0.1 ± 0.1	0.4 ± 0.1	-	210
Low S-Ash	44.8 ± 7.5	0.4 ± 0.1	0.1 ± 0.1	1.7 ± 0.2	-	185
S-Ash	34.1 ± 3.1	0.3 ± 0.1	0.1 ± 0.1	4.1 ± 0.5	-	130
High S-Ash	29.0 ± 1.9	0.2 ± 0.1	0.1 ± 0.1	3.8 ± 0.6	-	147
2D Br-S-Ash	31.7 ± 1.0	0.4 ± 0.1	0.1 ± 0.1	3.8 ± 0.2	0.9 ± 0.1	119
2D Br-Ash	35.6 ± 0.3	0.4 ± 0.1	0.1 ± 0.1	0.4 ± 0.1	0.7 ± 0.1	178

The results from the Hg⁰ pulse injection tests for the sulfur samples are shown in Figure 6.1. An effective sorbent for Hg⁰ capture by powdered activated carbon sorbents should have a low breakthrough (i.e. high Hg⁰ capture). The untreated Raw Ash captured mercury at low temperatures, but performed poorly above 100 °C, exhibiting the worst mercury capture among all the samples tested. Above 200 °C, all the sorbents in Figure 6.1 show high Hg⁰ breakthrough, indicating that they are not effective sorbents for Hg⁰ capture at these temperatures. However, at 200 °C (and below), the breakthrough of mercury is very low (<1%) for the S-Ash sorbent, indicating that the impregnation of biomass ash can capture mercury at typical powdered activated carbon temperatures (approximately 150 °C). In comparison, the Low-S-Ash exhibits higher Hg⁰ breakthrough than the S-Ash, and the High S-Ash Hg⁰ breakthrough is slightly higher than the S-Ash. It seems that the initial wood ash:sulfur impregnation ratio of the S-Ash is at its optimum value, as the lower and higher ratios led to less adequate mercury capture performance. The difference in mercury capture ability is interesting as the sulfur content of S-Ash and High S-Ash is similar and High S-Ash has a slightly higher specific surface area. It appears that the accessibility and/or the form of sulfur play a role in determining the effectiveness of loaded sulfur. Figure 6.2 Shows the SEM images of raw ash compared with the S-Ash and High S-Ash. The raw ash is the most porous (which agrees well with the result of the highest specific surface

area). S-Ash and High S-Ash appear to have different pore shapes compared to raw ash. S-Ash also has more mesopores than the other two samples (Figure 6.2). Since S-Ash (with more mesopores) exhibited a higher Hg^0 removal efficiency in the pulse injection test, the mesopores might actually be an important feature for Hg^0 capture during the short contact time experiment. In the case of the High S-Ash sample, it appears that some of the larger pores have been filled by sulfur, which makes it more difficult for mercury to access the micropores. It is possible that during the sulfur loading, the high amount of liquid S^0 present filled and blocked some of the pores during the 200 °C step, resulting in different surface sulfur distribution than when lower concentrations of S^0 were present during impregnation. The reduction in mercury capture by mesopore filling with sulfur has also been seen by others.^{20,25} The sulfur distribution on the S-Ash and High S-Ash was investigated using TEM mapping by EDS (Figure 6.3). The mapping shows that the bright spots seen on the image contain calcium. In the case of the S-Ash (Figure 6.3a), the sulfur is fairly evenly distributed across the sample. However, in High-S-Ash (Figure 6.3b), the bright spots of the sulfur seem to overlap with the calcium, suggesting that some of the sulfur may be bonded to calcium in the sample. Combining the results in Figures 6.1 and 6.3 indicate that the sulfur bonded to calcium may be less effective in the capture of mercury, making S-Ash a more effective at mercury capture than High S-Ash.

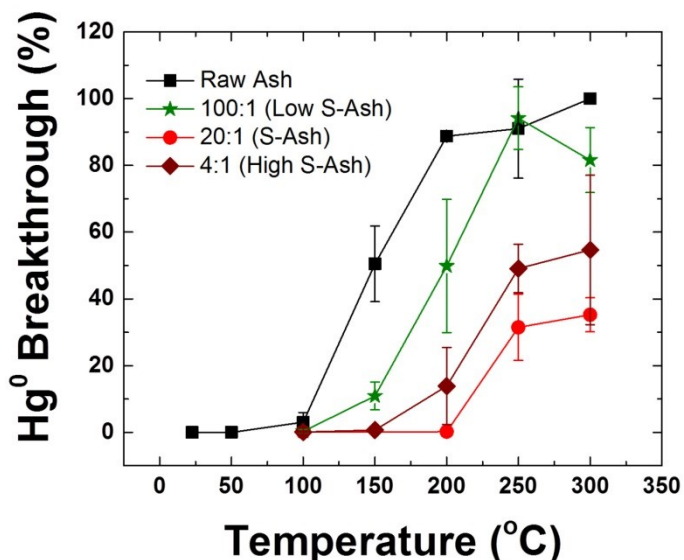


Figure 6.1. Mercury Breakthrough of sulfur-loaded samples.

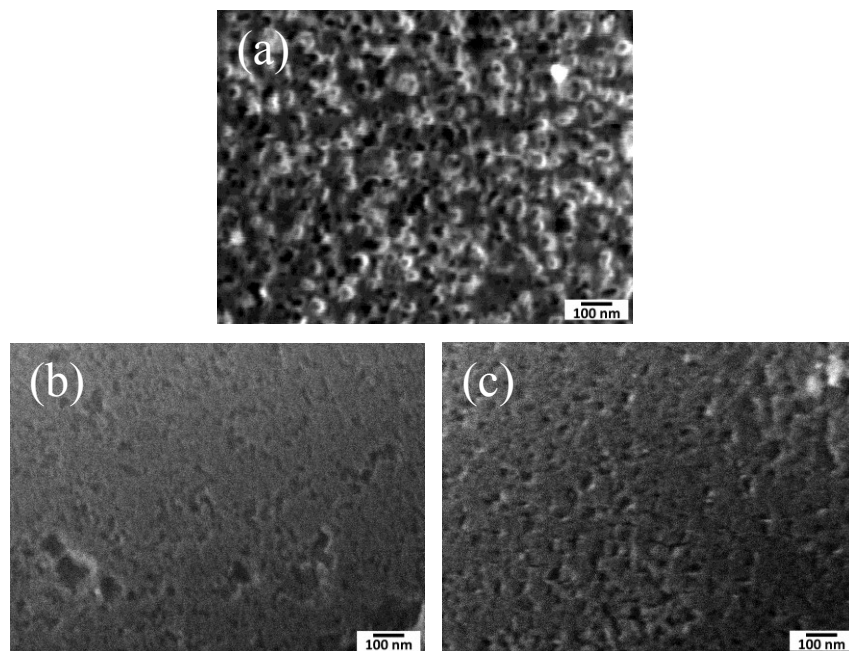


Figure 6.2. High resolution SEM images of (a) Raw Ash;⁴¹ (b) S-Ash; (c) High S-Ash.

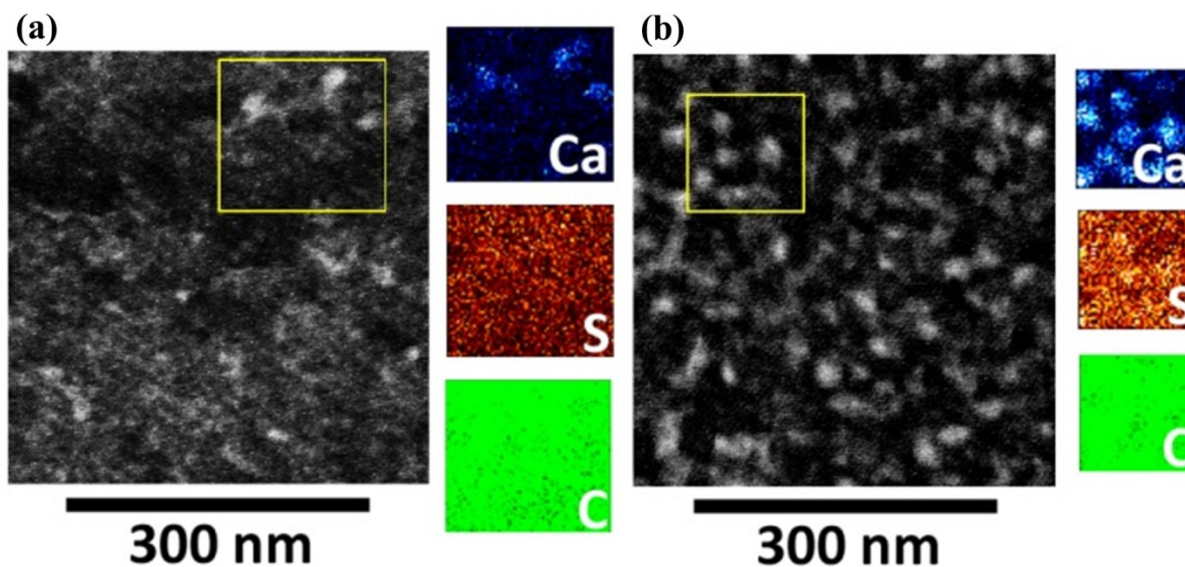


Figure 6.3. TEM images mapped by EDS for (a) S-Ash and (b) High S-Ash.

Based on the better Hg^0 capture capability (optimum sulfur loading level), S-Ash was chosen for bromination. The goal of Br impregnation was to improve mercury capture performance

(which would result in lower Hg^0 breakthrough). Figure 6.4 compares the results of Hg^0 pulse injection tests of the brominated S-Ash with non-brominated S-Ash and 2D Br-Ash (no sulfur). At high temperatures (e.g. 300 °C), both S-Ash and 2D Br-Ash exhibit significant Hg^0 breakthrough. However, when the sulfur and a small amount of bromine are combined, as in the 2D Br-S-Ash sample, the mercury capture is dramatically improved as shown by low breakthrough of the mercury pulse. This above additive improvement could be a result of different mercury capture mechanisms, i.e., different binding environment of mercury with the sulfur and bromine together on biomass ash. To confirm the different mercury binding mechanisms between the sorbents, mercury loading tests and subsequent XAS analysis were performed.

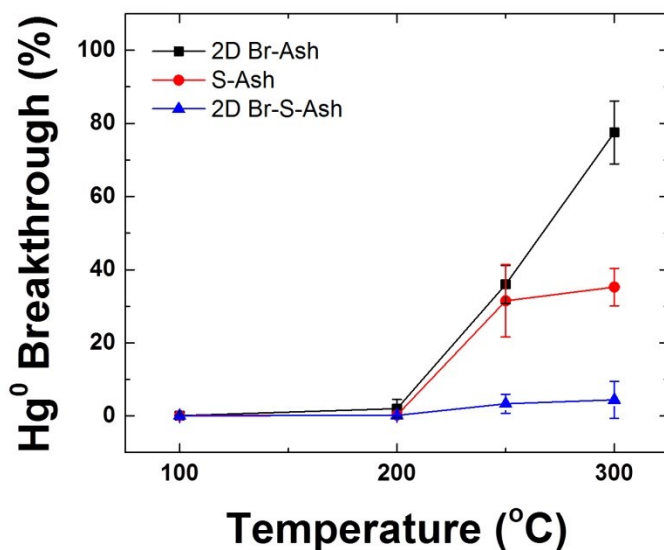


Figure 6.4. Mercury breakthrough of sulfur and low Br-Ash samples.

Mercury loading tests were conducted to compare mercury capture capacity of the sorbents over an extended period (24 h) and to prepare samples for XAS analysis. Figure 6.5 shows the results of mercury loading tests for all the samples studied. All the treatments of raw biomass ash increased Hg loading. Of the samples treated with sulfur only, the S-Ash has the greatest mercury uptake. The result for the S-Ash is similar to that of the maximum mercury uptake by an elemental sulfur-impregnated activated carbon (same impregnation temperature), reported by Liu et al.²⁹ to be 2200 ppm (Note: Testing by Liu et al. was at 140°C in a fixed bed reactor

using 100 mg sample, 1.0 L/min N₂ flow and 55 µg/m³ mercury inlet concentration, which is different from the testing conditions of the current study). It can also be seen in Figure 6.5 that the samples loaded with both bromine and sulfur (2D Br-S-Ash) outperformed the brominated (2D Br-Ash) or sulfur-impregnated (S-Ash) samples, even though 2D Br-S-Ash has a lower surface area than the other sorbents. The improved mercury capture performance demonstrates the benefit of combining both Br and S on the sorbent. Adding the mercury captured by brominated (2D Br-Ash) and sulfur-impregnated (S-Ash) samples results in a combined mercury capture of 4917ppm. This amount was only slightly higher than the amount captured by the combined sorbent (2D Br-S-Ash) that could be considered within the experimental error, as shown in Figure 6.5. The additive nature of the Hg⁰ capture by S and Br on the sorbent indicates that the sorbents can be engineered with varying Br and S concentrations to achieve a desired design of sorbent capacity, depending on the application conditions. Br utilization was calculated based on the total mercury that could theoretically bind with all of the bromine on the sorbent (BA100* in Figure 4.3 and 2D Br-Ash in Figure 6.5). The utilization improved for the 2D Br-Ash compared to the original Br-Ash, which was 18% compared to 2%, respectively. In a similar fashion, the S utilization was calculated for Low S-Ash, S-Ash and High S-Ash, and was <1% for all three samples.

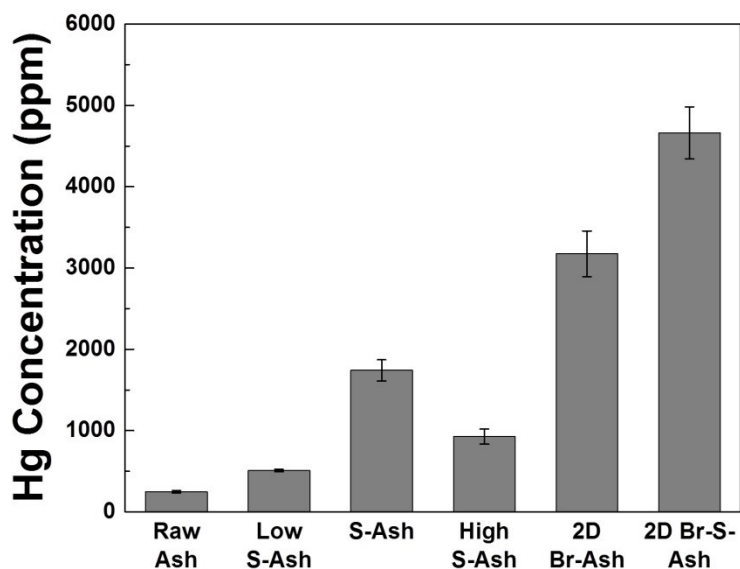


Figure 6.5. Mercury loading test results indicating the amount of Hg⁰ the sorbents are able to capture during a 24 hour period of mercury exposure in air at 100 °C.

The speciation of sulfur is known to impact removal of Hg^0 by activated carbon.^{3,20,24,29} Sulfur K-edge spectra were obtained for all the samples tested in this study to better understand the possible Hg^0 capture mechanisms and improve future sorbent design. The sulfur K-edge spectra containing the sulfur-impregnated sorbents can be seen in Figure 6.6a. Three dominant sulfur peaks can be seen, and show the differences between the S present in the raw ash and the sulfur-impregnated samples. The sulfur in the raw ash is predominantly in the oxidized (sulfate) form ($E_0 \sim 2481.6$ eV), while the sulfur loaded samples (Low S-Ash, S-Ash, High S-Ash and 2D Br-S-Ash) contain the sulfate peak as well as two others at $E_0 \sim 2472$ and 2474 eV. The peak at 2472 indicates sulfur in the reduced form (e.g. sulfur, S^0 , and sulfide, S^{2-}). The peak at 2474 eV is due to an intermediate sulfur species (e.g. sulfoxide and thiophene). Considering these results in addition to the mercury capture and loading results (shown in Figures 6.2 and 6.5), some observations can be made about the speciation of sulfur and the mercury uptake. The raw ash had a low mercury uptake and had sulfur predominantly in the form of sulfate, indicating that sulfate does not play a major role in the mercury removal by the functionalized sorbents. After sulfur addition, the amount (intensity) of S^0 and S^{2-} increases while the relative intensity of sulfate decreases. This shows that the loading procedure is performing well by increasing S^0 and S^{2-} , which are known to be more effective in Hg^0 capture.^{3,22} The amount of intermediate sulfur species also increases, but it is not known if these species are contributing to Hg^0 capture. Amplitude analysis was calculated from the fitted peak area to better understand the changes in sulfur speciation after sulfur loading (Figure 6.6b). The speciation of sulfur is quite different between the Low S-Ash, S-Ash and High S-Ash samples. From Low S-Ash to S-Ash, the amount of oxidized S decreases, while the intermediate and reduced sulfur species increases, along with the mercury capture (Figures 6.2 and 6.5). The High S-Ash sample also has a higher intermediate and reduced sulfur species content with lower oxidized S, however, the mercury uptake is lower than the S-Ash. Overall, higher concentrations of intermediate and reduced sulfur species may improve mercury capture, but if combined with pore blockage, low mesopore formation, or bonding of S to Ca (as described earlier), the addition of more reduced S species may no longer improve mercury capture.

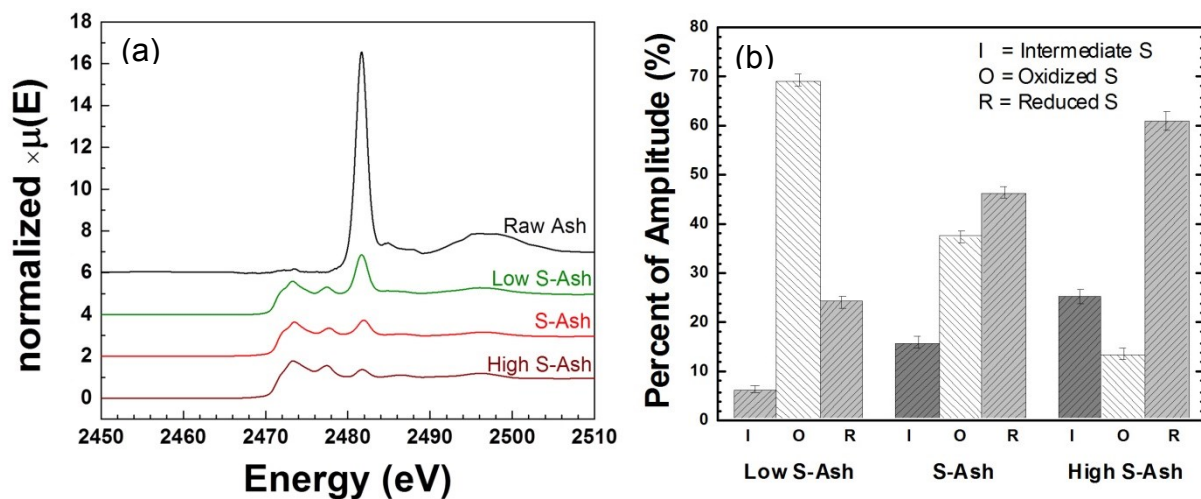


Figure 6.6. Sulfur K-edge results for varying sulfur contents. (a) FY Spectra; (b) S K-edge amplitude analysis providing speciation.

Sulfur K-edge spectra were also obtained for the S-Ash sample and 2D Br-S-Ash sample with and without Hg^0 (Figure 6.7a). The samples appear to have slightly more sulfate and less reduced sulfur species present after mercury capture. 2D Br-Ash (not shown) was found to be predominantly in the oxidized (sulfate) form. The changes in sulfur speciation after mercury exposure were also determined from the fitted peak area (Figure 6.7b). After exposure to Hg^0 , the S-Ash sample has an increased sulfate concentration (3.2% of sulfur species) and corresponding decreased intermediate and reduced sulfur compounds, likely due to oxygen exposure or reactions of Hg and sulfur, causing the oxidation of sulfur during the experiments. In comparison, the 2D Br-S-Ash sample had a much smaller difference in sulfur speciation (<0.6% of sulfur species) after exposure to Hg^0 . Comparing S-Ash to 2D Br-S-Ash, it can be seen that after Br addition, more S was oxidized (sulfate) and less of the S was in the intermediate and reduced forms. During the bromination procedure, the sample is exposed to air in a vacuum oven at 200 °C, so the oxidation could occur during that step. This oxidation before Hg^0 addition could explain why the 2D Br-S-Ash has less change in speciation after Hg^0 addition compared to S-Ash.

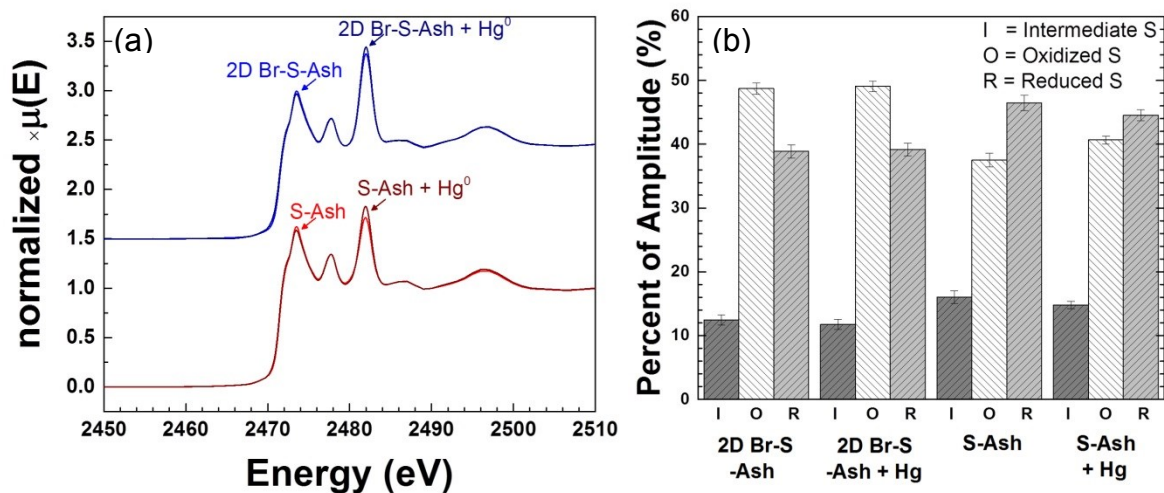


Figure 6.7. Sulfur K Edge comparing samples before and after Hg⁰ exposure. (a) FY Spectra (b) amplitude analysis providing speciation.

Hg L_{III} -edge data obtained for Hg-S-Ash, Hg-2D-Br-S-Ash and Hg-2D-Br-Ash (Figure 6.8) show very different binding environments between the 3 samples. The sample loaded with both Br and S appears to have a binding environment that is a combination of the other two samples (i.e. the spectra lies in between the two others). Inflection point difference (IPD) was calculated from the derivative spectra (inset Figure 6.8) and is given in Table 6.2. IPD values can give insight into the type of bonding environment around the Hg atoms. The higher the IPD, the higher the ionicity of the Hg bond.⁶ The IPD values for the samples were in the range of 7.4 – 7.7 eV, which is more ionic than the Br-Ash previously tested (IPD = 5.6).³

IPD is an approximate measure and should not be used alone to determine bonding environment, but can be used along with EXAFS to better understand the Hg⁰ speciation.³ Hg EXAFS were obtained to determine more precisely the bonding environment of the Hg species on the samples (Figure B3 in Appendix B), including the fits to the spectra as described in the experimental section (Table 6.2). In the case of S-Ash, the EXAFS data show that mercury is associated with sulfur and carbon on the ash, which is similar to the commercial activated carbon tested in our previous paper.³ In addition, the IPD value of 7.5 eV is similar to that seen by others for HgS.^{4,6} Amplitude values were also determined for Hg⁰ (Table 6.2, Figure 6.9), and show that the weighting of Hg coordination was predominantly with the sulfur species.

Considering the sulfur data shown above, it is interesting to note that there was no change in speciation in the sulfur spectra after Hg^0 exposure. However, if Hg^0 reacted with one sulfide species to form a different sulfide species, the new sulfide species would not be able to be distinguished from the rest of the reduced sulfur spectra. For example, the formation of HgS would be reflected in the reduced sulfur species peak of the sulfur K-edge spectra. If this species was formed, it would not be resolved in the sulfur K-edge spectra, making it difficult to determine the precise chemistry of the captured mercury. However, the bonding of Hg to S species indicates that the mercury capture mechanism for the S-Ash is likely similar to the mechanism previously proposed, which involves mercury oxidation, followed by subsequent binding to sulfur species on the sample.^{3,35} In the case of 2D Br-Ash, the mercury is associated with Br and carbon. It is interesting to note that even though the Br concentration is very low (<1%), the Hg is primarily associated with Br on the sorbent, indicating its importance in Hg^0 capture. The mechanism of Hg^0 removal is likely similar to that seen for Br-Ash involving surface enhanced oxidation of Hg and binding of oxidized Hg to Br species on the sorbent.³ The combined Br/S/Ash sample (2D Br-S-Ash), appears to be a combination of binding environments, with mercury associated with S, Br and C in this case. Given the margin of error in Figure 6.9, it is difficult to determine which species is dominant. Based on the XANES spectra and EXAFS modeling, the mechanism in this case is likely to be a blend of the mechanisms given for the S and Br samples, consisting of surface enhanced oxidation, followed by binding of the oxidized mercury to S, Br or C. The proposed mechanism for the combined Br-S-Ash sample is illustrated in Figure 6.10.

Table 6.2. Mercury XANES and EXAFS results summary.

Sample	IPD (eV)	k- range (Å)	Path	CN	Amp	R (Å)	σ^2 (Å ²)	ΔE (eV)	R- factor
2D Br-S-Ash +Hg	7.494	2-12	^c Hg-S	2	0.509 ±0.190	2.362 ± 0.022	0.003 ±0.004	3.37 ±2.08	0.001
			^b Hg-Br	2	0.460 ±0.338	2.547 ± 0.022	0.007 ±0.006		
			^a Hg-C	2	0.306 ±0.148	2.247 ± 0.118	0.013 ±0.026		
S-Ash +Hg	7.672	2-12	^c Hg-S	2	1.96 ±0.33	2.518 ± 0.012	0.010 ±0.003	7.83 ±1.34	0.007
			^a Hg-C	2	0.740 ±0.170	2.367 ± 0.021	-0.003 ±0.002		
2D Br-Ash +Hg	7.434	2-12	^b Hg-Br	2	0.956 ±0.138	2.506 ± 0.0081	0.006 ±0.001	-2.53 ±1.72	0.008
			^a Hg-C	2	0.612 ±0.361	2.164 ± 0.039	0.028 ±0.018		

^aCrystal structure from HgC₂ ⁴⁵ ^bCrystal structure from HgBr₂ ⁴⁶ ^cCrystal structure from Hg(mpHg)₂ ⁴⁷

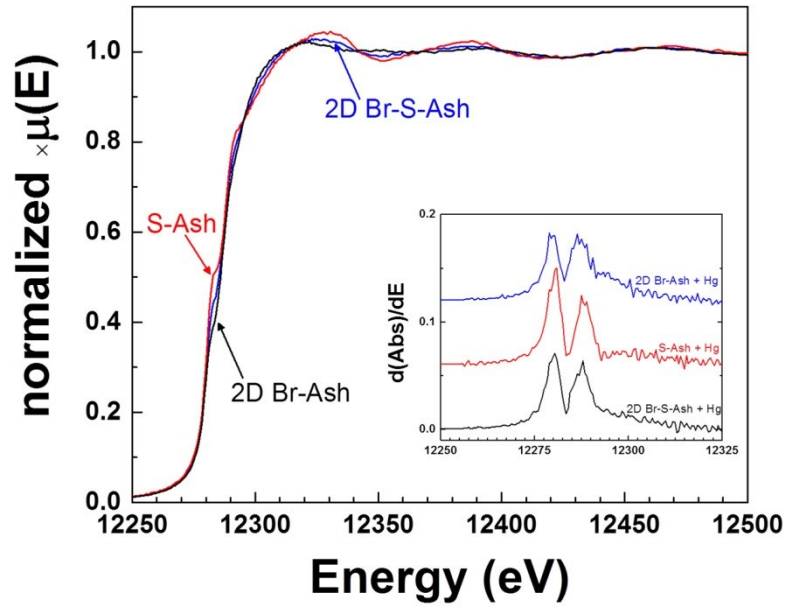


Figure 6.8. Mercury L_{III} -edge XANES spectra. Inset: First derivative of normalized XANES spectra.

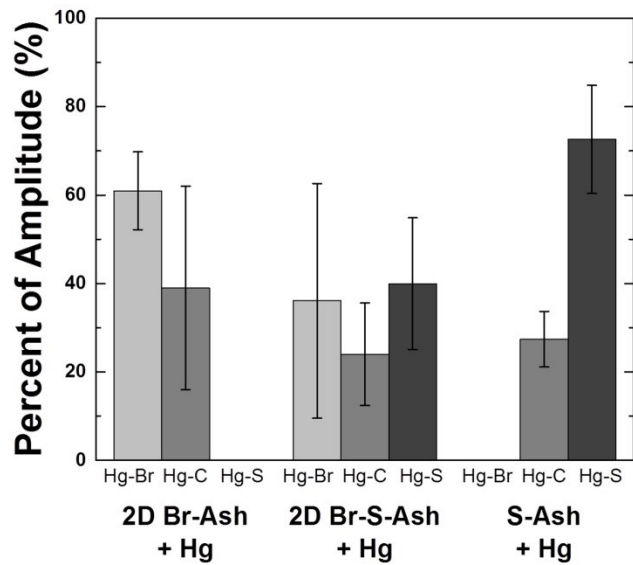


Figure 6.9. Mercury EXAFS amplitude analysis for the samples.

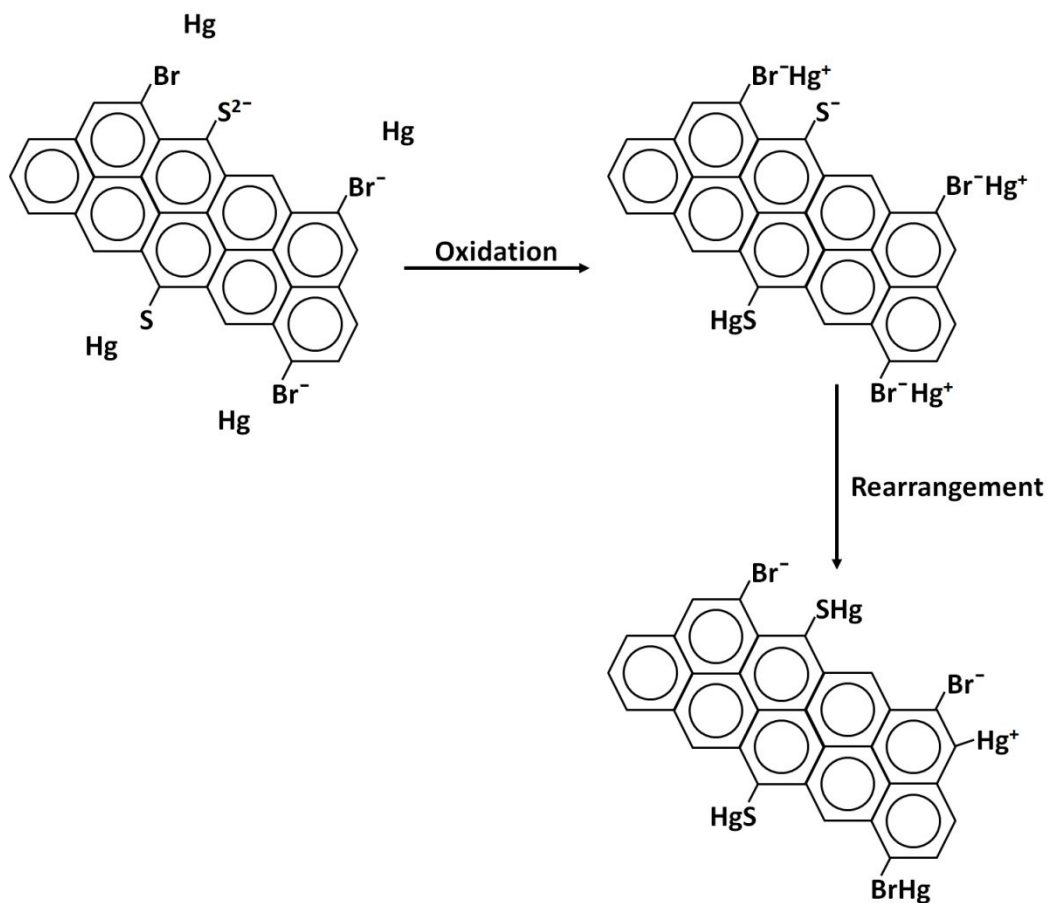


Figure 6.10. Illustration of proposed mechanism of Hg^0 capture by 2D Br-S-Ash. Fused rings represent carbon in wood ash.

The toxicity characteristic leaching procedure (TCLP) test was conducted for the S-Ash, 2D Br-Ash and 2D Br-S-Ash samples following the method described in Section 5.2. Results for the mercury and bromine leach tests are given in Tables B1 and B2, respectively (Appendix B). In addition to the new samples, the results for the Br-Ash are included for comparison. All samples in Table B1 are below the 0.2 mg/L target for mercury. The 2D Br-Ash sample has a higher mercury concentration in the leachate compared with the other samples, indicating that for low Br concentrations, addition of sulfur onto the ash appears to stabilize the mercury. The Br leaching test results (Table B2) show that the bromine concentrate in the leachate is much lower for samples 2D Br-Ash and 2D Br-S-Ash than the Br-Ash. This is due to a much lower bromine concentration on the samples. The 2D Br-S-Ash and 2D Br-Ash also have a lower Br % leached

compared to Br-Ash, indicating that the bromine present at low concentrations is more stable. The 2D Br-S-Ash was also tested for the case that was found to have the highest bromine and mercury leach in the expanded leach tests in section 5.3 (liquid:solid ratio of 2). The bromine and mercury concentrations in the leachate of 2D Br-S-Ash was significantly lower than the Br-Ash (Figure 6.11). In addition, the mercury concentration in the leachate of 2D Br-S-Ash was lower than the 0.2 mg/L limit set by the EPA.⁴⁸

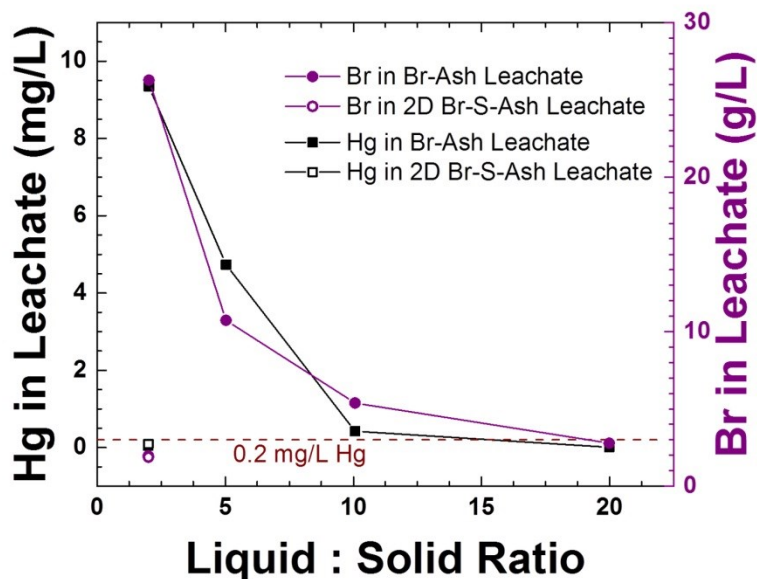


Figure 6.11. Hg and Br leached from 2D Br-S-Ash compared to original Br-Ash Sorbent. 0.2 mg/L line shows the limit imposed by the EPA for Hg leaching.⁴⁸

Combined sulfur-impregnation with low bromine impregnation on wood ash has resulted in a sorbent with good mercury capture capacity, potential lower costs and lower environmental impact due to lower leaching of Br and Hg. Follow-up tests in real flue gases can confirm the effectiveness of the combined Br-S-Ash sorbent for mercury capture.

6.4. References:

- (1) Yang, H.; Xu, Z.; Fan, M.; Bland, A.E.; Judkins, R.R. Adsorbents for capturing mercury in coal-fired boiler flue gas. *Journal of Hazardous Materials*. **2007**, *146*, p. 1-11.
- (2) Wilcox, J.; Sasmaz, E.; Kirchofer, A.; Lee, S.-S. Heterogeneous Mercury Reaction Chemistry on Activated Carbon. *J. Air Waste Manage. Assoc.* **2011**, *61*, 418–426.
- (3) Bisson, T. M.; MacLean, L.C.W.; Hu, Y.; Xu, Z. Characterization of Mercury Binding onto a Novel Brominated Biomass Ash Sorbent by X-ray Absorption Spectroscopy. *Environ. Sci. Technol.* **2012**, *46*, p. 12186–12193.
- (4) Hutson, N. D.; Attwood, B. C.; Scheckel, K. G. XAS and XPS characterization of mercury binding on brominated activated carbon. *Environ. Sci. Technol.* **2007**, *41*, 1747–1752.
- (5) Huggins, F. E.; Huffman, G. P.; Dunham, G. E.; Senior, C. L. XAFS examination of mercury sorption on three activated carbons. *Energy Fuels*. **1999**, *13*, 114–121.
- (6) Huggins, F. E.; Yap, N.; Huffman, G. P.; Senior, C. L. XAFS characterization of mercury captured from combustion gases on sorbents at low temperatures. *Fuel Proc. Technol.* **2003**, *82*, 167–196.
- (7) Uddin, M. A.; Ozaki, M.; Sasaoka, E.; Wu, S. Temperature-Programmed Decomposition Desorption of Mercury Species over Activated Carbon Sorbents for Mercury Removal from Coal-Derived Fuel Gas. *Energy Fuels*. **2009**, *23*, 4710–4716
- (8) Pavlish, J. H.; Sondreal, E. A.; Mann, M. D.; Olson, E. S.; Galbreath, K.C.; Laudal, D. L.; Benson, S. A. Status review of mercury control options for coal-fired power plants. *Fuel Process. Technol.* **2003**, *82*, 89–165.
- (9) Olson, E. S.; Azenkeng, A.; Laumb, J. D.; Jensen, R. R.; Benson, S. A.; Hoffmann, M. R. New developments in the theory and modeling of mercury oxidation and binding on activated carbons in flue gas. *Fuel Process. Technol.* **2009**, *90*, 1360–1363
- (10) Laumb, J. D.; Benson, S. A.; Olson, E. A. X-ray photoelectron spectroscopy analysis of mercury sorbent surface chemistry. *Fuel Process. Technol.* **2004**, *85*, 577– 585
- (11) Padak, B.; Brunetti, M.; Lewis, A.; Wilcox, J. Mercury Binding on Activated Carbon. *Environ. Prog.* **2006**, *25*, 319-326.

- (12) Granite, E. J.; Pennline, H.W.; Hargis, R. A. Novel Sorbents for Mercury Removal from Flue Gas. *Ind. Eng. Chem. Res.* **2000**, *39*, 1020-1029
- (13) Ho, T. C.; Ghai, A. R.; Guo, F.; Wang, K. S.; Hopper, J. R. Adsorption and Desorption of Mercury on Sorbents at Elevated Temperatures. *Combust. Sci. Tech.* **1998**, *134*, 263-289.
- (14) Qu, Z.; Chang, J. J.; Hsiung, T-L.; Yan, N.; Wang, H. P.; Dod, R.; Chang, S-G.; Miller, C. Halides on Carbonaceous Materials for Enhanced Capture of Hg⁰: Mechanistic Study. *Energy Fuels.* **2010**, *24*, 3534–3539
- (15) Liu, J.; Qu, W.; Zheng, C. Theoretical studies of mercury–bromine species adsorption mechanism on carbonaceous surface. *Proceedings of the Combustion Institute.* **2013**, *34*, 2811–2819.
- (16) Sasmaz, E.; Kirchofer, A.; Jew, A. D.; Saha, A.; Abram, D.; Jaramillo, T. F.; Wilcox, J. Mercury chemistry on brominated activated carbon. *Fuel.* **2012**, *99*, 188–196.
- (17) Wilcox, J.; Rupp, E.; Ying, S. C.; Lim, D. –H.; a, Suarez Negreira, A.; Kirchofer, A.; Feng, F.; Lee, K. Mercury adsorption and oxidation in coal combustion and gasification processes. *Int. J. Coal Geol.* **2012**, *90-91*, 4–20.
- (18) Sinha, R. K.; Walker Jr., P. L. Removal of mercury by sulfurized carbons. *Carbon.* **1972**, *10*, 754-756.
- (19) Daza, L.; Mendioroz, S.; Pajares, J. A. Mercury elimination from gaseous streams. *Appl. Catal. B. Environ.* **1993**, *2*, 277-287.
- (20) Feng, W.; Kwon, S.; Feng, X.; Borguet, E.; Vidic, R. D. Sulfur impregnation on activated carbon fibers through H₂S oxidation for vapor phase mercury removal. *J. Environ. Eng.* **2006**, *132*, 292-300.
- (21) Kwon, S.; Vidic, R. D. Evaluation of two sulfur impregnation methods on activated carbon and bentonite for the production of elemental mercury sorbents. *Environ. Eng. Sci.* **2000**, *17*, 303-313.
- (22) Feng, W.; Borguet, E.; Vidic, R. D. Sulfurization of a carbon surface for vapor phase mercury removal – II: Sulfur forms and mercury uptake. *Carbon.* **2006**, *44*, 2998-3004.
- (23) Morimoto, T.; Wu, S.; Uddin, M. A.; Sasaoka, E. Characteristics of the mercury vapor removal from coal combustion flue gas by activated carbon using H₂S. *Fuel.* **2005**, *84*, 1968-1974.

- (24) Hsi, H. C.; Chen, S.; Rostam-Abadi, M.; Rood, M. J.; Richardson, C. F.; Carey, T. R.; Chang, R. Preparation and Evaluation of coal-derived activated carbons for removal of mercury vapor from simulated coal combustion flue gases. *Energy Fuels*, **1998**, *12*, 1061-1070.
- (25) Hsi, H.-C.; Rood, M. J.; Rostam-Abadi, M.; Chang, Y.-M. Effects of sulfur, nitric acid, and thermal treatments on the properties and mercury adsorption of activated carbons from bituminous coals. *Aerosol Air Qual. Res.* **2013**, *13*, p. 730-738.
- (26) Hsi, H. C.; Rood, M. J.; Rostam-Abadi, M.; Chen, S.; Chang, R. Effects of sulfur impregnation temperature on the properties and mercury adsorption capacities of activated carbon fibers (ACFs). *Environ. Sci. Technol.* **2001**, *35*, 2785-2791.
- (27) Hsi, H. C.; Chen, C. T. Influences of acidic/oxidizing gases on elemental mercury adsorption equilibrium and kinetics of sulfur-impregnated activated carbon. *Fuel*. **2012**, *98*, 229-235.
- (28) Steijns, M.; Peppelenbos, A.; Mars, P. Mercury chemisorption by sulfur adsorbed in porous materials. *J. Colloid Interface Sci.* **1976**, *57*, 181-186.
- (29) Liu, W.; Vidic, R. D.; Brown, T. D. Optimization of sulfur impregnation protocol for fixed-bed application of activated carbon-based sorbents for gas-phase mercury removal. *Environ. Sci. Technol.* **1998**, *32*, 531-538.
- (30) Suresh Kumar Reddy, K.; Al Shoaibi, A.; Srinivasakannan, C. Gas-phase mercury removal through sulfur impregnated porous carbon. *J. Ind. Eng. Chem.* **2014**, *20*, 2969-2974.
- (31) Ie, I.-R.; Shen, H. Z.; Yuan, C.-S.; Hung, C.-H.; Chen, W.-H.; Jen, Y.-H. Single and dual adsorption of vapor-phase Hg^0 and/or HgCl_2 by innovative composite activated carbons impregnated with both S^0 and Na_2S . *Aerosol Air Qual. Res.* **2014**, *14*, 376-385.
- (32) Korpiel, J. A.; Vidic, R. D. Effect of sulfur impregnation method on activated carbon uptake of gas-phase mercury. *Environ. Sci. Technol.* **1997**, *31*, 2319-2325.
- (33) Ie, I. R.; Chen, W. C.; Yuan, C. S.; Hung, C. H.; Lin, Y. C.; Tsai, H. H.; Jen, Y. S. Enhancing the adsorption of vapor-phase mercury chloride with an innovative composite sulfur-impregnated activated carbon. *J. Hazard. Mater.* **2012**, *217-218*, 43-50.
- (34) Otani, Y.; Emi, H.; Kanaoka, C.; Uchijima, I.; Nishino, H. Removal of mercury vapor from air with sulfur-impregnated adsorbents. *Environ. Sci. Technol.* **1988**, *22*, 708-711.

- (35) Yao, Y.; Velpari, V.; Economy, J.; Design of sulfur treated activated carbon fibers for gas phase elemental mercury removal. *Fuel*. **2014**, *116*, 560-565.
- (36) Yan, N.; Qu, Z.; Chi, Y.; Qiao, S.; Dod, R. L.; Chang, S.; Miller, C. Enhanced elemental mercury removal from coal-fired flue gas by sulfur-chlorine compounds. *Environ. Sci. Technol.* **2009**, *43*, 5410-5415.
- (37) Qu, Z.; Yan, N.; Liu, P.; Guo, Y.; Jia, J. Oxidation and stabilization of elemental mercury from coal-fired flue gas by sulfur monobromide. *Environ. Sci. Technol.* **2010**, *44*, 3889-3894.
- (38) Saha, A.; Abram, D. N.; Kuhl, K. P.; Paradis, J.; Crawford, J. L.; Sasmaz, E.; Chang, R.; Jaramillo, T. F.; Wilcox, J. An X-ray photoelectron spectroscopy study of surface changes on brominated and sulfur-treated activated carbon sorbents during mercury capture: performance of pellet versus fiber sorbents. *Environ. Sci. Technol.* **2013**, *47*, 13695-13701.
- (39) Bandosz, T. J.; Ania, C. O. Surface chemistry of activated carbons and its characterization. In: *Activated Carbon Surfaces in Environmental Remediation*. Amsterdam; London: Elsevier, 2006. Edited by Bandosz, Teresa J. pages 159-229.
- (40) SunSirs China Commodity Data Group. 100 Spot Commodities Price Chart – 09/05/2014. <http://www.sunsirs.com/uk/sdetail.html>. Accessed May 10, 2014.
- (41) Bisson, T. M.; Xu, Z.; Gupta, R.; Maham, Y.; Liu, Y.; Yang, H.; Clark, M.; Patel, M. Chemical–mechanical bromination of biomass ash for mercury removal from flue gases. *Fuel*. **2013**, *108*, p.54-59.
- (42) Newville, M. EXAFS analysis using FEFF and FEFFIT. *J. Synchrotron Radiat.* **2001**, *8*, 96–100.
- (43) Ravel, B.; Newville, M. ATHENA, ARTEMIS, HEPHAESTUS: Data analysis for X-ray absorption spectroscopy using IFEFFIT. *J. Synchrotron Radiat.* **2005**, *12*, 537–541.
- (44) Zabinsky, S. I.; Rehr, J.J.; Ankudinov, A; Albers, R. C. Multiple scattering calculations of X-ray absorption spectra. *Phys. Rev. B: Condens. Mater. Phys.* **1995**, *52*, 2995-3009.
- (45) Wang, S.; Fackler, J. P. Mercury complexes with one dimensional chain structures. Syntheses and crystal structures of $[\text{Hg}(\text{C}_5\text{H}_4\text{NS})(\text{CH}_3\text{CO}_2)]_n$, $\text{Hg}(\text{C}_5\text{H}_4\text{NS})_2$, and $\text{Hg}(\text{CH}_2\text{P}(\text{S})\text{Ph})_2$. *Inorg. Chem.* **1989**, *28*, 2615–2619.
- (46) Braekken, H. The crystal structure of HgBr_2 . *Z. Kristallogr.* **1932**, *81*, 152–154.

- (47) Popović, Z.; Matković-Čalogović, D.; Hasić, J.; Sikirica, M.; Vikić-Topić, D. Binding of Mercury(II) by N-(2-mercapto-propionyl)glycine. Synthesis, IR and NMR Characterization. Crystal Structure of the 1: 2 Solvate of Bis[N-(propionyl-2-thiolato)- glycine]mercury(II) with 4-Methylpyridine. *Croatica Chemica Acta*. **1999**, *72*, 279-294.
- (48) Environmental Protection Agency. Hazardous waste characteristics, a user-friendly reference document. (2009)
<http://www.epa.gov/osw/hazard/wastetypes/wasteid/char/hw-char.pdf>
(Accessed April 14, 2014).

Chapter 7

Thesis Summary, Conclusions and Future Work

7.1. Results Summary and Conclusions

Biomass ash as a waste from combustion of wood ash was used as a carbon source material to prepare a brominated carbon sorbent (Br-Ash). The Br-Ash was found to be capable of efficiently capturing elemental mercury (Hg^0) in an argon atmosphere up to 390 °C, as well as from exposure to actual flue gases of a power plant. Thermogravimetric analysis showed that the bromine was thermally stable on the brominated ash with approximately 20% bromine loss upon heating to 650 °C, and was more stable than the commercial brominated activated carbon. The biomass ash achieved good mercury removal performance without any thermal or chemical activation treatment which reduces costs as compared to traditional activated carbons or other studies involving activating waste materials.

Leaching tests on the Br-Ash and commercial brominated activated carbon (Br-AC) sorbents showed that Br leaches considerably, but is slightly more stable on the Br-Ash than on commercial Br-AC. It is recommended that before disposal of brominated carbon materials, potential impacts of any leached Br should be considered and monitored. Leaching of bromine was not affected by mercury present on the Br-Ash samples (i.e. the samples with and without mercury lost the same amount of Br). After leaching of the Br, the leached Br-Ash and commercial Br-AC were still able to capture an injected pulse of mercury up to 250 °C, but not at higher temperatures. The leached bromine (or greater bromine concentration) appears to only be important for mercury capture at temperatures greater than 250 °C. The amount of mercury leached by the toxic characteristic leaching procedure was very low and is not anticipated to be a problem for the Br-Ash. Since mercury leaching is so low, it is possible to pretreat the sorbent by water washing in order to remove the Br before disposal, particularly if water quality limits are expected to be exceeded. The low leaching of mercury but high leaching of Br also indicate

that Hg is either not bound to Br or was bound to the Br that didn't leach. Alternatively, Hg⁰ could also be bound to carbon on the sorbent. Leaching tests were also conducted at various pH and liquid to solid ratios to estimate different possible landfill conditions. Mercury was found to leach at high pH, low pH and low liquid to solid mass ratios. For the tests at natural pH, mercury concentration in the leachate followed the same trend as Br concentration in the leachate. It is possible that the high Br concentration in the leachate is causing more Hg to leach from the sorbents at low liquid to solid mass ratios. The results of the leaching tests indicate that landfill conditions should be considered prior to sorbent disposal. It may also be beneficial to reduce the amount of Br in the waste material by water washing to remove Br before disposal. Redesigning the sorbent to reduce the Br could also be beneficial. Leaching tests on the sorbent and fly ash after pilot or plant scale tests would be beneficial to determine the optimum location for disposing of the ash/sorbent waste. Analysis of the Br-Ash before and after leaching by x-ray photoelectron spectroscopy indicated a higher amount of organically bound Br compared to metal-bound Br after leaching, indicating a lower stability of metal-bound Br (i.e. metal-bound Br tends to leach more than organically-bound Br).

A high amount of mercury was added to the Br-Ash sample for analysis by x-ray absorption spectroscopy. In the mercury loaded samples, the Hg was found to be associated with carbon and bromine on the Br-Ash, and was associated with sulfur on the commercial activated carbon and brominated activated carbon. The commercial activated carbons had sulfide groups not present in the Br-Ash, which were preferred for Hg⁰ capture according to hard/soft acid-base theory. Our results for the commercial samples supported previously suggested mechanisms of surface enhanced oxidation of mercury, followed by binding of the oxidized mercury to the sulfide species on commercial sorbents. In the case of the Br-Ash, a mechanism of surface enhanced oxidation, followed by binding of oxidized Hg to C near the Br on the surface, was proposed. Based on the results from this study, designing the Br-Ash sorbent to contain sulfide groups was proposed to further improve Hg⁰ capture while reducing Br requirements on the sorbent.

The sulfur impregnation method was designed involving heating the elemental sulfur with wood ash. An optimum sulfur loading level was achieved at a 20:1 carbon to sulfur mass ratio. The sorbent prepared at this sulfur concentration efficiently captured mercury in a pulse injection

test up to 200 °C. Above the 20:1 carbon to sulfur mass ratio, no additional sulfur was loaded onto the sorbent (after heating to 600 °C), and mercury capture decreased. Scanning electron microscope images showed more mesopores for the optimum S-Ash sample compared to the high S-Ash sample or raw ash sample before treatment. It is possible that mesopores may be more important than micropores for mercury capture over a short contact time, such as mercury pulse injection tests in the laboratory and powdered sorbent injection in power plant facilities. The optimum sulfur loaded sample was chosen for bromine impregnation. Considering the leaching test results for Br, a low bromine content was selected (0.7-0.9%) compared to the previous loading values (8%). Addition of the low Br content to the sulfur impregnated sample dramatically improved mercury capture and increased the capability of the sorbent to capture a mercury pulse from 200 °C to 300 °C. In addition, the amount of mercury captured during the 24 hour loading test also increased. The increase of mercury captured during the 24 hour loading test showed an additive effect of combining Br and S on the sorbent. The additive effect of combining Br and S indicates that the sorbents can be designed with varying Br and S contents, depending on target application for an optimum sorbent performance. Sulfate was not found to assist in mercury capture by the biomass ash sorbents. In comparison, increasing elemental sulfur and sulfide was found to improve mercury capture by the sorbents (as long as sulfur concentrations sufficiently low to avoid pore blockage). The concentration of intermediate sulfur species (e.g. sulfoxide and thiophene) increased with sulfur loading, but it was not known if the species contributed to mercury capture.

Mercury capture mechanisms were also suggested for the biomass ash sorbent containing Br and S. The mechanism of mercury capture by S-Ash involved oxidation of the mercury by the sorbent, followed by binding to S species. In the case of Br-Ash, the mechanism of mercury removal was proposed to involve oxidation of the Hg by the surface of the sorbent, followed by binding to C or Br (with more carbon bonds present if there was lower Br concentration on the sorbent). The binding mechanism of mercury on the Br-S-Ash sorbent was proposed to be a combination of the mercury capture mechanisms by Br-Ash and S-Ash, involving oxidation of the mercury followed by binding to S, Br, or C species present on the surface. Leaching tests by TCLP indicated that the Br-S-Ash had a lower concentration of Br and Hg in the leachate compared to the Br-Ash (with low Br content) and S-Ash. In addition, leaching tests in water at

low liquid:solid ratio showed a significantly lower amount of Hg and Br in the leachate from Br-S-Ash compared to Br-Ash.

In summary, an effective sorbent created from a waste biomass ash material has been studied and redesigned for improved mercury capture. When designing the sorbent, leaching characteristics of the mercury, as well as impregnated species, should be considered. In order to engineer sorbents to reduce environmental impacts while improving efficiency, bromine and sulfur were both impregnated on the sorbent. The combined Br and S impregnation provides an excellent opportunity for producing an effective mercury sorbent with reduced environmental concerns (for disposal) while creating a lower cost adsorbent.

7.2. Contributions to Original Knowledge

- The leaching characteristics of bromine from brominated biomass ash and commercial brominated carbon were determined for the first time.
- First time that x-ray photoelectron spectroscopy has been used to show that after leaching the bromine is predominantly organically bound, i.e. organically bound bromine is more stable than metal-bound bromine.
- Mechanism of mercury capture has been proposed for the biomass ash sorbents.
- Fundamental study led to design of novel sorbent by impregnation of both liquid bromine and elemental sulfur onto biomass ash for the first time. Also, this is the first study to suggest engineering sorbents for optimum mercury capture by adjusting content of bromine and sulfur on surface of carbon sorbents.

7.3. Future Work

- Simulated flue gas tests or tests in a slipstream of real flue gases are an important next step in this work to determine the effect of other flue gas components on mercury capture by the combined Br-S-Ash sorbent. Br and S concentrations on the sorbent could be further optimized from these tests.
- In situ x-ray absorption spectroscopy tests in simulated flue gases would provide further insight into mechanism of mercury capture by the sorbents.

- Pilot or full scale tests including leaching tests from the resulting fly ash + sorbent would determine mercury capture performance during powdered injection for the Br-S-Ash. Leaching tests should include Hg, Br and S analysis of the leachate at varying pH and liquid to solid mass ratios.
- It remains to be seen if fly ash containing the Br-Ash sorbent can be used by the concrete industry. Tests for concrete properties and mercury stability for this application would determine if fly ash can continue to be sold for this purpose after sorbent injection.
- Temperature optimization for the sulfur loading on the Br-S-Ash sorbent could reduce pore blockage effect for high sulfur loadings.
- A study of functional groups present on the raw ash. Functional group analysis will help explain why it is a good support despite low specific surface area and lack of pretreatment (no thermal or chemical activation process).
- Test of Br and S loading on other waste materials from different facilities.
- Other starting sulfur species such as dimethyl disulfide, sodium sulfide or carbon disulfide could also be investigated. Addition of these species to the biomass ash may produce different sulfur speciation, and could reduce pore blockage.
- Study the impact of micropores and mesopores on the biomass sorbent by increasing the amount of pores and studying mercury capture as a function of porosity (while considering functional groups).

Bibliography

- Andrews, J.C. Mercury speciation in the environment using X-ray absorption spectroscopy. *Structure & Bonding*. **2006**, *120*, 1-35.
- Arvelakis, S.; Crocker, C.; Folkedahl, B.; Pavlish, J.; Spliethoff, H. Activated carbon from biomass for mercury capture: effect of the leaching pretreatment on the capture efficiency. *Energy Fuels*. **2010**, *24*, 4445-4453.
- Bandosz, T. J.; Ania, C. O. Surface chemistry of activated carbons and its characterization. In: *Activated Carbon Surfaces in Environmental Remediation*. Amsterdam ; London : Elsevier, 2006. Edited by Bandosz, Teresa J. pages 159-229.
- Behrooz Ghorishi, S.; Keeney, R. M.; Serre, S. D.; Gullett, B. K.; Jozewicz, W. S. Development of a Cl-impregnated activated carbon for entrained flow capture of elemental mercury. *Environ. Sci. Technol.* **2002**. *36*, 4454-4459.
- Berlin, M.; Zalups, R. K.; Fowler, B. A. Mercury. In: *Handbook on the Toxicology of Metals 3rd ed*; Nordberg, G. F, Fowler, B. A., Nordberg, M., Friberg, L. T., Eds.; Academic Press, Inc: USA, 2007, pp 675-729.
- Bisson, T. M.; Xu, Z.; Gupta, R.; Maham, Y.; Liu, Y.; Yang, H.; Clark, M.; Patel, M. Chemical-mechanical bromination of biomass ash for mercury removal from flue gases. *Fuel*. **2013**, *108*, 54-59.
- Bisson, T. M.; MacLean, L. C. W.; Hu, Y.; Xu, Z. Characterization of mercury binding onto a novel brominated biomass ash sorbent by x-ray absorption spectroscopy. *Environ. Sci. Technol.* **2012**, *46*, 12186–12193.

- Braekken, H. The crystal structure of HgBr₂. *Z. Kristallogr.* **1932**, 81, 152-154.
- Brown, T.; Lissianski, V. First full-scale demonstration of mercury control in Alberta. *Fuel Process. Technol.* **2009**, 90, 1412-1418.
- Canadian Council of Ministers of the Environment. CANADA-WIDE STANDARDS for MERCURY EMISSIONS from COAL-FIRED ELECTRIC POWER GENERATION PLANTS http://www.ccme.ca/assets/pdf/hg_epg_cws_w_annex.pdf (Accessed July 1, 2014).
- Canadian Council of Ministers of the Environment. 2012 PROGRESS REPORT. http://www.ccme.ca/assets/pdf/pn_1518_cws_hg_coal_prgrs_rpt_2012.pdf (Accessed July 1, 2014).
- Cho, J. H.; Eom, Y.; Park, J.-M.; Lee, S.-B.; Hong, J.-H.; Lee, T. G. Mercury leaching characteristics of waste treatment residues generated from various sources in Korea. *Waste Management.* **2013**, 33, 1675-1681.
- Cotte, M.; Susini, J.; Metrich, N.; Moscato, A.; Gratziu, C.; Bertagnini, A.; Pagano, M. Blackening of Pompeian cinnabar paintings: X-ray microspectroscopy analysis. *Anal.Chem.* **2006**, 78, 7484-7492.
- Daza, L.; Mendioroz, S.; Pajares, J. A. Mercury elimination from gaseous streams. *Appl. Catal. B. Environ.* **1993**, 2, 277-287.
- De, M.; Azargohar, R.; Dalai, A. K.; Shewchuk, S. R. Mercury removal by bio-char based modified activated carbons. *Fuel.* **2013**, 103, 570-578.
- Douglas, B; McDaniel, D.; Alexander, J. Concepts and Models of Inorganic Chemistry, 3rd ed., John Wiley & Sons, Inc.: New York, U.S.A., **1994**
- Environmental Protection Agency. Characterization of Mercury-Enriched Coal Combustion Residues from Electric Utilities Using Enhanced Sorbents for Mercury Control. (2006) <http://www.epa.gov/nrmrl/pubs/600r06008.html> (Accessed August 9, 2014)

- Environmental Protection Agency. Hazardous waste characteristics, a user-friendly reference document. (2009) <http://www.epa.gov/osw/hazard/wastetypes/wasteid/char/hw-char.pdf> accessed on April 14, 2014.
- Eswaran, S.; Stenger, H. G. Gas-phase mercury adsorption rate studies. *Energy Fuels*. **2007**, *21*, 852-857.
- Fan, M.; Tong, S.; Jia, C. Q.; Mao, L.; Li, Y.; Zhang, X. *Adsorption and stability of mercury on different types of impregnated activated carbon*. Proceedings of the 2011 International Conference on Computer Distributed Control and intelligent Environmental Monitoring. Feb 19-20, 2011. Changsha, Hunan, China. pp.1929-1932.
- Feeley III, T. J.; Jones, A. P.; Brickett, L. A.; O'Palko, B. A.; Miller, C. E.; Murphy, J. T. An update on DOE's phase II and phase III mercury control technology R&D program. *Fuel Process. Technol.* **2009**, *90*, 1388-1391.
- Feng, W.; Borguet, E.; Vidic, R. D. Sulfurization of a carbon surface for vapor phase mercury removal – II: Sulfur forms and mercury uptake. *Carbon*. **2006**, *44*, 2998-3004.
- Feng, W.; Kwon, S.; Feng, X.; Borguet, E.; Vidic, R. D. Sulfur impregnation on activated carbon fibers through H₂S oxidation for vapor phase mercury removal. *J. Environ. Eng.* **2006**, *132*, 292-300.
- Galbreath, K. C.; Zygarlicke, C. J. Mercury transformations in coal combustion flue gas. *Fuel Process. Technol.* **2000**, *65–66*, 289 – 310.
- Gale, T. K.; Lani, B. W.; Offen, G. R. Mechanisms governing the fate of mercury in coal-fired power systems. *Fuel Process. Technol.* **2008**, *89*, 139-151.
- Granite, E. J.; Pennline, H.W.; Hargis, R. A. Novel Sorbents for Mercury Removal from Flue Gas. *Ind. Eng. Chem. Res.* **2000**, *39*, 1020-1029.
- Graydon, J. W.; Zhang, X.; Kirk, D. W.; Jia, C.Q. Sorption and stability of mercury on activated carbon for emission control. *J. Hazard. Mater.* **2009**, *168*, 978-982.

- Greenwood, N. N.; Earnshaw, A. Chemistry of the Elements, Pergamon Press: Oxford, U.K., **1984**.
- Gupta, R. P.; Xu Z.; Clark, I.; Yang, H. Bromination process. United States Patent No. 20100126345, May 27, 2010.
- Haitzer, M.; Aiken, G. R.; Ryan, J. N. Binding of mercury(II) to dissolved organic matter: The role of the mercury-to-DOM concentration ratio. *Environ. Sci. Technol.* **2002**, *36*, 3564-3570.
- Hesterberg, D.; Chou, J. W.; Hutchison, K. J.; Sayers, D.E. Bonding of Hg(II) to reduced organic sulfur in humic acid as affected by S/Hg ratio. *Environ. Sci. Technol.* **2001**, *35*, 2741-2745.
- Ho, T. C.; Ghai, A. R.; Guo, F.; Wang, K. S.; Hopper, J. R. Adsorption and Desorption of Mercury on Sorbents at Elevated Temperatures. *Combust. Sci. Tech.* **1998**, *134*, 263-289.
- Hoffman, J.; Ratafia-Brown, J. Preliminary cost estimate of activated carbon injection for controlling mercury emissions from an un-scrubbed 500 MW coal-fired power plant. http://www.alrc.doe.gov/technologies/coalpower/ewr/mercury/pubs/ACI_Cost_Final.pdf (Accessed August 4, 2014)
- Hsi, H. C.; Tsai, C. Y.; Kuo, T. H.; Chiang, C. S. Development of low-concentration mercury adsorbents from biohydrogen-generation agricultural residues using sulfur impregnation. *Bioresource Technol.* **2011**, *102*, 7470-7477.
- Hsi, H. C.; Chen, S.; Rostam-Abadi, M.; Rood, M. J.; Richardson, C. F.; Carey, T. R.; Chang, R. Preparation and Evaluation of coal-derived activated carbons for removal of mercury vapor from simulated coal combustion flue gases. *Energy Fuels*, **1998**, *12*, 1061-1070.
- Hsi, H. C.; Rood, M. J.; Rostam-Abadi, M.; Chen, S.; Chang, R. Effects of sulfur impregnation temperature on the properties and mercury adsorption capacities of activated carbon fibers (ACFs). *Environ. Sci. Technol.* **2001**, *35*, 2785-2791.

- Hsi, H. C.; Chen, C. T. Influences of acidic/oxidizing gases on elemental mercury adsorption equilibrium and kinetics of sulfur-impregnated activated carbon. *Fuel*. **2012**, *98*, 229-235.
- Hsi, H. C.; Rood, M. J.; Rostam-Abadi, M.; Chang, Y. M. Effects of sulfur, nitric acid, and thermal treatments on the properties and mercury adsorption of activated carbons from bituminous coals. *Aerosol Air Qual. Res.* **2013**, *13*, 730-738.
- Hu, Y. F.; Coulthard, I.; Chevrier, D.; Wright, G.; Igarashi, R.; Sitnikov, A.; Yates, B. W.; Hallin, E. L.; Sham, T. K.; Reininger, R. Preliminary Commissioning and Performance of the Soft X-ray Micro-characterization Beamline at the Canadian Light Source in: *SRI 2009: The 10th International Conference On Synchrotron Radiation Instrumentation Sep 27-Oct 02, 2009*, AIP Conference Proceedings, Melbourne: Australia, 2010, vol. 1234, pp. 343-346.
- Huber, M. L.; Laesecke, A.; Friend, D. G. The vapour pressure of mercury. National Institute of Standards and Technology <http://www.nist.gov/mml/properties/upload/NISTIR-6643.pdf> (Accessed February 3, 2012).
- Huffman, G. P.; Mitra, S.; Huggins, F. E.; Shah, N.; Vaidya, S.; Lu, F. Quantitative analysis of all major forms of sulfur in coal by x-ray absorption fine structure spectroscopy. *Energy Fuels*. **1991**, *5*, 574-581.
- Huggins, F. E.; Huffman, G. P. XAFS examination of mercury sorption on three activated carbons. *Energy Fuels*. **1999**, *13*, 114-121.
- Huggins, F. E.; Yap, N.; Huffman, G. P.; Senior, C. L.; XAFS characterization of mercury captured from combustion gases on sorbents at low temperatures. *Fuel Proc. Technol.* **2003**, *82*, 167-196.
- Huggins, F. E.; Dalai, A. K.; Wallace, K. W.; Smith, D.; Shewchuk, S. R. *Surface properties of two activated carbons before and after exposure to a Hg-containing power-plant flue-gas*. Proceedings of the Combined Power Plant Air Pollutant Control Mega Symposium. August 30-September 2, 2004, Washington DC.

- Hutson, N. D.; Attwood, B. C.; Scheckel, K. G. XAS and XPS characterization of mercury binding on brominated activated carbon. *Environ. Sci. Technol.* **2007**, *41*, 1747-1752.
- Ie, I. R.; Chen, W. C.; Yuan, C. S.; Hung, C. H.; Lin, Y. C.; Tsai, H. H.; Jen, Y. S. Enhancing the adsorption of vapor-phase mercury chloride with an innovative composite sulfur-impregnated activated carbon. *J. Hazard. Mater.* **2012**, *217-218*, 43-50.
- Ie, I.-R.; Shen, H. Z.; Yuan, C.-S.; Hung, C.-H.; Chen, W.-H.; Jen, Y.-H. Single and dual adsorption of vapor-phase Hg^0 and/or $HgCl_2$ by innovative composite activated carbons impregnated with both S^0 and Na_2S . *Aerosol Air Qual. Res.* **2014**, *14*, 376-385.
- Johnson, D. W.; Brown, J. H.; Martin, M. J.; Rumble, A. Coal's triple challenge for air regulation compliance: technology, measurement, and commercial. In *Power Plant Air Pollution Control 'Mega' Symposium 2012*, Proceedings of the Power Plant Air Pollutant Control "MEGA" Symposium, Baltimore, Maryland, USA, August 20-23, 2012; Curan Associates: Red Hook, NY, 2013; p. 1-13.
- Karatza, D.; Lancia, A.; Musmarra, D.; Zucchini, C. Study of mercury absorption and desorption on sulfur impregnated carbon. *Exp. Therm. Fluid Sci.* **2000**, *21*, 150-155.
- Keating, M. H.; Mahaffey, K. R.; Schoeny, R.; Rice, G. E.; Bullock, O. R.; Ambrose, R. B.; Swartout, J.; Nichols, J. W. Mercury Study Report to Congress, Volume I: Executive Summary, <http://www.epa.gov/ttn/caaa/t3/reports/volume1.pdf> (Accessed March 29, 2010).
- Korpiel, J. A.; Vidic, R. D. Effect of sulfur impregnation method on activated carbon uptake of gas-phase mercury. *Environ. Sci. Technol.* **1997**, *31*, 2319-2325.
- Kwon, S.; Vidic, R. D. Evaluation of two sulfur impregnation methods on activated carbon and bentonite for the production of elemental mercury sorbents. *Environ. Eng. Sci.* **2000**, *17*, 303-313.

- Laumb, J. D.; Benson, S. A.; Olson, E. A. X-ray photoelectron spectroscopy analysis of mercury sorbent surface chemistry. *Fuel Process. Technol.* **2004**, *85*, 577–585.
- Lee, S. J.; Seo, Y.; Jurng, J.; Lee, T. G. Removal of gas-phase elemental mercury by iodine- and chlorine-impregnated activated carbons. *Atmos. Environ.* **2004**, *38*, 4887-4893.
- Lee, S. H.; Rhim, Y. J.; Cho, S. P.; Baek, J. I. Carbon-based novel sorbent for removing gas-phase mercury. *Fuel*. **2006**, *85*, 219-226.
- Lennie, A. R.; Charnock, J. M.; Patrick, R. A. D. Structure of mercury(II)-sulfur complexes by EXAFS spectroscopic measurements. *Chem. Geol.* **2003**, *199*, 199-207.
- Li, Y. ; Murphy, P. D.; Wu, C. Y.; Powers, K. W.; Bonzongo, J. C. J. Development of silica/vanadia/titania catalysts for removal of elemental mercury from coal-combustion flue gas. *Environ. Sci. Technol.* **2008**, *42*, 5304–5309.
- Li, Y.; Murphy, P.; Wu, C. Y. Removal of elemental mercury from simulated coal combustion flue gas using a SiO₂-TiO₂ nanocomposite. *Fuel Process. Technol.* **2008**, *89*, 567–573.
- Li, X.; Lee, J.; Heald, S. XAFS characterization of mercury captured on cupric chloride-impregnated sorbents. *Fuel*. **2012**, *93*, 618-624.
- Liu, J.; Qu, W.; Zheng, C. Theoretical studies of mercury-bromine species adsorption mechanism on carbonaceous surface. *Proceedings of the Combustion Institute.* **2013**, *34*, 2811-2819.
- Liu, S.; Yan, N. ; Liu, Z.; Qu, Z.; Wang, H. P.; Chang, S.; Miller, C. Using bromine gas to enhance mercury removal from flue gas of coal-fired power plants. *Environ. Sci. Technol.* **2007**, *41*, 1405-1412.
- Liu, W.; Vidic, R. D.; Brown, T. D. Optimization of sulfur impregnation protocol for fixed-bed application of activated carbon-based sorbents for gas-phase mercury removal. *Environ. Sci. Technol.* **1998**, *32*, 531-538.

- Liu, W.; Vidic, R. D.; Brown, T. D. Impact of flue gas conditions on mercury uptake by sulfur-impregnated activated carbon. *Environ. Sci. Technol.* **2000**, *34*, 154-159.
- Liu Y.; Kelly, D. J. A.; Yang, H.; Lin, C. C. H.; Kuznicki, S. M.; Xu, Z. Novel regenerable sorbent for mercury capture from flue gases of coal-fired power plant. *Environ. Sci. Technol.* **2008**, *42*, 6205-6210.
- Luo, Z.; Hu, C.; Zhou, J.; Cen, K. Stability of mercury on three activated carbon sorbents. *Fuel Process. Technol.* **2006**, *87*, 679-685.
- Ma, J.; Liu, Z.; Liu, Q.; Guo, S.; Huang, Z.; Xiao, Y., SO₂ and NO removal from flue gas over V₂O₅/AC at lower temperatures - role of V₂O₅ on SO₂ removal, *Fuel Process. Technol.* **2008**, *89*, 242-248.
- Morimoto, T.; Wu, S.; Uddin, M. A.; Sasaoka, E. Characteristics of the mercury vapor removal from coal combustion flue gas by activated carbon using H₂S. *Fuel.* **2005**, *84*, 1968-1974.
- Moulder, J. F.; Stickle, W. F.; Sobol, P. E.; Bomben, K. D. *Handbook of X-ray Photoelectron Spectroscopy*; Physical Electronics USA, Inc., Chanhassen, MN, 1995.
- Naumkin, A. V.; Kraut-Vass, A.; Gaarenstroom, S. W.; Powell, C. J. NIST X-ray Photoelectron Spectroscopy Database: NIST Standard Reference Database Version 4.1, 2012. <http://srdata.nist.gov/xps/Default.aspx> (Accessed on February 1, 2014).
- Newville, M.; Livins, Y.; Yacoby, Y.; Rehr, J. J.; Stern, E.A. An improved background removal method for XAFS. *Jpn. J. Appl. Phys. Pt1.* **1993**, *32*, 125-127.
- Newville, M. EXAFS analysis using FEFF and FEFFIT. *Journal of Synchrotron Radiation.* **2001**, *8*, 96-100.
- Norit. "Norit activated carbons for mercury removal from power plant flue gas", http://www.norit-america.com/pdf/Mercury_Removal_Power_Plants_rev5.pdf (Accessed March 29, 2010).

Norit. Norit activated carbon datasheet – DARCO Hg.

<http://www.norit-america.com/product/darco-hg> (Accessed June 6, 2012)

Norit. Norit activated carbon datasheet – DARCO Hg-LH. <http://www.norit-america.com/product/darco-hg-lh> (Accessed June 6, 2012)

Nugent, O., The Acid Rain Primer, 2-29,

<http://www.pollutionprobe.org/Publications/ARP06dwnldpage.htm> (Accessed June 22, 2009).

Olson E. S.; Azenkeng, A.; Laumb, J. D.; Jensen, R. R.; Benson, S. A.; Hoffman, M. R. New developments in the theory and modeling of mercury oxidation and binding on activated carbons in flue gas. *Fuel Process. Technol.* **2009**, *90*, 1360-1363.

Otani, Y.; Emi, H.; Kanaoka, C.; Uchijima, I.; Nishino, H. Removal of mercury vapor from air with sulfur-impregnated adsorbents. *Environ. Sci. Technol.* **1988**, *22*, 708-711.

Padak, B.; Brunetti, M.; Lewis, A.; Wilcox, J. Mercury Binding on Activated Carbon. *Environ. Prog.* **2006**, *25*, 319-326.

Paulik, F.; Paulik, J.; Buzágh-Gere, É.; Arnold, M. Examination of the decomposition of CaBr_2 with the method of simultaneous TG, DTG, DTA and EGA. *J. Therm. Anal.* **1979**, *15*, 271-277.

Pavlish, J. H.; Sondreal, E. A.; Mann, M. D.; Olson, E. S.; Galbreath, K. C.; Laudal, D. L.; Benson, S. A. Status review of mercury control options for coal-fired power plants. *Fuel Process. Technol.* **2003**, *82*, 89-165.

Pearson, R. G. Hard and Soft Acids and Bases. *Survey of Progress in Chemistry.* **1969**, *5*, 1-52.

Popović, Z.; Matković-Čalogović, D.; Hasić, J.; Sikirica, M.; Vikić-Topić, D. Binding of Mercury(II) by N-(2-mercaptopropionyl)glycine. Synthesis, IR and NMR Characterization. Crystal Structure of the 1: 2 Solvate of Bis[N-(propionyl-2-thiolato)- glycine]mercury(II) with 4-Methylpyridine. *Croatica Chemica Acta.* **1999**, *72*, 279-294.

- Presto, A. A.; Granite, E. J. Impact of sulfur oxides on mercury capture by activated carbon. *Environ. Sci. Technol.* **2007**, *41*, 6579-6584.
- Qu, Z.; Chang, J. J.; Hsiung, T.; Yan, N.; Wang, H. P.; Dod, R.; Chang, S.; Miller, C. Halides on carbonaceous materials for enhanced capture of Hg⁰: mechanistic study. *Energy Fuels*, **2010**, *24*, 3534-3539.
- Qu, Z.; Yan, N.; Liu, P.; Guo, Y.; Jia, J. Oxidation and stabilization of elemental mercury from coal-fired flue gas by sulfur monobromide. *Environ. Sci. Technol.* **2010**, *44*, 3889-3894.
- Ravel, B.; Newville, M. ATHENA, ARTEMIS, HEPHAESTUS: Data analysis for X-ray absorption spectroscopy using IFEFFIT. *Journal of Synchrotron Radiation*. **2005**, *12*, 537-541.
- Reddy, B. M.; Durgasri, N.; Vinod Kumar, T.; Bhargava, S. K. Abatement of gas-phase mercury-recent developments. *Catal. Rev.- Sci. Eng.* **2012**, *54*, 344-398.
- Riddle, S. G.; Tran, H.H.; DeWitt, J. G.; Andrews, J. C. Field, laboratory, and X-ray absorption spectroscopic studies of mercury accumulation by water hyacinths. *Environ. Sci. Technol.* **2002**, *36*, 1965-1970.
- Rupp, E. C.; Wilcox J. Mercury chemistry of brominated activated carbons – packed-bed breakthrough experiments. *Fuel*. **2014**, *117*, 351-353.
- Saha, A.; Abram, D. N.; Kuhl, K. P.; Paradis, J.; Crawford, J. L.; Sasmaz, E.; Chang, R.; Jaramillo, T. F.; Wilcox, J. An X-ray photoelectron spectroscopy study of surface changes on brominated and sulfur-treated activated carbon sorbents during mercury capture: performance of pellet versus fiber sorbents. *Environ. Sci. Technol.* **2013**, *47*, 13695-13701.
- Sasmaz, E.; Kirchofer, A.; Jew, A. D.; Saha, A.; Abram, D.; Jaramillo, T. F.; Wilcox, J. Mercury chemistry on brominated activated carbon. *Fuel*. **2012**, *99*, 188-196.

- Seneviratne, H. R.; Charpentreau, C.; George, A.; Millan, M.; Dugwell, D. R.; Kandiyoti, R. Ranking low cost sorbents for mercury capture from simulated flue gases. *Energy Fuels*, **2007**, *21*, 3249-3258.
- Sinha, R. K.; Walker Jr., P. L. Removal of mercury by sulfurized carbons. *Carbon*. **1972**, *10*, 754-756.
- Skodras, G.; Diamantopoulou, I.; Zabaniotou, A.; Stavropoulos, G.; Sakellaropoulos, G. P. Enhanced mercury adsorption in activated carbons from biomass materials and waste tires. *Fuel Process. Technol.* **2007**, *88*, 749-758.
- Srivastava, R. K.; Hutson, N.; Martin, B.; Princiotta, F.; Staudt, J., Control of mercury emissions from coal-fired electric utility boilers, *Environ. Sci. Technol.* **2006**, *40*, 1385-1393.
- Steijns, M.; Peppelenbos, A.; Mars, P. Mercury chemisorption by sulfur adsorbed in porous materials. *J. Colloid Interface Sci.* **1976**, *57*, 181-186.
- SunSirs China Commodity Data Group. 100 Spot Commodities Price Chart – 09/05/2014. <http://www.sunsirs.com/uk/sdetail.html>. (Accessed May 10, 2014).
- Suresh Kumar Reddy, K.; Al Shoaibi. A.; Srinivasakannan, C. Gas-phase mercury removal through sulfur impregnated porous carbon. *J. Ind. Eng. Chem.* **2014**, *20*, 2969-2974.
- Tong, S.; Fan, M.; Mao, L.; Jia, C. Q. Sequential extraction study of stability of adsorbed mercury in chemically modified activated carbons. *Environ. Sci. Technol.* **2011**, *45*, 7416–7421.
- Uddin, M. A.; Ozaki, M.; Sasaoka, E.; Wu, S. Temperature-Programmed Decomposition Desorption of Mercury Species over Activated Carbon Sorbents for Mercury Removal from Coal-Derived Fuel Gas. *Energy Fuels*. **2009**, *23*, 4710–4716
- Union of Concerned Citizens, Environmental impacts of coal power: air pollution. http://www.ucsusa.org/clean_energy/coalswind/c02c.html (Accessed June 22, 2009).

United Nations Minamata Convention on Mercury. <http://www.mercuryconvention.org/>
(Accessed May 23, 2014).

US EPA Method 1311 toxicity characteristic leaching procedure. Fed. Regist. 55 (1992) 11798–11877. www.epa.gov/osw/hazard/testmethods/sw846/pdfs/1311.pdf
(Accessed December 5, 2013)

Valupadas, P. Alberta mercury regulation for coal-fired power plants. *Fuel Process. Technol.* **2009**, *90*, 1339–1342.

Vidic, R. D.; Siler, D. P. Vapor-phase elemental mercury adsorption by activated carbon impregnated with chloride and chelating agents. *Carbon*. **2001**, *39*, 3-14.

Vitolo, S.; Pini, R. Deposition of sulfur from H₂S on porous adsorbents and effect on their mercury adsorption capacity. *Geothermics*. **1999**, *28*, 341-354.

Wang, S.; Fackler, J. P. Mercury complexes with one-dimensional chain structures. Syntheses and crystal structures of [Hg(C₅H₄NS)(CH₃CO₂)]_n, Hg(C₅H₄NS)₂, and Hg(CH₂P(S)Ph)₂. *Inorg. Chem.*, **1989**, *28*, 2615-2619.

Wilcox, J.; Sasmaz, E.; Kirchofer, A.; Lee, S-S. Heterogeneous Mercury Reaction Chemistry on Activated Carbon. *Journal of the Air & Waste Management Association*. **2011**, *61*, 418-426.

Wilcox, J.; Rupp, E.; Ying, S. C.; Lim, D. -H.; a, Suarez Negreira, A.; Kirchofer, A.; Feng, F.; Lee, K. Mercury adsorption and oxidation in coal combustion and gasification processes. *Int. J. Coal Geol.* **2012**, *90-91*, 4–20.

World Health Organization, Bromide in drinking-water: Background document for development of WHO Guidelines for Drinking-water Quality (2009)
http://www.who.int/water_sanitation_health/dwq/chemicals/Fourth_Edition_Bromide_Final_January_2010.pdf (Accessed April 14, 2014).

- Wu, J.; Chen, J.; Zhang, S.; He, P.; Fang, J.; Wu, Y. Removal of gas-phase elemental mercury by bromine-impregnated activated carbon. *Adv. Mater. Res.* **2012**, 356-360, 1660-1663.
- Yan, N.; Qu, Z.; Chi, Y.; Qiao, S.; Dod, R.L.; Chang, S.; Miller, C. Enhanced elemental mercury removal from coal-fired flue gas by sulfur-chlorine compounds. *Environ. Sci. Technol.* **2009**, 43, 5410–5415.
- Yang, H.; Xu, Z.; Fan, M.; Bland, A.E.; Judkins, R.R., Adsorbents for capturing mercury in coal-fired boiler flue gas, *J. Hazard. Mater.* **2007**, 146, 1-11.
- Yao, Y.; Velpari, V.; Economy, J.; Design of sulfur treated activated carbon fibers for gas phase elemental mercury removal. *Fuel.* **2014**, 116, 560-565.
- Yoon, S. J.; Diener, L. M.; Bloom, P. R.; Nater, E. A.; Bleam, W. F. X-ray absorption studies of CH_3Hg^+ -binding sites in humic substances. *Geochim. Cosmochim. Acta.* **2005**, 69, 1111-1121.
- Zabinsky, S. I.; Rehr, J. J.; Ankudinov, A.; Albers, R.C. Multiple-scattering calculations of X-ray absorption spectra. *Phys. Rev. B: Condens. Mater. Phys.* **1995**, 52, 2995-3009.
- Zeng, H.; Jin, F.; Guo, J. Removal of elemental mercury from coal combustion flue gas by chloride-impregnated activated carbon. *Fuel.* **2004**, 83, 143-146.
- Zhao, L.; Liu, Q.; Wu, J.; Zhang, C.; Wu, Y.; Zha, J.; Yang, S.; Hu, C. Study on the removal of mercury in the simulated flue gas by biomass activated carbon. *Adv. Mater. Res.* **2014**, 864-867, 1519-1524.

Appendix A

Additional Figures for Chapter 4

The composition of commercial activated carbon samples and brominated ash samples is determined by bulk x-ray fluorescence. Bromine K-edge XANES spectra is presented showing similar Br-bonding environment in all samples.

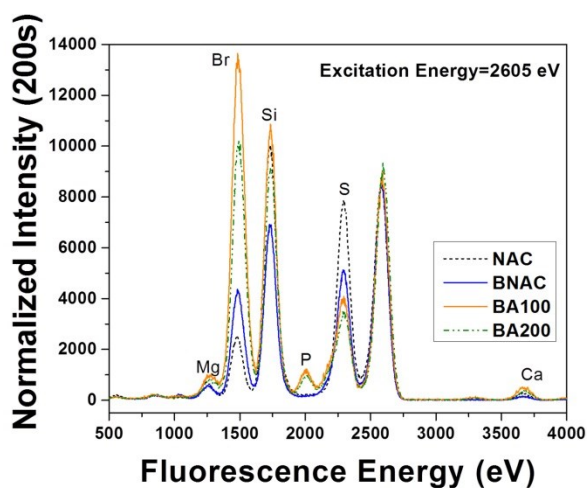


Figure A1. Bulk X-ray fluorescence spectra of each sample. Excitation energy at 2605 eV.

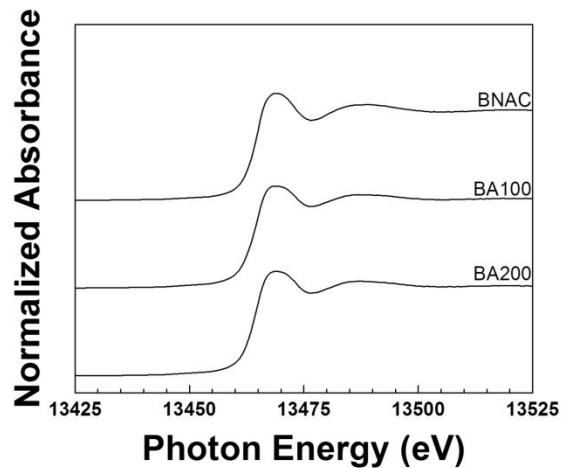


Figure A2. Bromine K-edge XANES spectra for the activated carbon sorbents ($E_0 = 13,474$ eV).

Appendix B

Additional Figures and Tables for Chapter 6

Sulfur and mercury loading schematics are presented, along with mercury EXAFS fitting results. Leach test results are also shown for the sorbents.

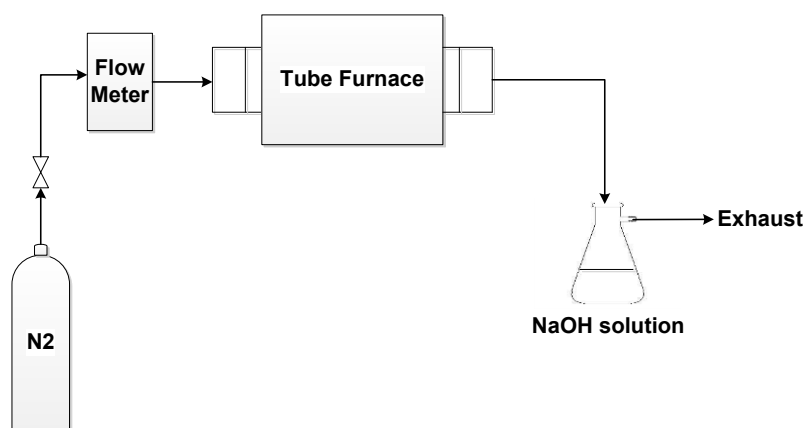


Figure B1. Schematic of sulfur loading setup.

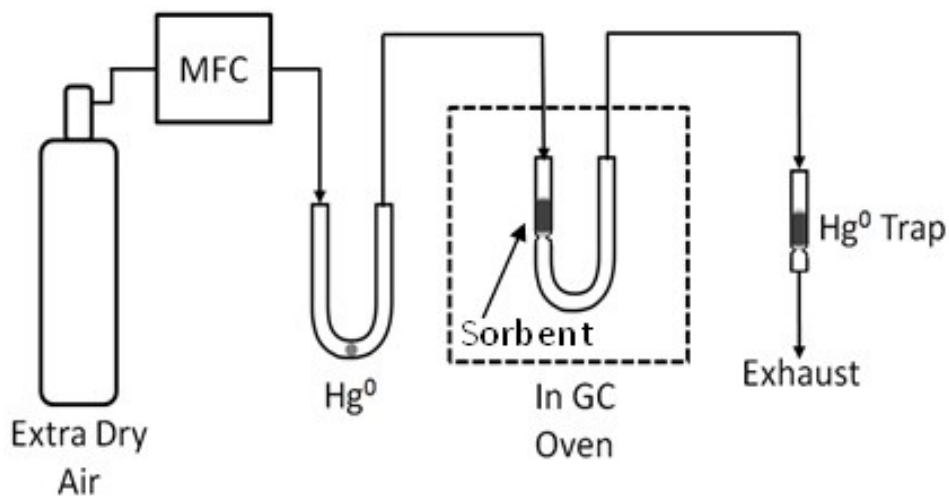


Figure B2. Hg⁰ loading experimental setup.

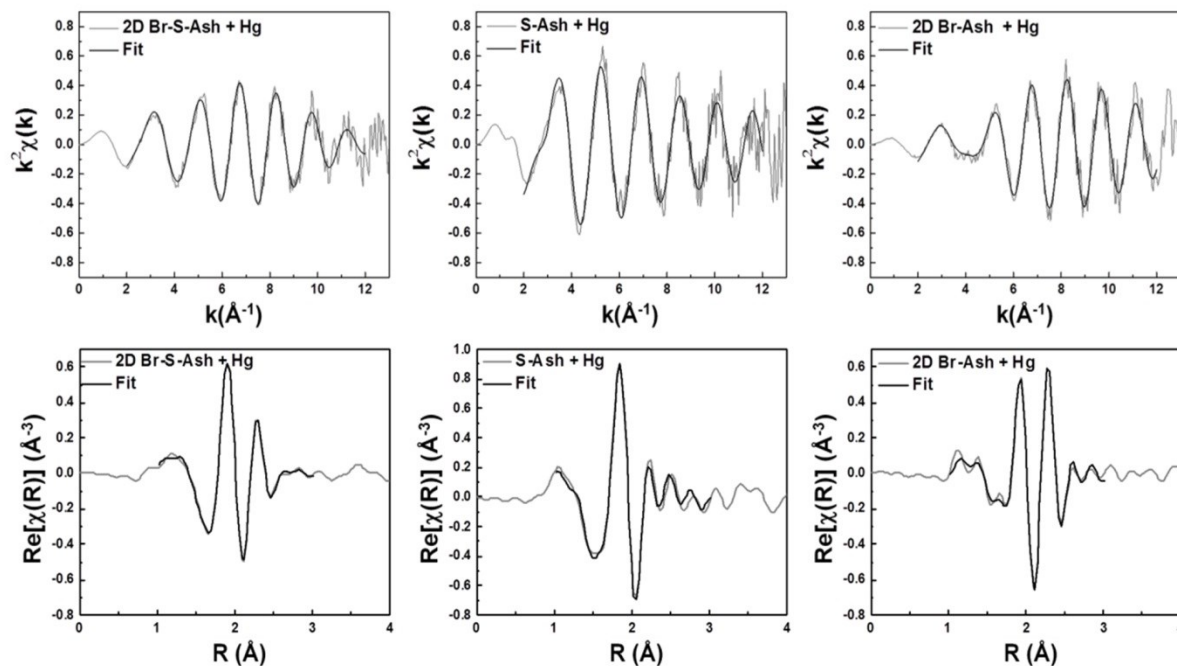


Figure B3. Mercury EXAFS fitting.

Table B1. Hg leach test results using TCLP leaching method.

	Average mg/L	+/-	Average %	+/-
Br-S-Ash	0.01	0.00	0.05	0.05
2D Br-Ash	0.18	0.13	0.7	0.7
2D Br-S-Ash	0.02	0.01	0.1	0.1
Br-Ash	0.01	0.00	0.05	0.01

Table B2. Br leach test results TCLP leaching method.

	Average mg/L	+/-	Average %	+/-
2D Br-Ash	145	10.0	42.1	2.8
2D Br-S-Ash	209	15.6	46.9	3.6
Br-Ash	2630	37	70.9	3.6